AN INVESTIGATION OF COHESION IN ILLITE

WILLIAM R. ROGERS

AN INVESTIGATION OF COHESION IN ILLITE

by

Lt. William R. Rogers, CEC, USN

A Thesis submitted to the Faculty
of the Department of Civil Engineering
in Partial Fulfillment of the
Requirements for the Degree of
MASTER OF CIVIL ENGINEERING

TABLE OF CONTENTS

LIST OF TABLES

LIST OF FIGURES

FOREWORD

The author wishes to express his appreciation to Professor E. J. Kilcawley, Head of the Division of Soil Mechanics and Sanitary Engineering, Department of Civil Engineering, for his suggestion in the selection of this topic and for his guidance throughout the investigation.

Particular acknowledgement to Associate Professor S. V. Best, also of the Division of Soil Mechanics, for his assistance and suggestions in carrying out the experiments.

Lt. J. E. Powell, CEC, USN and Lt. C. C. Heid, CEC, USN generously conducted tests and produced curves for X-ray Diffraction and Differential Thermal Analysis, respectively.

ABSTRACT

The investigation of the variance of cohesion in a saturated illite clay with respect to normal stresses, rates of strain and preconsolidation necessarily concerns itself with the general subject of shear resistance. The original Coulomb equation, $s = c + \sigma \tan\phi$, treated cohesion as a constant value for a particular soil. Later modifications led to the Krey-Tiedeman equation, $s = p_c \tan\phi_c + \sigma \tan\phi$, which presented cohesion as a variable. It is shown in this work that cohesion is a variable but much more complex than $c = p_c \tan\phi_c$

Recent investigations by J. M. Turnbull (Ref. 14) support the theory that cohesion reaches high values for fine clays under large normal stresses. Turnbull suggested criteria which would enable a determination of true cohesion, true angle of friction and capillary normal stress from shearing resistance tests at two or more rates of strain. The criteria, presented in the form of six laws, was found inapplicable to a saturated illite.

Direct shear tests were made on saturated illite samples preconsolidated to 1, 2 and 4 tons/sq.ft. at two rates of strain: .02 in/min and .003 in/min. The results were plotted in a manner after Hvorslev (Ref. 5) to obtain the true angle of friction and the

true cohesion.

True cohesion was found not only to vary directly with normal stress but also to be dependent upon the rate of strain and pore pressure. The relationship of these factors is so extremely complicated that no criteria could be evolved from the limited number of tests performed.

Both the angle of internal friction and intrinsic pressure vary inversely with rate of strain. There is strong evidence that the angle of internal friction is not constant for a given normal stress at a given rate of strain, under saturated conditions.

PART I

INTRODUCTION

A. Statement of Problem

The investigation which forms the subject of this thesis was undertaken to determine the applicability of J. McNeill Turnbull's (Ref. 14) six laws pertaining to the shearing resistance of soils to a saturated illite clay. The six laws recommended as suitable for use in the design of proposed structures and propounded as valid at various rates of strain on any particular sample of soil under uniform testing conditions are:

1. Proportionality between capillary normal stress and rates of strain.
2. Unique point of intersection for curves representing maximum shearing resistance at each rate of strain. (Fig. VIII)
3. Unique point of intersection, at the same maximum shearing resistance as the unique point of Law 2, of the curves representing the solution of Coulomb's equation for a particular applied normal stress at each rate of strain. (Fig. VIII)
4. Unique point of intersection for the cohesion curves at each rate of strain. (Fig. VIII)

5. Magnitude of true cohesion and true internal friction for any particular value of maximum shearing resistance is the same at each rate of strain.
6. Angle of internal friction at each rate of strain has a constant value for all normal stresses.

Two changes in nomenclature have been made by the writer in describing normal stresses. Instead of the term capillary normal pressure the writer uses the term intrinsic pressure under the assumption that no dependable capillary pressure exists in a completely saturated condition. Secondly, the term vertical load is substituted for applied normal stress as a matter of convenience.

Resistance of soils to shearing forces is basically the most important factor which confronts a foundation engineer. Shearing strength depends upon the cohesion and internal friction of a soil.

Cohesion was formerly assumed to be independent of all applied pressures. It is now generally acknowledged that cohesion is related to normal pressure in much the same manner as internal friction, but to a lesser degree. How much significance this relation has to the foundation engineer is yet to be determined. It is the intention of this work to record the effects of

normal pressure on a nearly pure illite under the supposition that in taking a known clay mineral and showing the variation of cohesion with normal pressure an appreciation can be had of its affect on a given cohesive soil of which illite forms one of the major constituents.

Many factors enter the determination of the shearing strength of a cohesive soil: angle of internal friction; intrinsic pressure; major, intermediate and minor principal stresses; intergranular stress; neutral stress; cohesion; colloidal phenomena; shear speed; drainage condition; moisture content; air content; gradation; molecular structure and chemical composition; past history; density. From this list it becomes apparent that any attempt to isolate cohesion would be impossible. However, with reasonable care and control, cohesion can be studied as a part of the shearing strength when these factors are ascertained or nullified.

There is a school of thought in Soil Mechanics that to divide shear strength into two major components is of questionable value in practice. One can see immediately that such an attitude is justified on the basis of simplicity and has not only appeal to the practicing engineer but is the ultimate goal of any strength invertigation. On the other hand, a complete

knowledge of choesive action may be the key to more accurate evaluations and predictions of the bearing capacity of cohesive soils.

To study the problem one series of direct shear tests were run on the illite at vertical loads of $\frac{1}{4}$, $\frac{1}{2}$, 1, 2 and 4 tons/sq.ft. Using the maximum values of shear resistance obtained from this series, a curve of maximum shearing resistance was established. Next, a series of direct shear tests were run at vertical loads of $\frac{1}{4}$, $\frac{1}{2}$, 1 and 2 tons/sq.ft. on samples preloaded to 4 tons/sq.ft. Similar tests were run on samples preloaded to 1 and 2 tons/sq/ft. From maximum shearing resistance values determined by the latter series of tests, three additional curves could be plotted to show true cohesion and the angle of internal friction at a particular rate of strain.

The entire procedure was performed at two rates of strain: .02 in/min and .003 in/min. These rates were the extremes obtainable on the test machine without modifications thereto.

A rate of strain of .02 in/min on illite, a relatively impermeable material as compared to natural soil mixtures, is well within the limitations established for the quick-consolidated test. Drainage, while not actually prohibited by sealing the specimens, was effectively impaired by the characteristic impermeability inherent to illite.

An intermediate condition between a quick-consolidated test and a drained test exists for the case of a rate of strain of .003 in/min. There is evidence of some drainage, but not to the fullest extent possible under an unlimited time duration.

A description of the clay mineral illite complete with x-ray diffraction, differential thermal curves, source, geological age and physical properties is given in Part IV. Most work undertaken and reported in the literature on shear testing and cohesion generally does not define the material tested in such detail. The writer has found this to be one possibility for the variations and even disagreements reported by different investigators.

B. Historical Review

Very little literature is available on the subject of cohesion as treated by the theory that it is functionally dependent on preconsolidation loads. Extensive use has been made of the Turnbull (Ref. 14) paper in this investigation.

Hogentogler (Ref. 4) cites a cohesive soil investigation in which the internal angle of friction increases with an increase in preconsolidation load, and that the importance of cohesion decreases im comparison.

Hvorslev (Ref. 5) appears to have been the first to report the relation of cohesion to preconsolidation loads. Only excerpts from the original Danish texts have been located. These excerpts show no allowance for variations in rate of strain or intrinsic pressure.

Modern texts on Soil Mechanics still tender the original Coulomb theory of constant cohesion.

PART II

THEORY

A. General

Shearing strength of a soil is its ability to withstand shearing stresses. Failure occurs in the form of slipping when its maximum resistance is exceeded. Shear strength is made up of internal friction (resistance due to interlocking of particles) and cohesion (resistance due to the molecular attraction between particles).

In most clay soils the shearing strength is derived primarily from cohesion and secondarily from internal friction. Both factors vary with moisture content and density, thus they depend upon the state of soil before loading, and drainage conditions during the process of loading and shearing.

To develop the theory of shearing strength of a soil the classical beginning is with Coulomb's equation $S = c + \sigma \tan \phi$ where:

S = shearing strength

σ = normal pressure on the failure plane

c = apparent cohesion independent of normal pressure

ϕ = angle of friction

It will be shown in the following development that c is actually dependent upon normal pressure.

B. Development of Theory

1. Sliding Friction

Consider a body shown in Fig. 1. P_n is a vertical force acting on the body whereas P_t acts horizontally in such a manner as to tend to produce sliding. The resultant R of the two forces P_n and P_t acts at angle α the angle of obliqity. When P_t reaches a magnitude that will actually produce sliding, the angle α increases to a maximum angle ϕ which is the angle of friction. The term tan ϕ is the coefficient of friction.

Then for a condition of incipient sliding we have $P_t = P_n \tan \phi$ or $S = \sigma \tan \phi$

where $S = \frac{P_t}{A}$

$\sigma = \frac{P_n}{A}$

The physical properties of the body and the plane determine the value of ϕ. Roughness of the surface, absorbed films or forces of attraction will effect the value of ϕ for any given material.

2. Stress at a Point

To have an appreciation of shearing stress, a review of the stresses at any point in a solid is of great value. Consider the point O, Fig. 2, which represents any point in a stressed body. OX represents the major

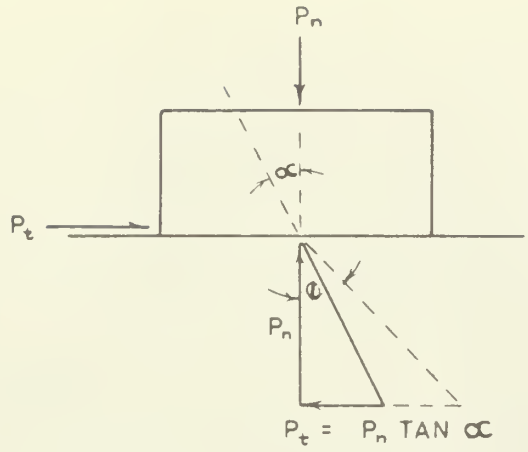

FIG. I ILLUSTRATION OF ANGLE OF FRICTION

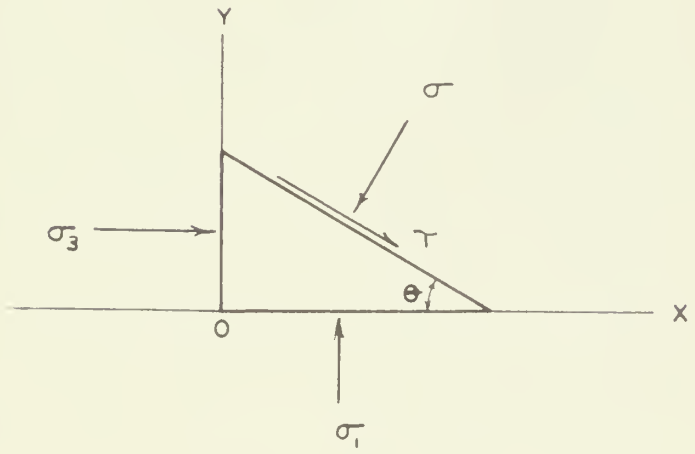

FIG. II STRESS AT A POINT

principal plane and OY represents the minor principal plane; in other words, the planes which intersect at 90° and have zero shearing stress.

For equilibrium to exist on the inclined plane in terms of unit stresses the following equations hold:

$$\sigma = \sigma_3 \sin^2\theta + \sigma_1 \cos^2\theta$$
$$= \sigma_3 + (\sigma_1 - \sigma_3)\cos^2\theta$$

and $$\tau = (\sigma_1 - \sigma_3)\sin\theta\cos\theta$$

3. Mohr Diagram

Stress at a point can most easily be shown graphically by means of the Mohr diagram. The Mohr diagram is composed of two major parts: the Mohr circle of stress and the Mohr envelope.

The Mohr circle of stress is a locus of points which represent normal stresses as abscissas and shearing stresses as ordinates for all values of θ defined above. The center of the circle is located on the abscissa and cuts the abscissa at (normal stress on major principal plane) and (normal stress on minor principal plane) as shown in Fig. III. Thus a point on the circle represents the coordinates of stress on some plane. This characteristic gives an excellent visualization of the orientation of various planes.

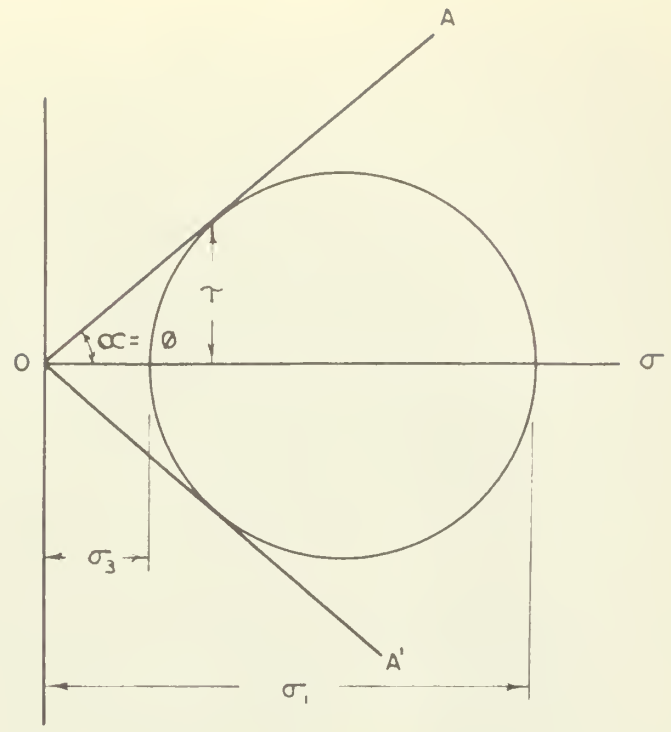

FIG. III MOHR DIAGRAM

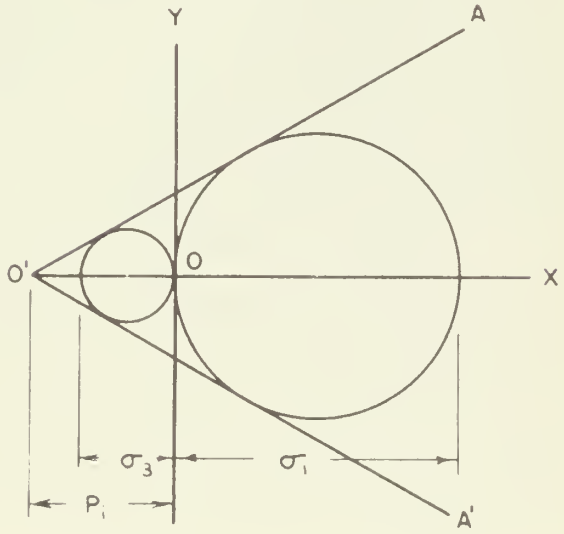

FIG. IV MOHR DIAGRAM ILLUSTRATING INTRINSIC PRESSURE

The Mohr envelope is shown as the lines OA and OA'; in this case the maximum value of the angle of obliqity is shown tangent to the Mohr circle and therefore is equal to ϕ. On any plane the shearing stress is $\tau = \sigma \tan\alpha$ and for cohesionless soils then $s = \sigma \tan\phi$

From the foregoing, the Mohr theory of rupture can be expressed for any Mohr circle within the Mohr envelope as representing a stable condition whereas any circle tangent to the envelope represents a condition of immenent failure.

The Mohr envelope is characteristic for a given material and is entirely independent of imposed stresses. On the other hand, the Mohr circle is independent of the material and represents only the imposed stresses.

Mohr's theory of rupture may be applied satisfactorily to soils with the following limitations:

1. Intermediate principal stress has no appreciable effect on shear strength.
2. No variablesother than pressure have any effect on shear strength.

Both of these limitations are found to a small degree in soils and will vary with density, structure, speed of shear and other variables mentioned previously. Taylor (Ref. 11) states that most of these factors have minor effects.

To carry through the Mohr's theory of rupture for cohesive soils a depiction of tensile properties will be shown. Under tensile conditions intrinsic pressure, pressure which has been applied some time in the past and has increased the intergranular attraction of the mass, becomes of major importance.

If a body has tensile strength it is readily shown on the Mohr diagram as a normal stress to the left of the origin of coordinates. The minor principal stress is thus represented as a negative value as shown in Fig. IV. Under the assumption that the Mohr envelope is a straight line, O'A can be drawn tangent to the Mohr circle, which represents failure of a mass under tension and compression respectively. The distance O'O represents the intrinsic pressure P_i.

The intercept of O'A on the OY axis then represents cohesion in a soil and $C = P_i \tan \phi$ from which $S = P_i \tan \phi + \sigma \tan \phi$ indicating that Coulomb's assumption of cohesion being constant is an over simplification of the problem.

C. Cohesion

Cohesion is presented in a variety of ways by authors dealing with the subject. An excellent means of gaining a broad understanding of cohesion as it pertains to soils is to study these presentations.

Terzaghi (Ref. 12): The bond between the soil particles is called cohesion.

If one makes a series of slow tests on a clay with a given initial water content after increasing the pressure on the samples from zero to different values σ_1, σ_2, etc., one gets an equation,

$$s = c + \sigma \tan \phi$$

If one makes another series of tests on specimens of the same material after preceding consolidation of samples under a pressure which is higher than the test pressures one gets another equation

$$s = c' + \sigma \tan \phi'$$

wherein c' is consiberably higher than c and ϕ' considerably smaller than ϕ. Hence using Coulomb's equation in connection with clays, the reader should remember that the values c and ϕ contained in this equation represent merely two empirical coefficients in the equation of a straight line. The term cohesion is retained only for historical reasons. It is used as an abbreviation of the term apparent cohesion. In contrast to the apparent cohesion, the true cohesion represents that part of the

shearing resistance of a soil which is a function only of water content. It includes not only c in Coulomb's equation but also an appreciable part of $\sigma \tan \phi$. There is no relation between apparent and true cohesion other than by name.

In order to visualize the difference between apparent and real cohesion we consider again a material whose cohesion increases with increasing compaction. By making a series of shear tests with the material we obtain

$$s = c + \sigma \tan \phi$$

However, when investigating which part of the shearing resistance of the material is due to sohesion we obtain

$$s = c + \frac{\sigma_1 + \sigma_3}{2} N + \sigma \tan \phi_f$$

Where N is an empirical factor, σ_1 and σ_3 represent the extreme principal stresses of failure, and ϕ_f is the angle of internal friction of failure.

Comparing the two preceding equations we find that the true cohesion of the material is equal not to c but to

$$c_c = c + \frac{\sigma_1 + \sigma_3}{2} N$$

If the entire pressure on the clay is transmitted from grain to grain the true cohesion is never smaller than the apparent cohesion.

Krynine (Ref. 7): There are two kinds of cohesion in soils: (a) true cohesion, caused by the mutual attraction of particles due to molecular forces;

(b) apparent cohesion, due to the action of moisture films. For instance, dry sand, especially fine sand, becomes cohesive when moist. This is so because surface tension in this case acts at the surface of the film and holds the grains together. In a general case, true cohesion in soils is small and may be disregarded. Some exceptions, however, are (a) dense gravels composed of both coarse and fine particles, the latter acting as a "binder" which cements the whole mass; and (b) compact sands and a few other soils.

In the following discussion apparent cohesion only will be considered. To make a soil mass cohesive, the moisture content should be adequately but not exceedingly high. If, for instance, a given soil is very cohesive when containing 15 per cent of moisture by dry weight, it mas be less cohesive when containing 5 or 25 per cent of moisture. In the former case these may not be moisture enough to form films on all particles of the mass, and in the latter case the surface tension may be removed by the excess of water. The "optimum" value of moisture content, corresponding to maximum cohesion, should be determined for each soil experimentally. It is assumed that cohesion in soils does not depend on the value of normal stress. This may be true in the case of metals or rocks, but is an approximation in soils, since

in this case the normal stress controls the moisture content and the latter controls cohesion. Cohesion may be developed in any direction within the body.

Taylor (Ref. 11): Materials which can be called solid have strength which can not be attributed to any visible source of pressure. This condition often may be described as a result of a pressure which was exerted on the material at some time in the past, the effects of which have in some way been retained.

A stiff clay, loaded and compressed in past ages by overlying strata, provides another example of retained pressure. When a specimen of such a soil is removed from the ground and protected from evaporation or increase in water content, a large portion of the intergranular pressure is retained by capillary action at the surface of the specimen. In this condition pore water is in tension, and the pressure on the sample is capillary pressure. The shearing strength which is caused by capillary pressure is sometimed called apparent cohesion. In some clays most of this pressure is lost in a short time if the specimen is placed under water, because submergence destroys the surface menisci, the sample swells, and the tension in the water soon is dissipated. A simple but common test to determine the degree to which this process occurs is called the slaking test, which consists simply in visually noting how fast and to what degree the sample slakes, or falls apart,

when placed below water. The strength lost during the slaking test is apparent cohesion or strength due to capillary pressure.

Some clays in such a test lose practically all their intergranular pressure, and others lose practically none. In those which lose only a minor portion of their strength, pressure must be retained by some type of bond in the adsorbed water adjacent to the points where grains touch or nearly touch. Water in this form is highly plastic and will flow, but flow is at a very slow rate. If a submerged specimen is given sufficient time, the retension of pressure contributed by this bound water may gradually be lost, but the adjustment may require decades, whereas only minutes or hours are required for apparent cohesion to disappear. This relatively permanent type of strength is called true cohesion and is said to be caused by intrinsic pressure. A clay which actually has started to pass into the category of shale may have a large amount of true cohesion.

Many modern concepts relative to intrinsic pressure are of hypothetical nature, but it may at least be said that when loads are applied to a solid some type of intrinsic attraction or bond either exists or comes into action to resist the relative displacement of adjacent particles. The shearing strength which a material possesses by virtue of its intrinsic pressure is given

the general name cohesion. Since failure will not result unless additional stresses are applied there will seldom be a failure in which cohesion is the entire shearing strength.

Tschebotarioff (Ref. 13): True cohesion is produced by the actual bond which develops at the surfaces of contact of clay particles as a result of electro chemical forces of attraction. It is dependent on a great number of factors, the study of most of which falls within the provinces of soil physics and colloidal chemistry.

Baver (Ref. 1): Cohesion in wet soils takes place between the molecules of the liquid phase that exists as bridges or films between adjacent particles.

For cohesion between colloidal-clay particles, he states: the colloidal material is responsible for the cementation of primary particles into stable aggregates. It should be expected that the formation of secondary particles from primary separates would be related to the amount of finer particles in the soil that may serve as material to be aggregated.

Russel (Ref. 9): Each particle is surrounded by an electric double layer, the outer one being diffuse and consisting of cations, while the inner layer consists of negative charges presumably anchored on the surface of the particle. The cations in the diffuse layer move about in the water in the same way as they do in

a complex anion, as pictured in the Debye-Hückel theory of strong electrolytes. Since the water molecules possess a dipole moment, they tend to be oriented along the lines of electric force radiating from each ion in the diffuse layer and from each free charge on the surface of the clay particle. Every cation and particle is thus surrounded by an envelope of oriented water molecules, and the orientation manifests itself as an apparent adsorption or immobilization of water by the clay. Some of the water molecules near an electric charge may be so strongly oriented that they appear bound to it, their heat motion merely making them oscillate about lines of force, while those further away from the charge possess only a statistical orientation around it. A clay particle in a dilute suspension can therefore be pictured as consisting of a central core surrounded by a surface carrying a negative charge. Around each negative charge is an envelope of water molecules which are strongly oriented the nearer they lie to the charge. Outside this surface are the cations, also possessing envelopes of oriented water molecules. Some cations are so close to a negative charge on the surface of a clay particle that the two water envelopes belonging to these charges overlap and the water molecules in this region are oriented in their joint field. This orientation is very strong since the negative end of the water dipole is attracted to the cation and the positive end to the par-

ticle's surface.

As the water is removed the deflocculater clay suspension becomes more concentrated and an increasing proportion of the water molecules becomes oriented in the joint field of a positive and a negative charge. It is reasonable to assume that a certain number of cations will share their oriented envelopes with two clay particles. A linking system is thus set up consisting of: particle - oriented wetting molecule - cation - oriented wetting molecule - particle.

As removal of water proceeds, an increasing proportion of cations share their water envelopes with two clay particles, and so the number of links increases. The links also become stronger, because they become shorter. In consequence, the cohesion of the clay particles increases.

Nichols (Ref. 8), applies the concept of the cohesion of moisture films to plate-shaped particles. The cohesive force of a water film between two particles is given by the formula:

$$c = \frac{K 4 \pi r T \cos \alpha}{d}$$

Where K is constant, r the radius of the particles, T the surface tension α the angle of contact between the liquid and the particle (generally assumed zero) and d the distance the particles are apart.

Then for a given size and number of particles, the cohesive force should vary inversely with the moisture content.

D. Conditions Affecting Maximum Shearing Resistance In A Clay

Many factors enter the determination and prognosis of shearing strength in a clay. These factors are often so interelated that it becomes impossible to designate their boundary conditions with any degree of accuracy. A partial list of these factors follow:

Friction Angle. It is widely recognized that the friction angle can vary over a wide range for a given soil in as much as it is not a constant soil property; independent of precompression, drainage and other variables.

Cohesion. Also recognized as a variable property which depends predominately upon grain size and shape, moisture content and mineralogical composition.

Intergranular Pressure. As another of the parameters of Coulomb's equation, intergranular pressure is perhaps most easily defined as the pressure acting normal to the surface of failure when failure is occuring.

Speed of Shear. Results of tests will be strongly affected by the amount of drainage which takes place prior to failure. Generally, the higher the rate of shear the less the amount of drainage in a cohesive soil, and a consequent reduction in shearing resistance. Plastic resistance, a phenomena related to speed at which shearing strain occurs in viscous and plastic

materials, acts to increase the instantaneous shearing strength of the soil at higher rates of speed.

Colloids. Actually, the total effect of colloidal phenomena is just beginning to unfold. Only recently has sufficient emphasis been placed on this factor as a possibility of answering some of the unexplained mysteries which are still associated with shearing strength.

Intrinsic Pressure. Previously defined, this property is the key to much of the dependable shearing strength of a cohesive soil. As shown by this thesis, the intrinsic pressure due to past loading is a dependable source of shearing strength.

Void Ratio. There has been long established a linear relationship between the void ratio and the logarithm of the compressive strength of a given clay, and therefore, since shearing stress is a function of the intergranular principal stresses and the friction angle, it too has a similar relationship. The relationship shows that as void ratio decreases strength increases.

Water Content. Water content will vary the shearing strength of a clay over a considerable range. As already shown, the addition of water to a dry soil will cause apparent cohesion which will increase the shearing strength of a moist soil to an optimum value. Beyond this value the pore spaces are completely filled and a decrease in shear strength is exhibited.

For saturated soils part of the external load is carried by the water in the voids until consolidation is complete. Since free water has no shearing strength, any increase in load will have little effect until further consolidation takes place.

Air Content. The effect of entrained air in a nearly saturated clay is complicated by the relationships between applied pressure, gas volume and shearing strength. Since gas is compressible there is a change in void ratio, because of the curvature of the bubble surface the pressure of the gas is larger than pore water pressure, and lastly there may be some gas going into solution. Consolidated-undrained shear tests have shown that a small amount of air will cause a decrease in shearing strength as compared to a fully saturated soil.

E. Types of Shear Tests

Generally shear tests are classified into three groups:

(a) Drained test (S-test or slow test): the samples are consolidated and sheared at speeds slow enough to allow complete drainage.

(b) Consolidated-undrained test (Q_c-test or quick-consolidated test): samples are consolidated and sheared under conditions of no drainage.

(c) Quick-consolidated (Q-test or quick test): sample is subjected to an applied pressure under conditions of no drainage and immediately sheared.

Using the above tests different values of c and ϕ may be expected from the same soil at any given state and load.

The variation in values is due largely to the effects of pore water pressure. Pore water pressure, (u), reduces the total intergranular stress as follows:

$$\sigma_e = \sigma - u$$

Where σ_e is the effective intergranular stress or in terms of Coulomb's equation $s = c + (\sigma - u) \tan \phi$

Testing performed in this thesis was carried out under drained conditions with the exception that the speeds were too high to permit complete drainage. Therefore, the tests would fall in a category intermediate between a true Drained Test and a Consolidated-undrained Test.

F. Effects of Preconsolidation

Investigators have shown that if a clay is completely remolded at a water content sufficient to give it a semi-liquid consistency and several samples of the mixture are consolidated under various pressures then subjected to direct shear at the same pressures, the maximum shearing stresses will occur on a straight line plotted directly proportional to the consolidation pressure. The slope of the line, which is a function of the angle of friction, will vary with the rate of shear.

Under the same conditions, but subjected to various normal stresses less than a given preconsolidation pressure, the maximum shearing stress again will occur on a straight line but at a higher value. The slope of a line plotted in this manner will be flatter than the first case.

Hvorslev (Ref. 5), reports that a family of lines plotted as in the latter case, Fig. V, for a series of preconsolidation pressures will be parallel, and that their angle with the horizontal could be considered the true angle of friction.

Hogentogler (Ref. 4), on the other hand shows that with increased consolidation pressures the so-called friction angle increases for such a plot as in Fig. VI.

Effect Of Preconsolidation Load On Shear Strength Of Clay

Showing Differences In Findings Of True Angle Of Friction And Variation Of Cohesion

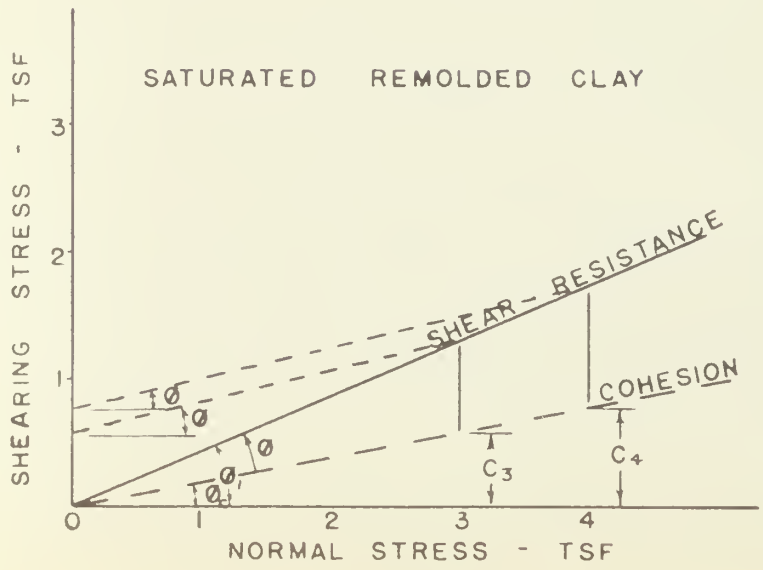

FIG. V (AFTER HVORSLEV[4])

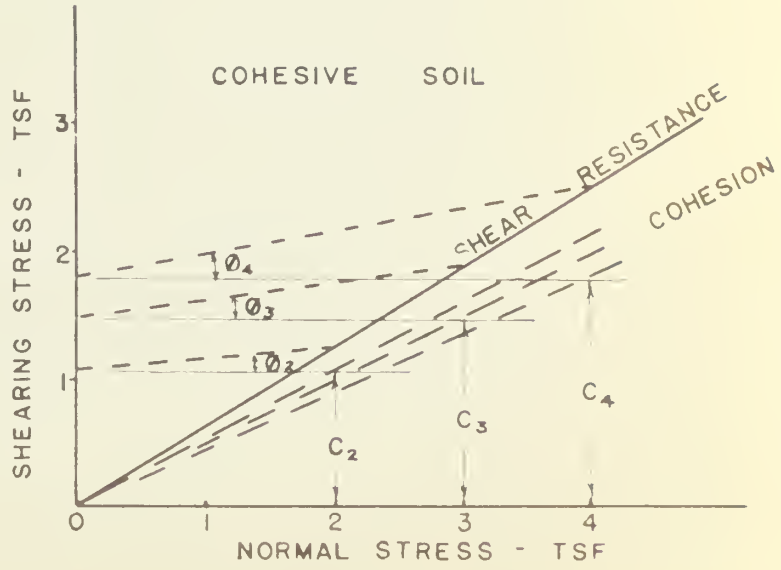

FIG. VI (AFTER HOGENTOGLER[3])

The Krey-Tiedeman formula $S = P_c \tan \phi_c + \sigma \tan \phi$ was developed from experiments similar to those of Hvorslev, where $\phi_c = \phi_1 - \phi$ shown in Fig. V. Here, for the first time, is introduced the concept that cohesion is a variable dependent upon intrinsic pressure.

Tchebotarioff (Ref. 13), indicates that the differences in the findings of Hvorslev and Hogentogler could be due to unequal opportunities for sample expansion. Such an explanation is valid from the standpoint of the theory of consolidation, but is not necessarily substantiated in light of the incomplete knowledge of conditions which existed at the time of the experiments. It will be noted that if expansion is to be considered a factor in determining shear strength, the Krey-Tiedeman formula does not satisfy this imposition.

G. The Effect of Water Content on the Strength of Clays

The state of water within the soil mass undoubtedly is the most important factor concerning the subject of water content. Free water and water existing as films imparts entirely different strengths to the soil.

For each soil there is an optimum moisture content for a specific degree of compaction at which maximum densification can be obtained. Capillary stress decreases with increase in moisture content above the optimum and, conversely, increases below the optimum value. Cohesion, however, is a maximum at the optimum moisture content.

High values of the liquid limit are indicative of a high percentage of colloids. Since cohesion varies directly with the amount of colloids due to the large total effective surface area per unit volume, the higher liquid limits also indicate higher cohesion.

H. The Effect of Rate of Shear on Clays

In drained shear tests the objective is to obtain a shearing resistance unaffected by pore water pressure. By allowing sufficient time for drainage to occur as shearing stress is applied the effects of pore water pressure are reduced. A constant rate of strain is preferred to a constant rate of stress in determining maximum shearing resistance, because of the ease with which strain can be controlled. Actually, the rate which will produce the minimum pore water pressure depends entirely upon the permeability of the sample.

Turnbull (Ref. 14), reports that a rate of strain of .007 inches per hour or less will have very little effect on the maximum shearing resistance of capillary normal pressure of a cohesive soil.

Turnbull also has found that for two rates of strain the maximum shearing resistance versus applied normal stress curves intersect at a common point characteristic for a particular soil. At lower normal stresses the curve for slower rate of strain passes below that of the faster rate. These tests were performed on samples at optimum moisture content. Therefore, a corresponding decrease in capillary normal stress resulted in slower rates of strain. Since the capillary normal stress is due to the capillary forces set up in the moisture films on the soil particles, the effect of

the increase in the rate of strain is to develop an excess resistance in the soil. For higher normal stresses a gain in maximum shearing strength at the slower rate of strain is due to the reduction of pore water pressures developed in the interstitial moisture and air by the strain set up along the plane of failure.

I. Determination of True Cohesion by Direct Shear

An initial maximum shearing resistance curve for a cohesive soil is established by shear tests at several vertical loads, represented by the line A_1A_4 in Fig. VII. A_1A_4 is then extrapolated to meet the abscissa at O'. The intrinsic pressure in the material is thus represented by O'O. The value of OA, commonly assumed to be cohesion, actually is comprised of true cohesion and internal friction.

To find the value of true cohesion additional tests are required on preconsolidated samples. For example, specimens are loaded to a value of N_4 then sheared at lesser values of N, thus establishing the curve A_4A_1' which is extrapolated to C'_4. The value of $O'C'_4$ represents the true cohesion and whose angle with the horizontal represents the true angle of internal friction.

Coulomb's equation can then be written as $S_n = O'C'_n + (OO' + ON_n \tan \phi)$ for a particular value of vertical load.

The ordinate distance between lines A_OA_4 and $A_O'A_4$ represents the increase of true cohesion due to an increase of vertical load, hence the value OC'_4 is the true cohesion under a vertical load N_4.

Similarly, for any value of preconsolidation corresponding curves can be drawn to obtain the true cohesion for the preconsolidation load required.

Since the ordinate value $O'C'_4$ represents true cohesion under vertical load N_4 it can be represented on the ordinate A_4N_4 as C_4N_4 and the line $O'C_4$ is the true cohesion curve for the preconsolidation load N_4.

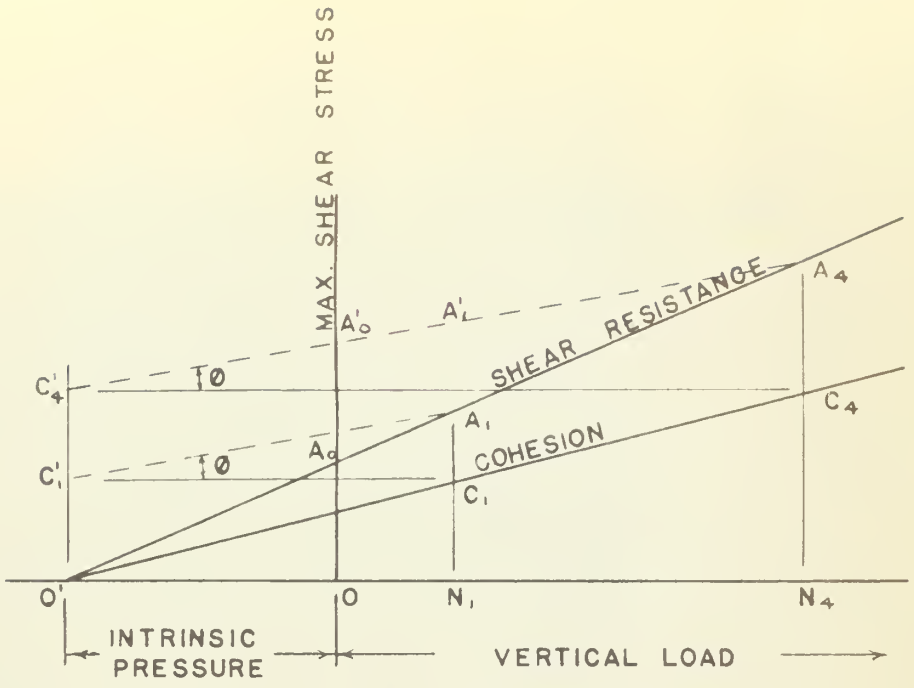

FIG. VII SHEARING RESISTANCE OF COHESIVE SOIL

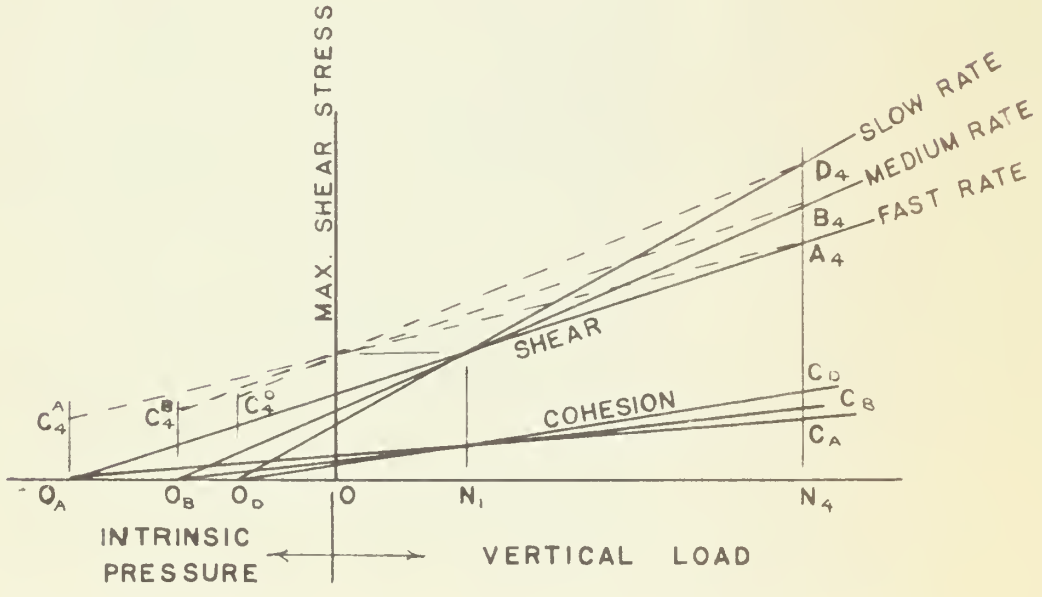

FIG. VIII RELATIONSHIP BETWEEN SHEARING RESISTANCE AT VARIOUS RATES OF STRAIN AND TRUE COHESION

PART III

APPARATUS

A. Constant Rate of Strain Direct Shear Machine

The direct shear apparatus used herein consisted of a round brass cylinder 2½ inches in diameter split horizontally at the level of the center of the soil sample which was held between metal grills fastened to porous plates. A vertical load applied to the same by means of dead weights caused a pressure across the plane of rupture between the upper and lower parts of the cylinder. Gradually increasing the horizontal load applied to the upper part of the box caused failure along the rupture plane. The ultimate shear stress at failure is obtained by dividing the maximum horizontal load by the cross-sectional area of the sample.

Figure IX shows the Soiltest Model D-110 Direct Shear Machine manufactured by Soil Testing Services, Evanston, Illinois.

B. Consolidometer

Figures X and XI show the Soilest Model C-280 Loading Frame with an 8:1 lever arm ratio, and the two Soilest Model C-251 Consolidometer Rings also manufactured by Soil Testing Services, Evanston, Illinois which were used in this experiment.

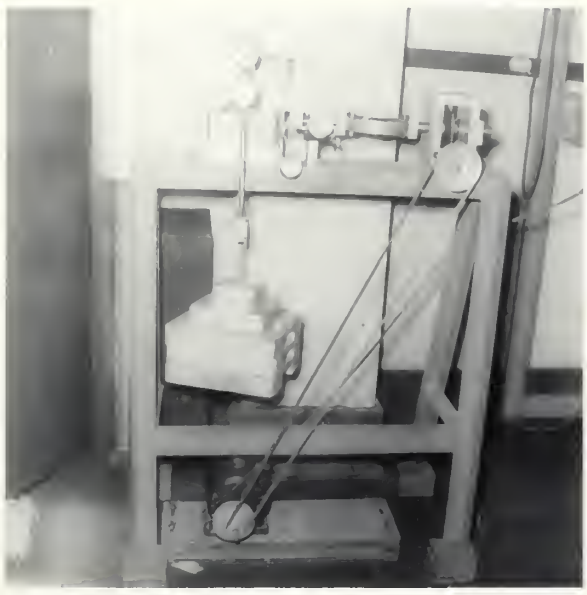

Fig. IX Direct Shear Machine with 2 tons per square foot vertical load

Fig. X Consolidometer

C. Preload Apparatus

To expedite the test schedule eight preloaders, shown in Figures XII and XIII were fabricated, each consisting of:

1 Lucite Tube, 2½" i.d.,2-3/4" o.d.
3 inches long

2 Plaster of Paris Plates, 2½" dia.,
½" thick with 1/16" dia. holes for
drainage

1 Follower, 2" dia. Croloy Type 347
Thin Wall Tubing, 3 inches long

1 Copper dish, 3½" dia.

1 Stand

1 Loading Platform, 3/4" plywood 4"x12"

1 Set of weights consisting of 5 lb. and
10 lb. steel plates, 25 lb. bag of lead
shot, and 2lb. lead shot container

D. Mixing Apparatus

Figure XV shows the mixing apparatus consisting of:

1 Universal Mixer

1 Spatula

1 Mixing Bowl

2 Battery jars

Fig. XI Rear view of consolidometer with direct shear machine in rear

Fig. XII View of preload apparatus

Fig. XIII Close up of preload cylinder

Fig. XIV Mixing Apparatus consisting of Universal Mixer and bowl, two battery jars, and Spatula. Preload cylinders and plaster of paris porous plates also shown.

PART IV

MATERIAL - ILLITE

A. Description

Illite, variously called hydromica, potash clay mineral or even illidromica, is a term proposed by Grim (Ref. 3), Bray and Bradley as a general term to include the mica-like clay minerals which have a 10-A c-axis spacing and substantially no expanding lattice characteristics. The general formula is $(OH)_4 K_y(Si_{8-y} \cdot Al_y)(Al_4 \cdot Fe_4 \cdot Mg_4 \cdot M_{g6})O_{20}$ where y is frequently equal to 1.0 to 1.5. Both biotite and muscovite crystallizations may occur, likewise dioctahedral and trioctahedral types.

Characteristically, the illites are small, poorly defined flakes (30A thick, 0.1-0.3 micron in diameter) commonly grouped together in irregular aggregates. A distinct hexagonal outline may show in some illites, whereas no such evidence is exhibited in others.

B. Occurrence

Illite is found in sedimentary and hydrothermal deposits and to a limited extent in metamorphic deposits and occurs in a wider range of soils than generally supposed as apparent from the following list:

a. In red and grey podsolic soils usually in quantities up to 10%.
b. In prairies soils formed under grass cover in the northern hemisphere.
c. Dominant in Chernozem soils formed under grass cover with 12-25 inches annual rainfall and cool climate.
d. Dominant in California desert soils.
e. Occasionally found in red and yellow podsols in small quantities.
f. Occurs in varying amounts in Planosols and Rendzina soils.
g. Generally predominate in arid soils together with montmorillonite.
h. Abundant in deep-sea clays of recent origin possibly formed by alteration of montmorillonite in sea water.
i. Alluvium deposits of Mississippi River and its tributaries show a dominace of illite as compared to other clay minerals.

j. Glacial deposits of unweathered till and loess are dominated by illite.

k. Pre-Mesozoic sediments are composed largely of illite and chlorite types of clay minerals.

l. Dominant clay mineral in most shales and slates.

m. Present in limestones and dolomites.

Illite is formed from the weathering of feldspar, disintegration of muscovite and alteration of montmorillonite.

C. Source of Material

The material used for testing was purchased from the Illinois Clay Products Company, Joliet, Illinois, who claim exclusive production under the trade name Grundite Bond Clay. Grundite is a high strength high permeability bond for foundary sand and possesses great durability.

Kerr and Kulp (Ref. 6) locate the source as follows: "Clay occurs in a clay pit of the Illinois Clay Products Co. in the Goose Lake area northwest ½ northeast, ¼ section 11 township 33N, Range 83 about 7 miles east of Morris in Grundy County, Illinois".

The "Grundite" layer of clay lies above three underclays separated by three minor coal seams. Its origin dates to cyclothemic activity of early Pennsylvanian time.

The impurities of samples tested Kerr, Main and Hamilton (Ref 6) showed impurities on the order of 10%: 3% pyrite, and 2% each of quartz, sericite, limonite and plagioclase. A quantitative X-ray Diffraction examination of the samples used in this experiment showed a higher precentage of impurities.

D. Properties

A sieve analysis is shown in Fig. XV

Specific Gravity: 2.76

Liquid Limit: 60%

Plastic Limit: 32%

Plastic Index: 28%

Void Ratio before consolidation: 2.53

Void Ratio after 4 tons/sq.ft. consolidation: .97

Percent Air Content of saturated sample before consolidation: 1.98%

Percent Air Content of saturated sample after 4 tons/sq.ft. consolidation: no measurable quantity.

Grading Curve For Illite

FIG. XV

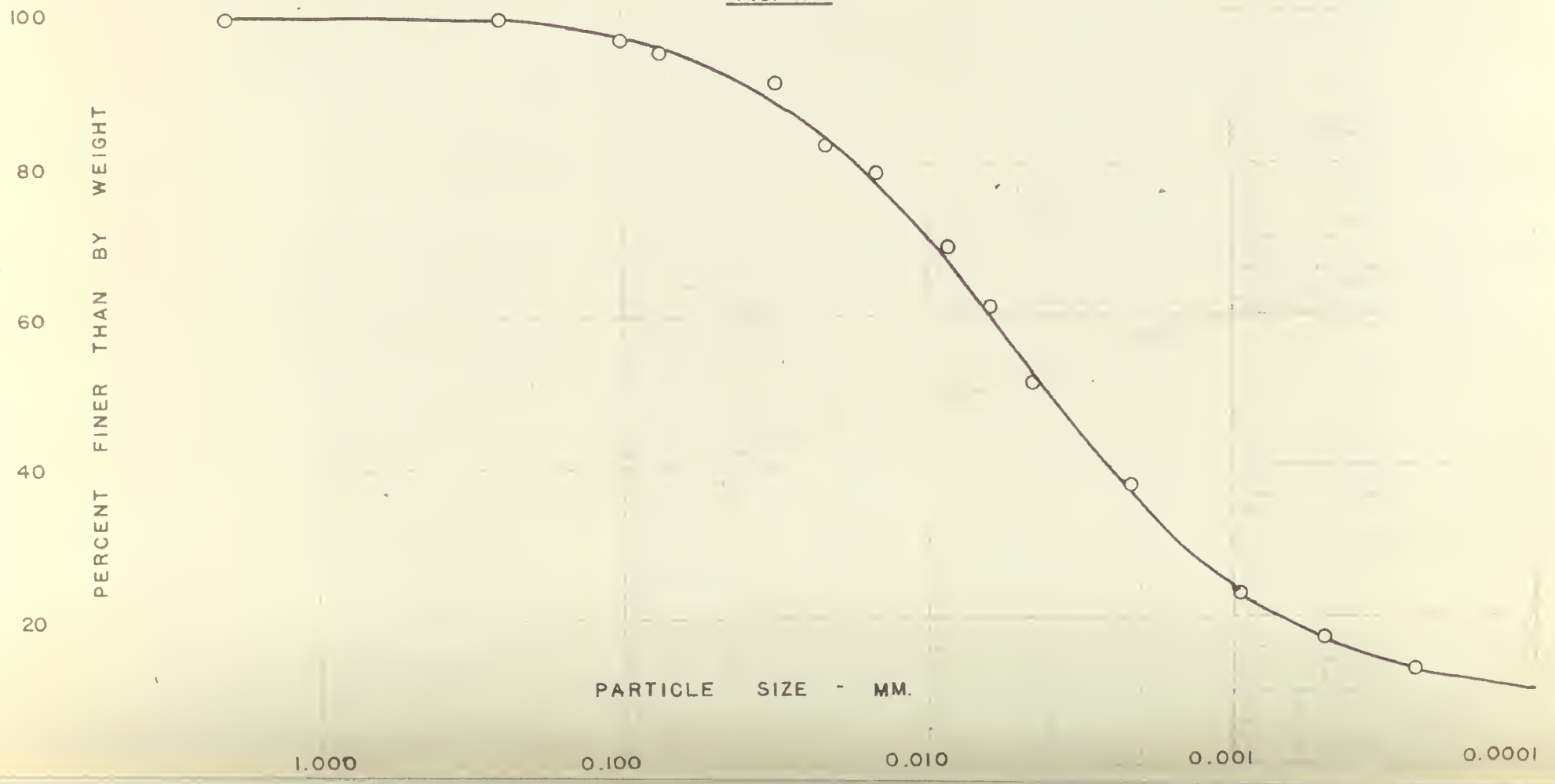

E. X-Ray Diffraction

1. Qualitative

An X-ray diffraction strip chart was run on the test Illite sample from the (2 θ) angle of 10^{o} to 70^{o} . (Fig. XVI) This chart shows the major peak intensities that are characteristic of the type material and locates their (2 θ) angles. Application of the Bragg equation $n\lambda = 2d\sin\theta$ then gives the "d" or lattice spacing for each intensity peak.

By comparison, this strip chart is nearly identical to the strip chart of standart Morris, Illinois illite since the characteristic peaks are the same. The only variance is a slightly less intensity of the peak in the test illite. This leads to the conclusion that the test illite is a Morris, Illinois illite but of a higher percentage of impurities.

2. Quantitative

Having classified the test illite, it was then possible to plot a calibration curve using the standard Morris, Illinois and an internal-standard (Zinc Sulfite) mixed by weight ratio (G_I/G_S) - where

G_I= weight of Standard Morris Illite clay

G_S= weight of internal standar (Zinc Sulfite)

Diffraction strip charts were then run for

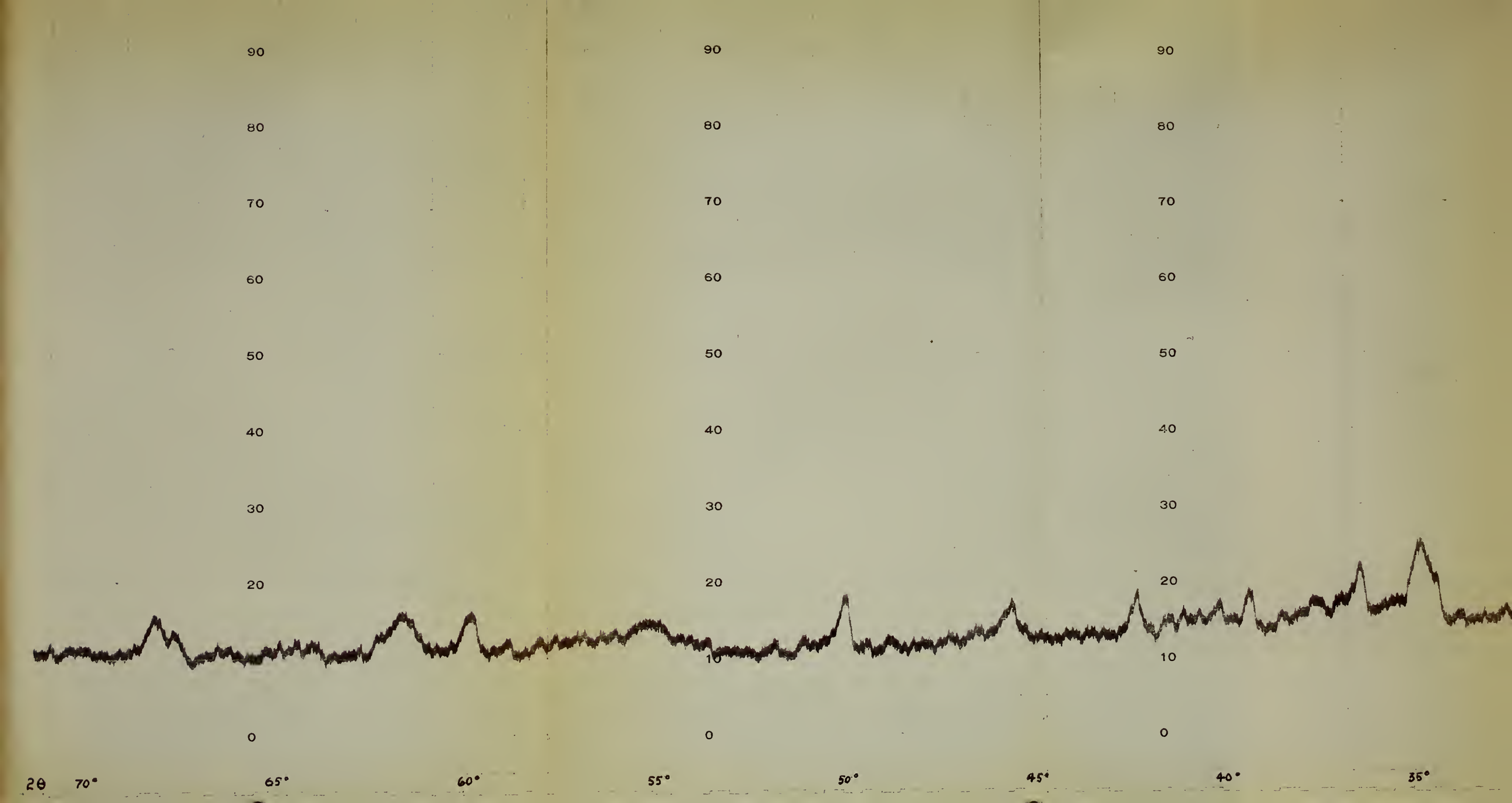
90
80
70
60
50
40
30
20
10
0
2θ 70° 65° 60° 55° 50° 45° 40° 35°

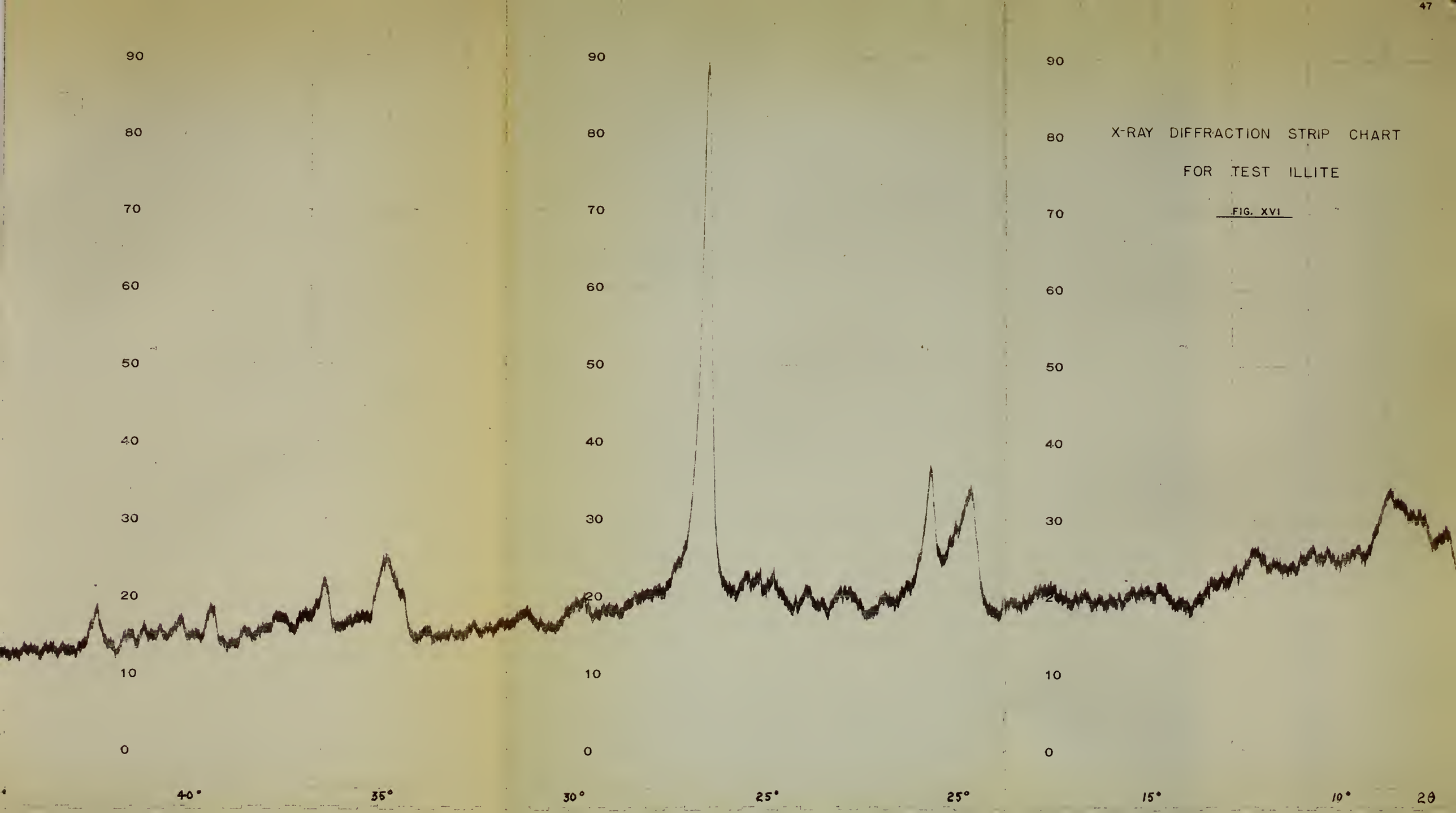

X-RAY DIFFRACTION STRIP CHART

FOR TEST ILLITE

FIG. XVI

these mixtures and the relative peak heights observed (H_I/H_S) - where H_I= height of Standard Morris Illite

H_S= height of internal standard peak.

The calibration curve was then plotted as (G_I/G_S) vs (H_I/ H_S) (Fig. XVII).

To obtain the quantity of test illite using this curve, a mixture of 1 gram test Illite, 1 gram Standard, 1 gram Diluent was prepared and a diffraction strip chart run (Fig. XVIII). The resulting H_I/H_Sratio was then plotted on the calibration curve and the resulting percent of illite, as can be seen from the dash line on the enclosed curve, is shown to be 84%. The test illite is then approximately 84% of the Standard Morris, Illinois illite and 16% foreign material. Since Kerr & Kulp (Ref. 6) found 10% impurities in the Standard Morris illite, then the test illite contains approximately 75% illite and 25% foreign material.

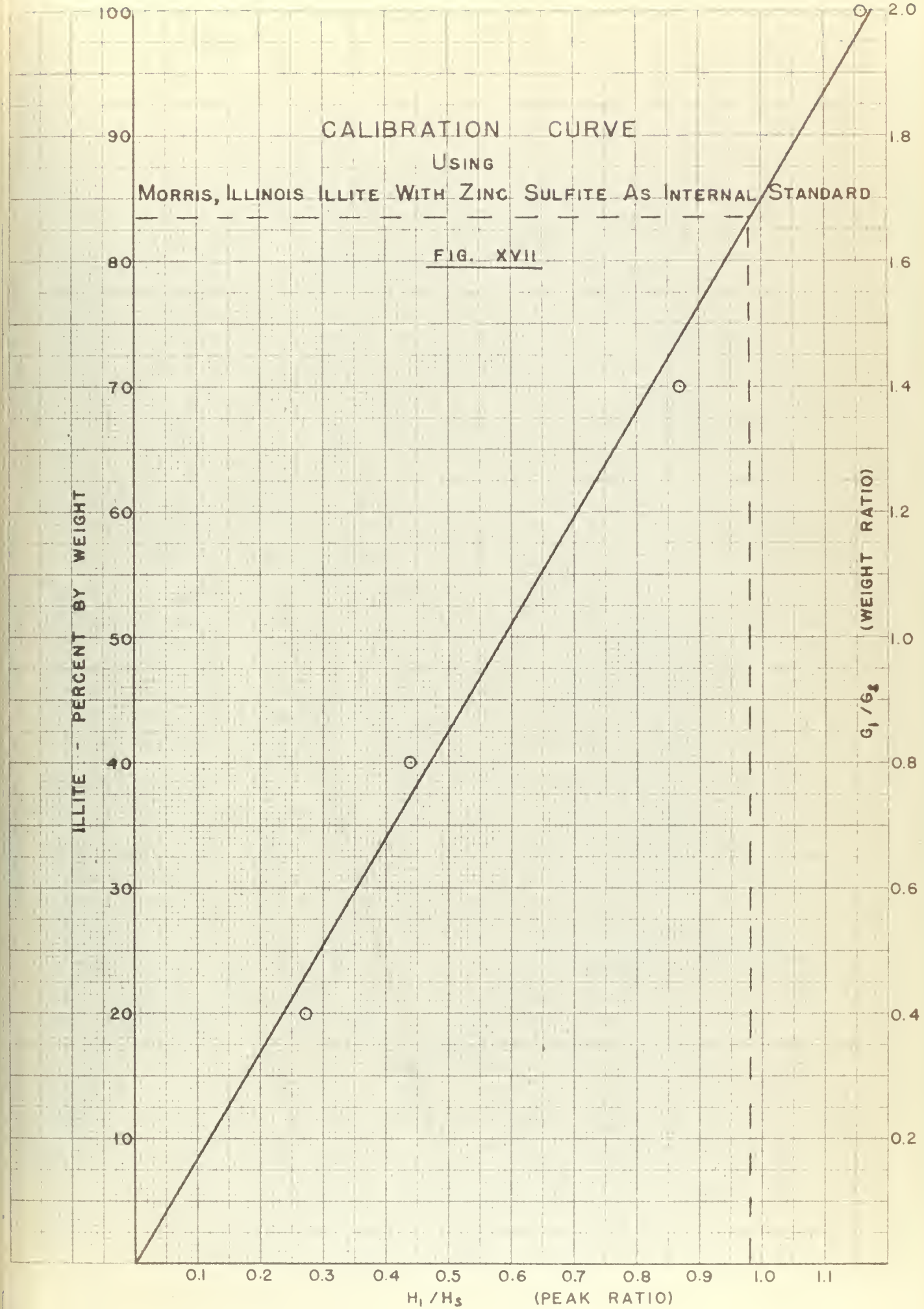
CALIBRATION CURVE
USING
MORRIS, ILLINOIS ILLITE WITH ZINC SULFITE AS INTERNAL STANDARD
ILLITE - PERCENT BY WEIGHT
100
90
80
70
60
50
40
30
20
10
2.0
1.8
1.6
1.4
1.2
1.0
0.8
0.6
0.4
0.2
G_I / G_S (WEIGHT RATIO)
0.1
0.2
0.3
0.4
0.5
0.6
0.7
0.8
0.9
1.0
1.1
H_I / H_S (PEAK RATIO)

FIG. XVII

X-RAY DIFFRACTION STRIP CHART FOR QUANTITATIVE ANALYSIS

FIG. XVIII

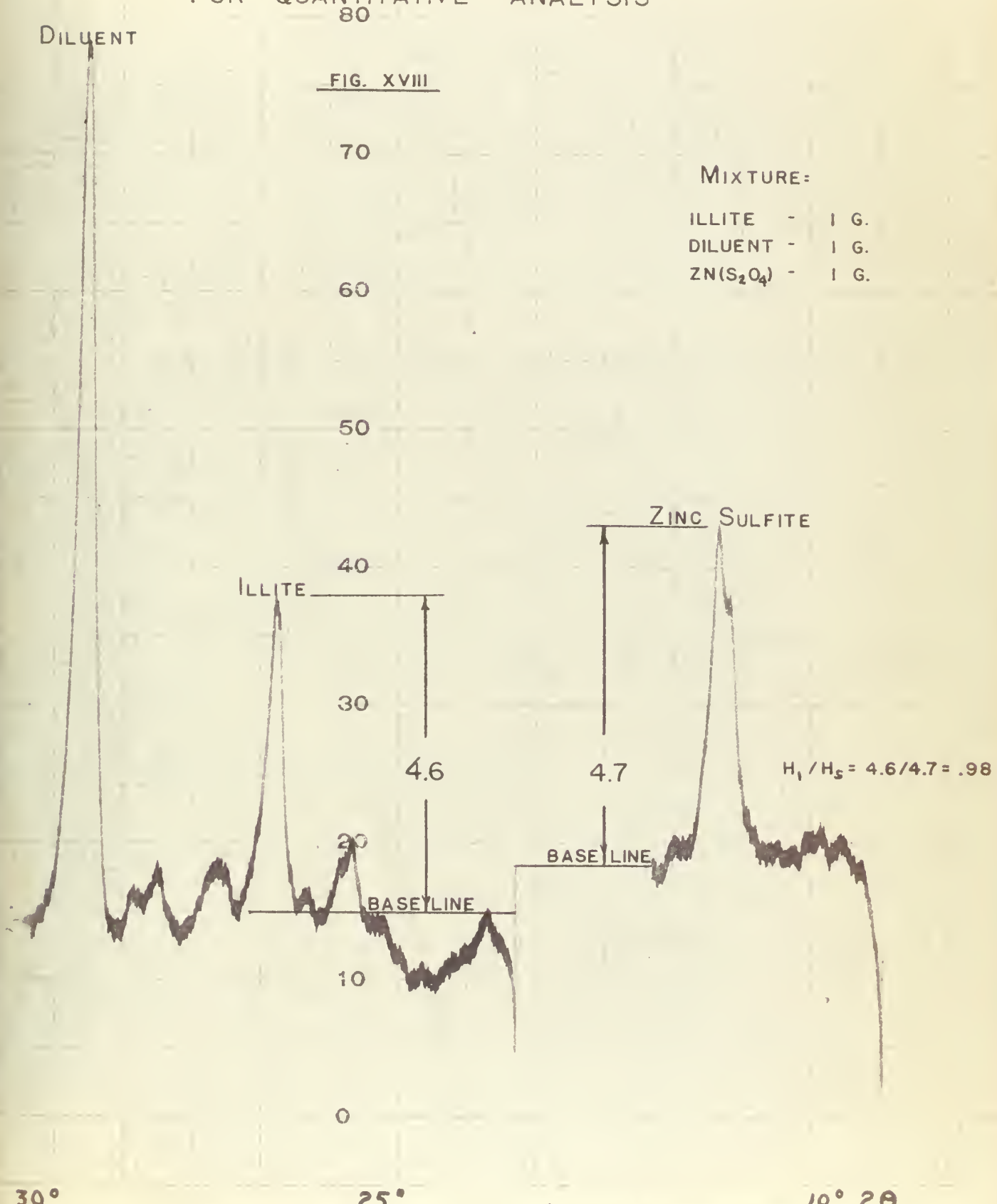

F. Differential Thermal Analysis

1. General Characteristics

Characteristic differential thermal curves for illite have three endothermic reactions with peaks occurring about 140°-180°, 550°-650° and 850° to 950° centigrade. Also, an exothermic peak frequently occurs between 900°-1000° centigrade. The height and temperature interval of the second endothermic peak varies with different samples as similarly the final portion of the curve.

In general, the first endothermic reaction is taken as the loss of the water held between the basal planes of the lattice structure; the second endothermic reaction is the loss of lattice water; while the third endothermic reaction is associated with the final destruction of the illite structure. The exothermic reaction is associated to some extent with the formation of spinel.

2. Characteristics of Test Sample

The test illite follows the typical curve with endothermic peaks at 165°, 575°, and 900° centigrade. A large exothermic reaction occurred from 300° to 540° centigrade. This range is also the range at which the oxidation reactions of organic materials occur.

To determine whether organic material was pre-

sent a differential thermal analysis was made in a helium atmosphere. Organic material heated in such a medium cannot obtain oxygen necessary for combustion and theoretically would not show the exothermic reaction which appears when run in air. A comparison of the curves in Fig. XIX indicates that organic material was present.

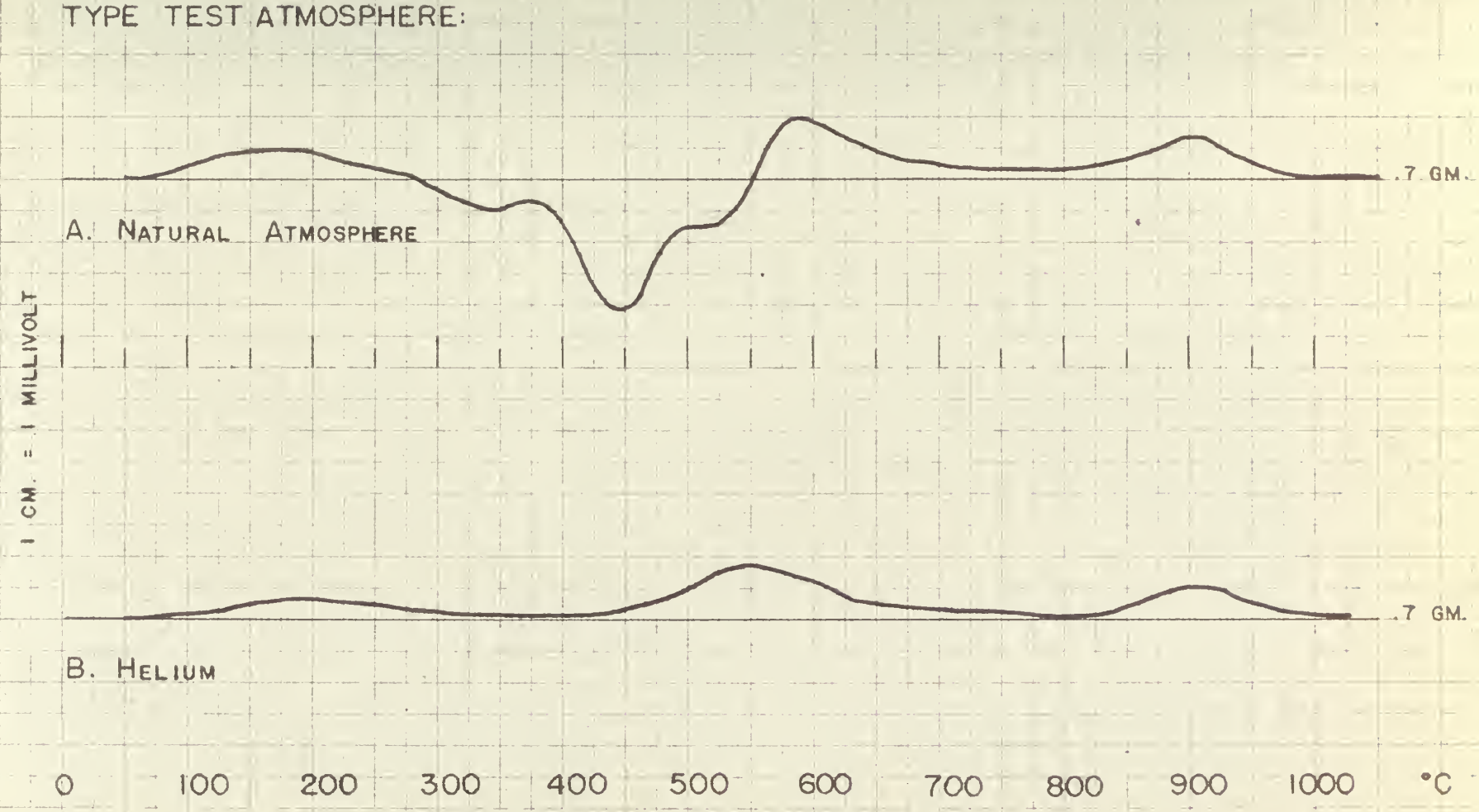

DIFFERENTIAL THERMAL CURVES FOR

MORRIS, ILLINOIS ILLITE

FIGURE XIX

PART V

METHOD OF PROCEDURE

A. Sample Preparation

Illite was mixed with distilled water for 30 minutes with the Universal Mixer at a moisture content of approximately 85%, then placed in two battery jars and allowed to stand completely covered with water for a period of at least 48 hours. Prior to loading in the preload apparatus, the material was again mixed for 30 minutes after drawing off the excess water.

The sample then was placed in the preload apparatus with a spatula using extreme care to prevent incorporating air voids. At a moisture content above 80% there was little difficulty in attaining a uniform mixture comparatively free of air voids.

Each sample was then loaded to $\frac{1}{4}$ tons/sq.ft. and allowed to consolidate for 24 hours. Thereafter, the sample was loaded in accordance with the test schedule through successive loads of $\frac{1}{2}$, 1 and 2 tons/sq.ft. Upon reaching the ultimate load in the preload apparatus the sample was removed and placed in a consolidometer under the same load as last attained in preloading. For example, if the sample had been subjected to $\frac{1}{2}$ tons/sq.ft. in preloading it was placed in the consolidometer at that load, and held there until secondary consolidation was evidenced by a consolidation

rate of 1/10,000" per hour.

Preloading was restricted to a maximum of 2 tons/sq.ft. because of heavy direct dead loads involved and the limitations of the apparatus. The preload samples were tended daily for the purpose of replenishing the water in the copper dish and in the tube, thus keeping them submerged at all times.

As soon as secondary consolidation began the sample was loaded to the next higher increment or placed in the direct shear machine as called for by the test schedule.

B. Shear Test

Standard procedure was used for direct shear. Two rates of strain, .02 in/min and .003 in/min were used in this experiment. In most cases the amount of shear strain was limited to 0.25 inches since the peak point in every test was reached earlier, and because there is some doubt as to the value of data beyond a strain of .25 inches due to the reduction of shear area of the sample and the effects of cohesion between clay and the upper and lower frames of the shear box.

The first series of tests, which established the maximum shearing resistance curves at the two rates of strain, consisted of consolidating and shearing two samples at each vertical load of $\frac{1}{4}$, $\frac{1}{2}$, 1, 2 and 4 tons/sq.ft.

A second series, similarly consisting of two samples each and preconsolidated to 4 tons/sq.ft., was sheared at vertical loads of $\frac{1}{4}$, $\frac{1}{2}$, 1 and 2 tons/sq.ft. respectively.

The third series was preconsolidated to 2 tons/sq.ft and sheared at $\frac{1}{4}$, $\frac{1}{2}$ and 1 tons/sq.ft. respectively. Lastly, a fourth series was preconsolidated to 1 ton/sq.ft. and sheared at $\frac{1}{4}$ and $\frac{1}{2}$ tons/sq.ft.

Moisture content was determined for each test after shear by taking a specimen from the center portion of the sheared sample.

The test schedule is shown in Table I. It will be noted that time effects were minimized by the systematic use of the two consolidometers.

TABLE I

Test Schedule Showing Load and Date Applied

Date	Vertical Load and Test Rate		Consolidometer Number		Preload Apparatus Number							
April	.02 in/min	.003 in/min	1	2	1	2	3	4	5	6	7	8
22			¼	¼								
23					¼	¼	¼	¼	¼	¼	¼	¼
24												
25	¼	¼	¼	¼								
26			½	½	¼	¼	½	½	½	½	½	½
27	½	½	½	½			¼	¼				
28			1	1					1	1	1	1
29	1	1	1	1	½	½	½	½	¼	¼		
30			2	2								
31	2	2	2	2	1	1	1	1	½	½	¼	¼
May												
1			4	4								
2					2	2			1	1	½	½
3	4	4	2	2	¼	¼	2	2				
4			4	4								
5	2	2	2	2	½	½	¼	¼	2	2	1	1
6			4	4								
7	1	1	2	2	1	1	½	½	¼	¼	2	2
8			4	4								
9	½	½	2	2	2	2	1	1	½	½	¼	¼
10			4	4								
11												
12												
13												
14	¼	¼	2	2	¼	¼	2	2	1	1	½	½
15	1	1	2	2	½	1	¼	¼	2	2	1	1
16	½	½	2	2	1		½	½	¼	¼		
17	¼	¼	1	1			1	1	½	½	¼	¼
18	½	½	1	1								
19	¼	¼	2	1								
20	1	½										
21												
22			2									
23	½		¼									
24	½		½									
25			1									
26			2									
27	1											

Note: Loads in tons per square foot.

PART VI

RESULTS

A. Comparison With Proposed Laws

Considerable disagreement with the six laws proposed by Turnbull is evidenced by the data in this series of tests. From Fig. XXV the following statements are shown:

Law: 1. Proportionality between capillary normal stress and rates of strain.

Results showed that with a decrease in the rate of strain the intrinsic pressure increased, in other words a reversal of the law.

2. Unique point of intersection for the curves representing maximum shearing resistance at each rate of strain.

The two test curves diverge slightly without intersecting, for any projection of positive values of maximum shearing resistance.

3. Unique point of intersection, at same maximum shearing resistance as the unique point of Law 2, of curves representing the solution of Coulomb's equation for a particular applied normal stress at each rate of strain.

Since there was no intersection in Law 2, it follows that this condition could not satisfied.

4. Unique point of intersection for the cohesion curves at each rate of strain.

   The cohesion curves intersect to the left of the origin at a shearing resistance of 0.01 tons/sq.ft. and an intrinsic pressure of 0.16 tons/sq.ft.; whereas, Turnbull implies that they should intersect to right of the origin at the same value of vertical load as the intersection of the curves for Law 2.

5. Magnitude of true cohesion and true internal friction for any particular value of maximum shearing resistance is the same at each rate of strain.

   This means that if a point selected on one maximum shearing resistance curve is projected horizontally to another maximum shearing resistance curve, the corresponding values of true cohesion should be equal. The discrepancy on this point is quite large. The geometry of Fig. XXV disallows any possibility of the equality to exist.

6. Angle of internal friction at each rate of strain has a constant value for all normal stresses.

At the .02 in/min rate of strain there is close agreement, the values being 5° at 4 tons/sq.ft., $6\frac{1}{2}^{\circ}$ at 2 tons/sq.ft., and 5° at 1 ton/sq.ft.

For the .003 in/min rate, however, there is a clear trend to decrease the angle of internal friction from 14° to 11° with the increase in preconsolidation from 1 ton/sq.ft. to 4 tons/sq.ft.

B. General Findings

1. Cohesion

   a. Proportional to vertical load at both rates of strain. (Fig. XXIV)

   b. Proportional to rate of strain. (Fig. XXV)

2. Maximum Shearing Resistance

   a. Wide degree of scattering for vertical loads less than 0.5 tons/sq.ft. (Fig. XXV)

   b. For preconsolidation at 4 tons/sq.ft. there is a definite trend to fall off the straight line when sheared at vertical loads of less than 1 ton/sq.ft. shown by solid lines on back curves in Fig. XXIV.

   c. Varies inversely with rate of strain.

   d. Composite plots of the shearing resistance curves at various perload conditions, given in the Appendix, are shown in Figures XX, XXI, XXII and XXIII.

3. Intrinsic Pressure

   a. Varies inversely with rate of strain. (Fig. XXV)

4. Angle of Internal Friction

   a. Varies inversely with rate of strain. (Fig. XXIV)

b. Relatively constant for rate of strain of .02 in/min. (Fig. XXIV)

c. Varies inversely with preconsolidation load at a rate of strain of .003 in/min. (Fig.XXIV)

5. Moisture Content

a. Relationship to vertical load, Fig.XXVI, shows higher moisture content at higher rate of strain.

b. The moisture content on the unloaded curves drops below the moisture content value for full preload at the faster rate of strain, then rises.

c. Figure XXVII shows the relationship to maximum shear strength. It is obvious from this plot that moisture content has considerable variance within a small range. However, the points approximate a straight line for the maximum shearing resistance curve, as well as the unloaded curves. The pattern of average slopes for the latter show a close degree of uniformity.

d. The entire span of moisture content at maximum shear strengths for preconsolidation between $\frac{1}{4}$ and 4 tons/sq.ft is

only 20%, and falls between 31.5% and 51.5%.

6. Compression and Expansion during Shear

a. Compression was greater at the slower rate for the maximum shearing resistance curve in all instances.

b. For the unloading curve at 4 tons/sq.ft. preconsolidation, there was expansion in every test, except for a vertical load of 2 tons/sq.ft., at the faster rate. There was no clear trend as to relative amounts of expansion at either rate.

c. For the unloading curves at 2 tons/sq.ft. and 1 ton/sq.ft. preconsolidation, the magnitude of expansion was greater for the faster rate at maximum shear resistance.

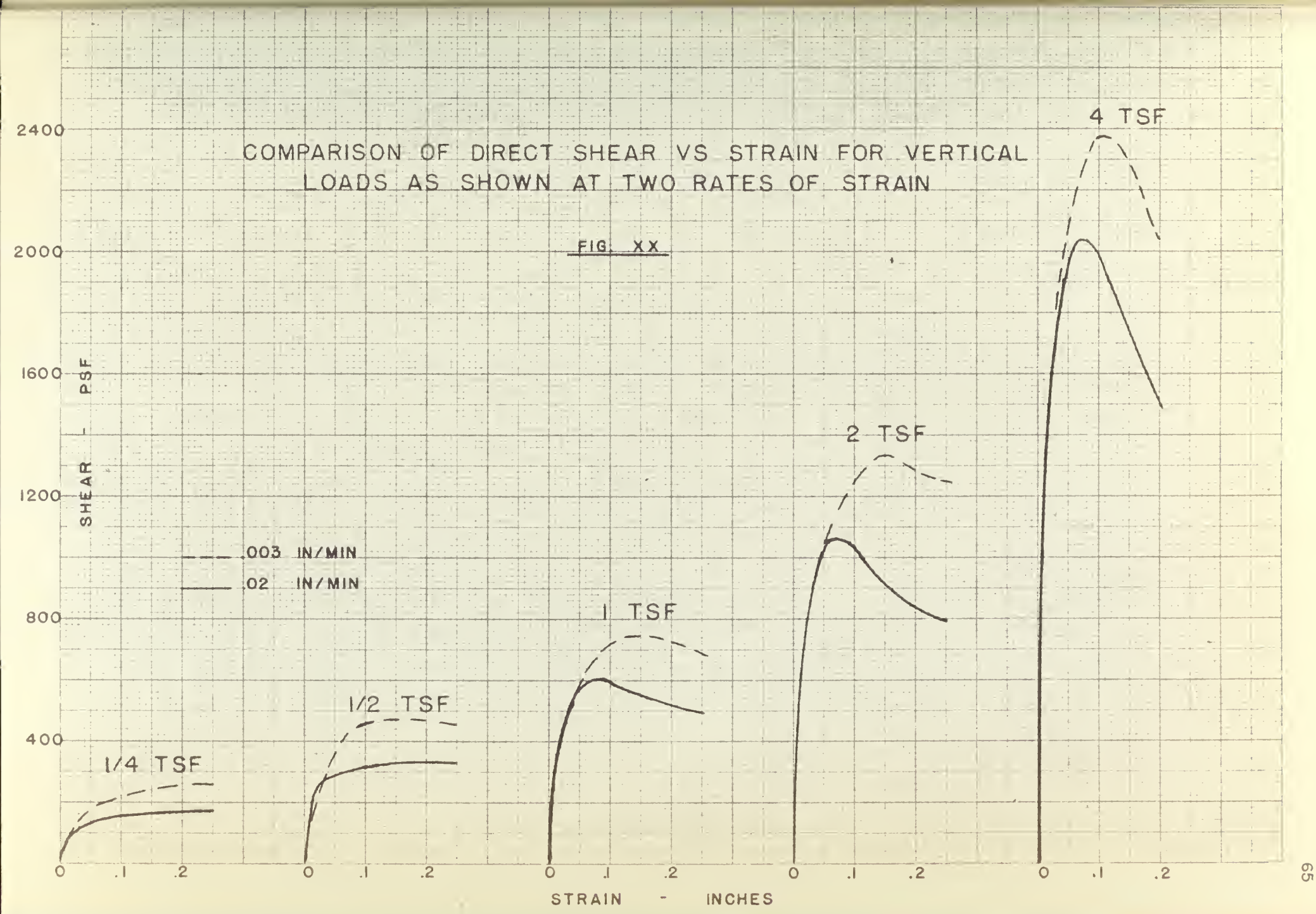
COMPARISON OF DIRECT SHEAR VS STRAIN FOR VERTICAL LOADS AS SHOWN AT TWO RATES OF STRAIN
FIG. XX
SHEAR - PSF
2400
2000
1600
1200
800
400
.003 IN/MIN
.02 IN/MIN
1/4 TSF
1/2 TSF
1 TSF
2 TSF
4 TSF
0
.1
.2
STRAIN - INCHES

COMPARISON OF DIRECT SHEAR VS STRAIN FOR VERTICAL LOADS AS SHOWN AFTER 4 TSF PRELOAD AT TWO RATES OF STRAIN

FIG. XXI

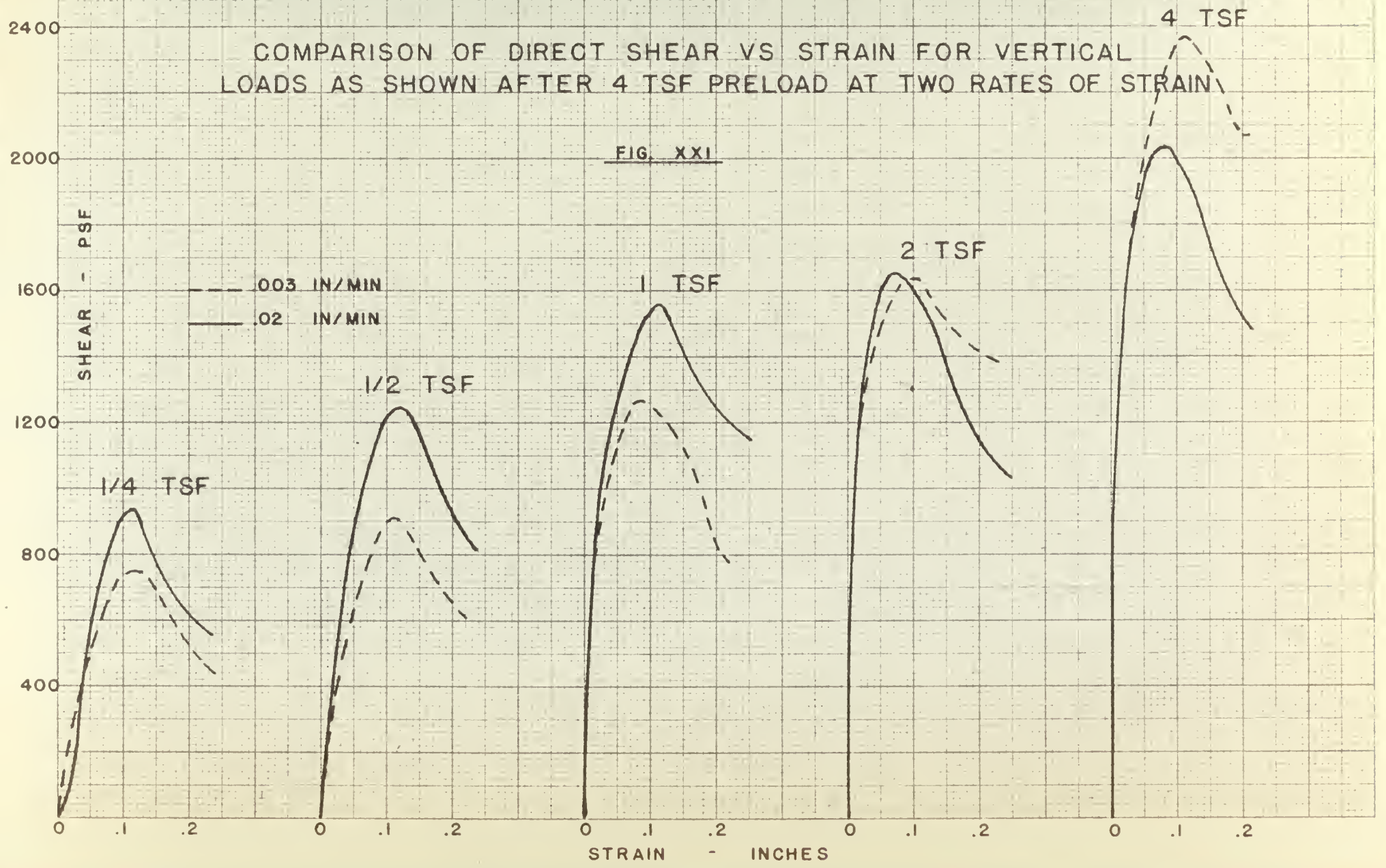

COMPARISON OF DIRECT SHEAR VS STRAIN FOR VERTICAL LOADS AS SHOWN AFTER 2 TSF PRELOAD AT TWO RATES OF STRAIN

FIG. XXII

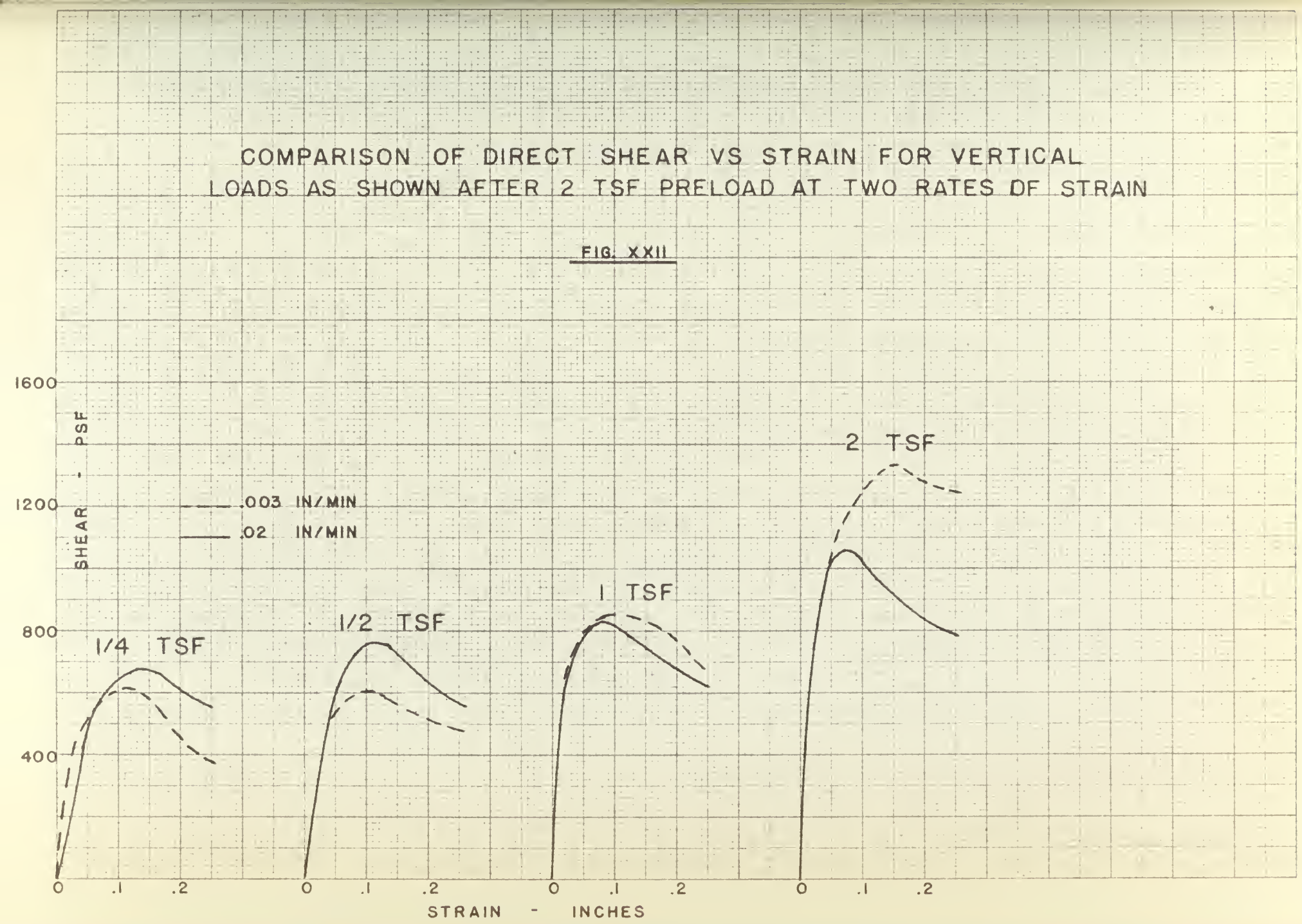

COMPARISON OF DIRECT SHEAR VS STRAIN FOR VERTICAL LOADS AS SHOWN AFTER 1 TSF PRELOAD AT TWO RATES OF STRAIN

FIG. XXIII

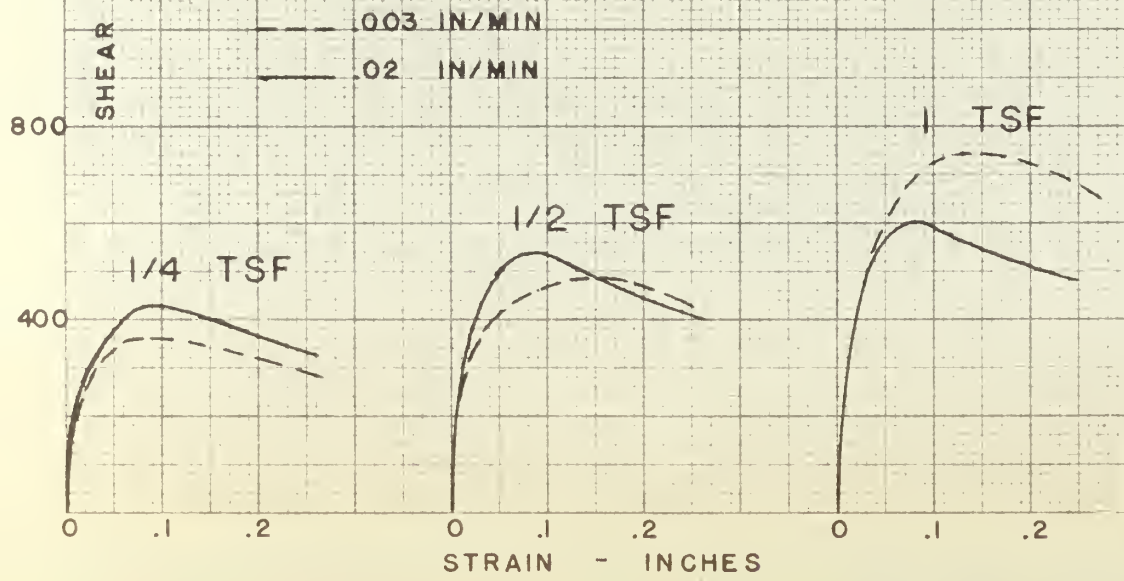

Relation Of Shearing Resistance And Cohesion

FIG. XXIV

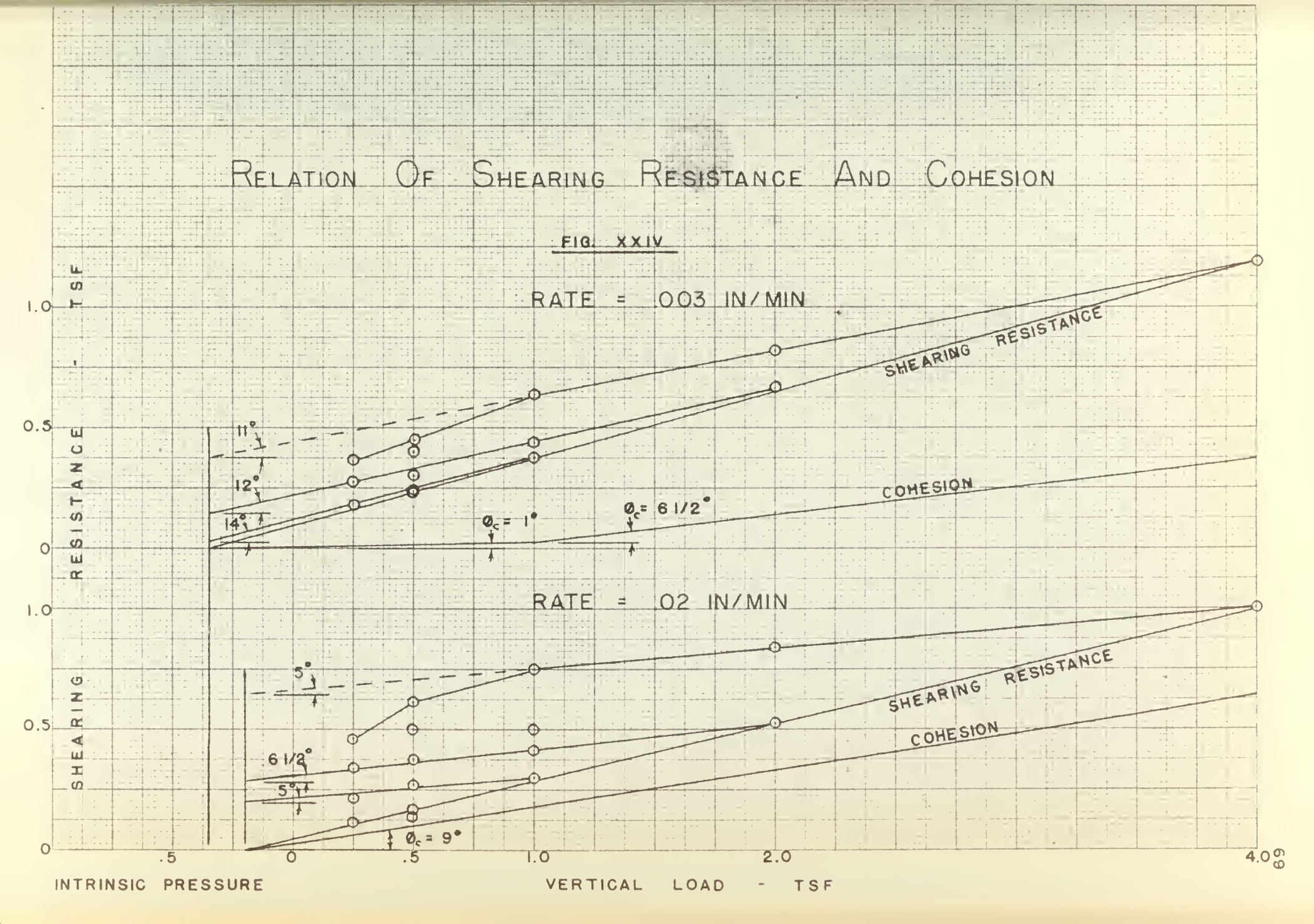

Relation Of Shearing Resistance And Cohesion At Two Rates Of Strain

FIG. XXV

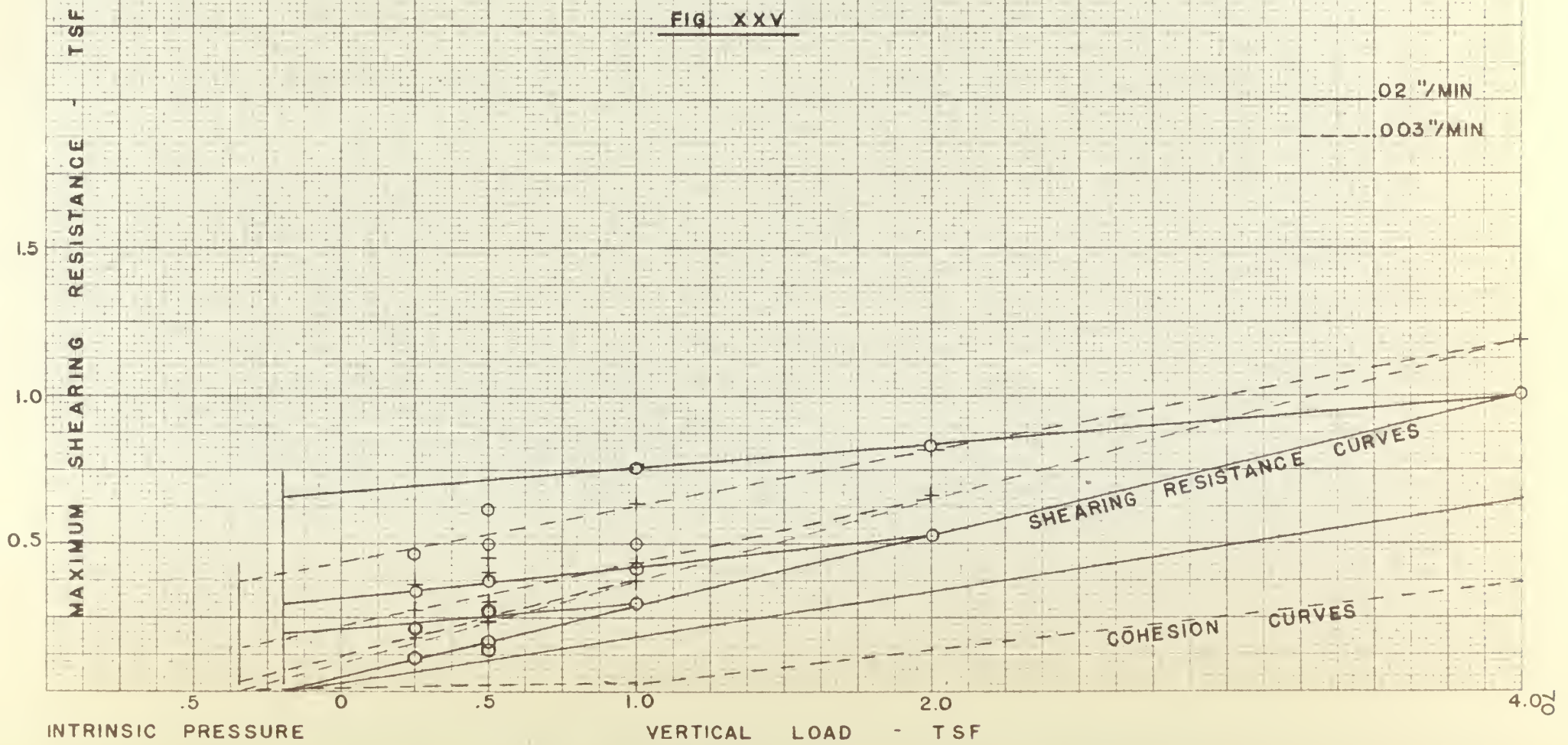

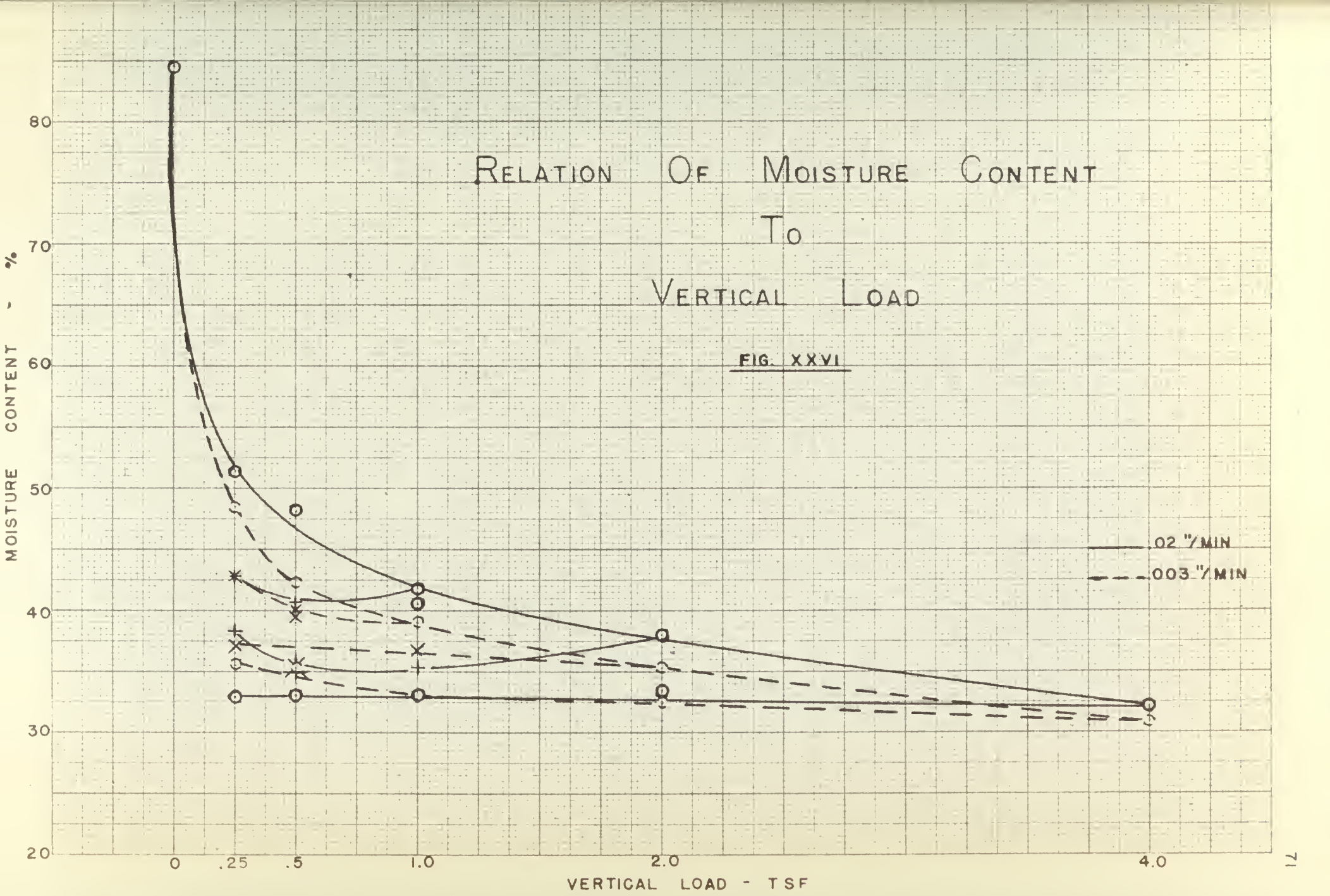
RELATION OF MOISTURE CONTENT
TO
VERTICAL LOAD
FIG. XXVI
MOISTURE CONTENT - %
80
70
60
50
40
30
20
0
.25
.5
1.0
2.0
4.0
VERTICAL LOAD - TSF
.02 "/MIN
.003 "/MIN

Relation Of Moisture Content To Shear Strength

FIG. XXVII

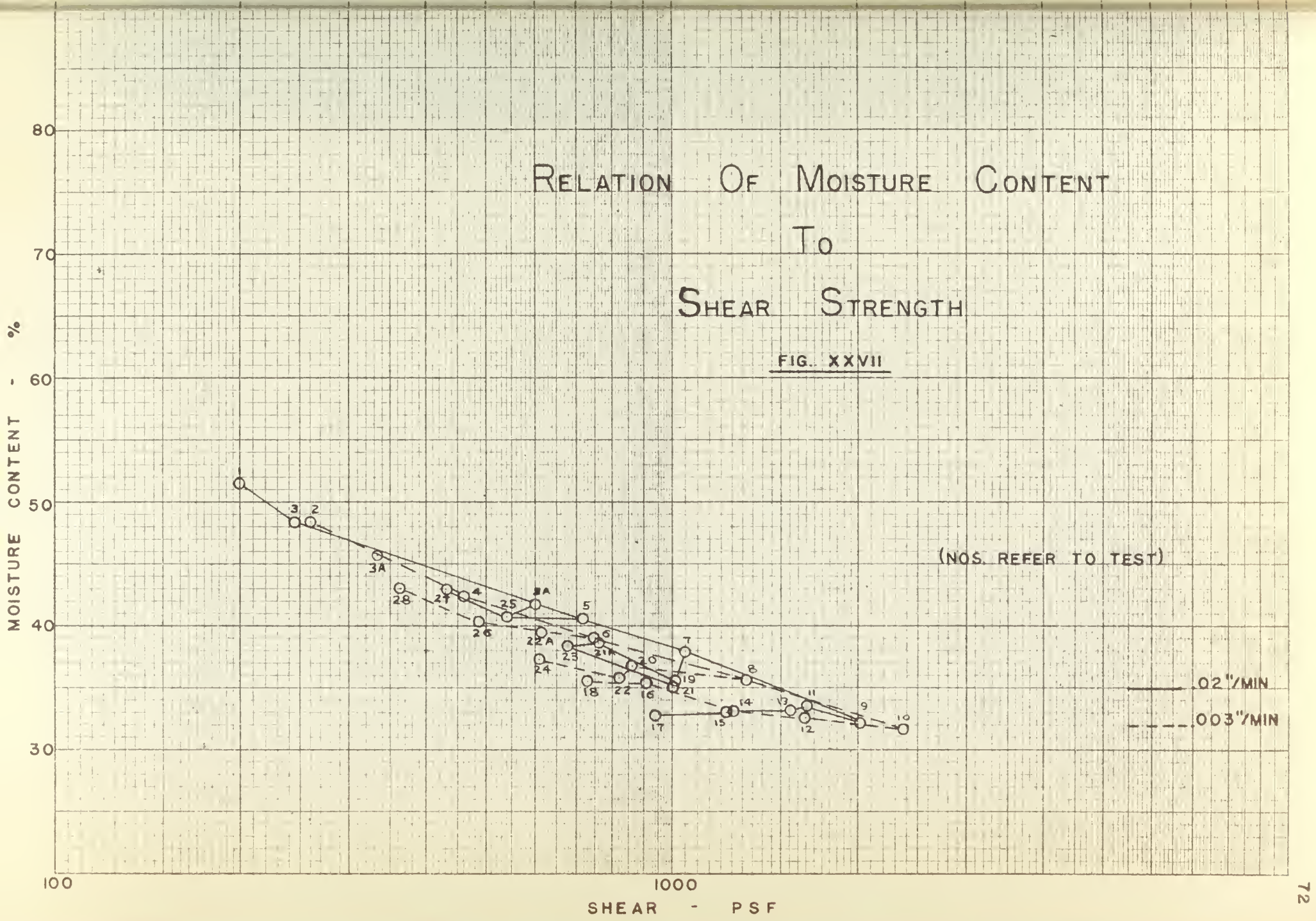

C. Test Values

1. Table 2 shows the values of maximum shear intensity at the various preload and vertical load conditions.
2. Table 3 shows the values of cohesion at the vertical loads used in the test.
3. Intrinsic Pressures:

   0.20 tons/sq.ft. @ .02 in/min

   0.35 tons/sq.ft. @ .003 in/min

4. Angle of internal friction:

Preload (tons/sq.ft.)	Rate of Strain	
	.02 in/min	.003 in/min
4	5°	11°
2	$6\frac{1}{2}^{\circ}$	12°
1	5°	14°

TABLE 2

Maximum Shear Intensity (TSF) At Various Vertical Loads

Vertical Load (TSF)	1/4		1/2		1		2		4	
Rate in/min	.02	.003	.02	.003	.02	.003	.02	.003	.02	.003
Preload (TSF)										
1/4	.100	.133								
1/2			.167	.233						
1	.215	.182	.270	.243	.299	.371				
2	.337	.303	.378	.307	.413	.429	.528	.664		
4	.469	.364	.617	.454	.775	.631	.825	.822	1.007	1.18

TABLE 3

Cohesion For Various Vertical Loads

	Cohesion - (TSF)		Angle of True Cohesion (ϕ_c)	
Vertical Load (TSF)	Rate in/min .02	.003	Rate in/min .02	.003
1/4	.060	.006	9°	1°
1/2	.100	.012	9°	1°
1	.175	.025	9°	1°
2	.325	.140	9°	6°
4	.650	.375	9°	6°

PART VII

DISCUSSION

As indicated in Part VI considerable deviation from Turnbull's laws occurred. There is, of course, no single answer as to the reasons for the digressions. Evidence presented herein is insufficient to dispute the validity of the laws to general applications, but it is adequate to question their unrestricted use. There are three major areas to be examined insofar as these results are concerned to educe possible reasons for discordance: method of testing; test conditions; and nature of the material.

The first area, method of testing, was performed under laboratory conditions using time worn direct shear techniques with care and continuity. A complete review of the procedure after conclusion of the tests brought forth absolutely no reason to suspect this area as a cause of the dissimilarities.

The second area, test conditions, seems to hold the key to the problem. Test conditions include such items as the establishment of pore water pressure, rates of strain, drainage conditions, and intergranular pressures. Since pore pressure reduces the intergranular pressure, and cohesion has been defined by

Terzaghi (Ref. 12) as a function of intergranular pressure, it follows that the magnitude of cohesion will depend to some extent upon pore water pressure.

For a saturated condition of less than 2% air voids, as developed in this experiment, pore pressure was induced during shear at both rates of strain. This is born out by the higher moisture content and the decrease in intrinsic pressure at the faster rate. Also, the increase in shearing strength at the slower rate is a common effect of pore pressure.

The increase in shearing resistance may be associated with any of the following:

(a) Increase in the apparent angle of internal friction.

(b) Increase in both internal friction and cohesion.

(c) Or a large increase in one of the above and a loss in the other.

Examining the data it is found that the angle of internal friction increases as the rate of strain decreased, the maximum shear resistance increased but the cohesion decreased with a decrease in rate of strain. This would appear contrary to the theory that cohesion is a function of intergranular pressure and that it should vary inversely with pore pressure. Likewise, the highest value of intrinsic pressure is found not with the highest

cohesion but with the lesser cohesion. Showing that the plotted intrinsic pressure is a variable dependent upon factors other than preconsolidation.

That cohesion decreases with a decrease in rate of strain may be explained on the basis of high pore pressures, which existed during the faster rate, reduced intergranular pressure and the reduced interlocking effect of the larger particles. But the true cohesion force between smaller particles is largely unaffected by pore water pressure since pore pressure does not exist between particles whose cohesive force is greater than pore pressure. As slower rates of strain pore pressure is reduced through drainage thus the shearing resistance is increased. The cohesive force is subordinate to the increased friction and relaxation occurs in which cohesive forces are dissipated during the slower strain.

There are indications that the cohesion curve is not a straight line function. In Fig. XXIV the cohesion curve at the .003 in/min rate was plotted with an inflection point at 1.0 ton/sq.ft. Actually, at each change in the angle of internal friction there is a corresponding change in slope of the cohesion curve, but because these changes were small, with the one exception, average slopes were plotted. Fig. XXIV also

shows that there is definitely no linear function between vertical loads smaller than approximately 25% of the preconsolidation load. Increased relative expansion during shear at the lighter loads is the cause. This is an extremely important point since conceivably the smaller load values are the ones most generally encountered in foundation practice and if expansion is permitted the shear resistance will decrease rapidly. Within this range of vertical loads the Turnbull laws definitely do not apply.

The moisture content of a saturated test sample has a direct relationship to the maximum shearing resistance, and is an indication of preloading and vertical loading at the time of shear. It was found, however, that the moisture content at a given preload and vertical shearing load under uniform test conditions varied an average of five percent, measured after shear, with corresponding variations is maximum shearing resistance. The reasons for moisture variations are beyond the scope of this thesis, but the fact is suggestive of the degree of accuracy to be expected. Moisture continuity should not be assumed for saturated samples of the same material, but should firmly established for each test.

Of the third area, nature of the material, little can be said that is not available elsewhere. Each constitutent of a soil imparts a complicated re-

lationship to the overall physical properties. Only by extensive, painstaking investigation of these constituents, singly and in groups, can a pattern of reaction be established. Much work has been done with a wide variety of soils, but too often the description and identification of the constituents has been neglected, consequently such work can not be utilized to the fullest extent. The practice of using place-name soils without proper analysis of the minerological character should be abolished.

Skempton (Ref. 10) brings out an interesting point regarding the possible relationship between true cohesion and the mineralogy of clays. Data is cited which relates the geologic age, method of derivation, and method of aging of clays to their colloidal activity, showing that colloidal inactivity increases ϕ and decreases cohesion. He found that European clays of the Triassic and Jurassic ages were considerably more active than certain younger North American clays, namely samples from the Chicago, Illinois area.

The illite clay used in this thesis was obtained at Morris, Illinois not far, geographically, from Chicago. Kerr and Kulp (Ref. 6) established that this illite originated in the cyclothemic activity of early Pennsylvanian time. From the Liquid Limit-Plastic Limit-Clay fraction relationship the illite falls within the class of "normally active" clays.

Turnbull's experiments were developed at an optimum moisture content for each soil and at rates of strain varying from .05 in/min to unlimited duration. He states that the curve for the shearing resistance for a saturated soil is parallel to those at optimum moisture content but have normal stress approximately one-third less. He points out the difficulty of completely saturating an impermeable soil. Also, the statement is made that the angle of internal friction remains the same in both the optimum moisture and saturated conditions.

The results of this experiment do not sustain these arguments. Again emphasis should be placed upon the variations of pore water pressure depending upon drainage conditions, rate of shear, and vertical load which will certainly cause corresponding variations in the observed values of shearing resistance and for which absolutely no allowance is made.

The unique points of intersection of the curves representing maximum shearing resistance, solutions to Coulomb's equation, and cohesion at each rate of strain are inapplicable and have no practical value for the conditions under which this experiment was performed. Any significance of these points has been completely lost apparently because of the saturated condition.

The findings of this thesis serve best as a warning that the proposed laws are not satisfied for a saturated illite clay, and secondly, as the first phase of an investigation which eventually may lead to the correlation of true cohesion in a saturated soil with capillary normal stress in a non-saturated soil. The unloading curves definitely show that cohesion is not constant for any given soil but will vary widely (75 per cent at 4 tons/sq.ft. preconsolidation in this case) depending upon the rate of strain, normal stress, and preconsolidation. Further work is necessary to establish the effects of rate of strain upon cohesion in a saturated soil.

PART VIII

CONCLUSIONS

1. Cohesion increases with normal stress.
2. The magnitude of cohesion depends upon rate of strain, normal stress, moisture content, the mineralogical nature and fineness of the clay.
3. Turnbull's laws were not proven applicable to a saturated clay.
4. For normal stress less than 75 per cent of the preconsolidation stress, the shearing resistance ceases to be a straight-line function. A large error on the unsafe side would be introduced if so assumed.
5. A vigorously accurate mathematical expression for cohesion is not a simple relation but an extremely complex variable. Present cohesion formulas can only be applied within narrow limitations to express its true value.
6. Further studies should be made at higher vertical loads and with a wider range of rates of strain to establish the full scope of cohesion variations, both at optimum moisture and saturated conditions.

PART IX

SUMMARY

The test data proves conclusively that true cohesion exists as a dependable force which increases proportionately with normal stress. Further tests on saturated illite are required to ascertain the full effects of pore pressure and rate of strain. Such a program conceivably could be carried out for all major clay minerals before satisfactory foundation design criteria becomes available.

PART X

LITERATURE CITED

1. Baver, L.D. Soil Physics, John Wiley and Sons, 1948, 398 pp.

2. Capper and Cassie. Mechanics of Engineering Soils, McGraw-Hill, 1953, 315 pp.

3. Grim, R.E. Clay Mineralogy, McGraw-Hill, 1953, 384 pp.

4. Hogentogler, C.A. Engineering Properties of Soils, McGraw-Hill, 1937, 434 pp.

5. Hvorslev, M.J. Ueber die Festigkeitseigenschaften gestoerter bindiger Boeden, Copenhagen, 1937, 159 pp.

6. Kerr, P.F. Reference Clay Mineral, API Research Project 49, Columbia Univ., 1951.

7. Krynine, D.P. Soil Mechanics, McGraw-Hill, 1941, 451 pp.

8. Nichols, M.L. The dynamic properties of soil. I. An explanation of the dynamic properties of soils by means of colloidal films, Agr. Eng. 12: 259-264 pp, 1931.

9. Russell, G.W. The interaction of clay with water and organic liquids as measured by specific volume changes and its relation to the phenomena of crumb formation in soils. Phil. Trans. Roy. Soc. London, 233 A: 361-389 pp, 1934.

10. Skempton, A.W. Possible Relationship between True Cohesion and the Mineralogy of Clays. 2nd Int. Conf. S.M.&F.E. Vol. VII, 1948, 45-46 pp.

11. Taylor, D.W. Fundamentals of Soil Mechanics, Wiley & Sons, 1948, 700 pp.

12. Terzaghi, K. Theoretical Soil Mechanics, Wiley & Sons, 1946, 510 pp.

13. Tschebotarioff, G.P. Soil Mechanics, Foundations and Earth Structures, McGraw-Hill, 1951, 655 pp.

14. Turnbull, J.M. Shear Resistance of Soils, Reprint from Commonwealth Eng., April-May 1952, 17 pp.

PART XI

APPENDIX

TEST DATA

Shear Strength At Zero Vertical Load And Zero Preload

MOISTURE CONTENT 84.6 %

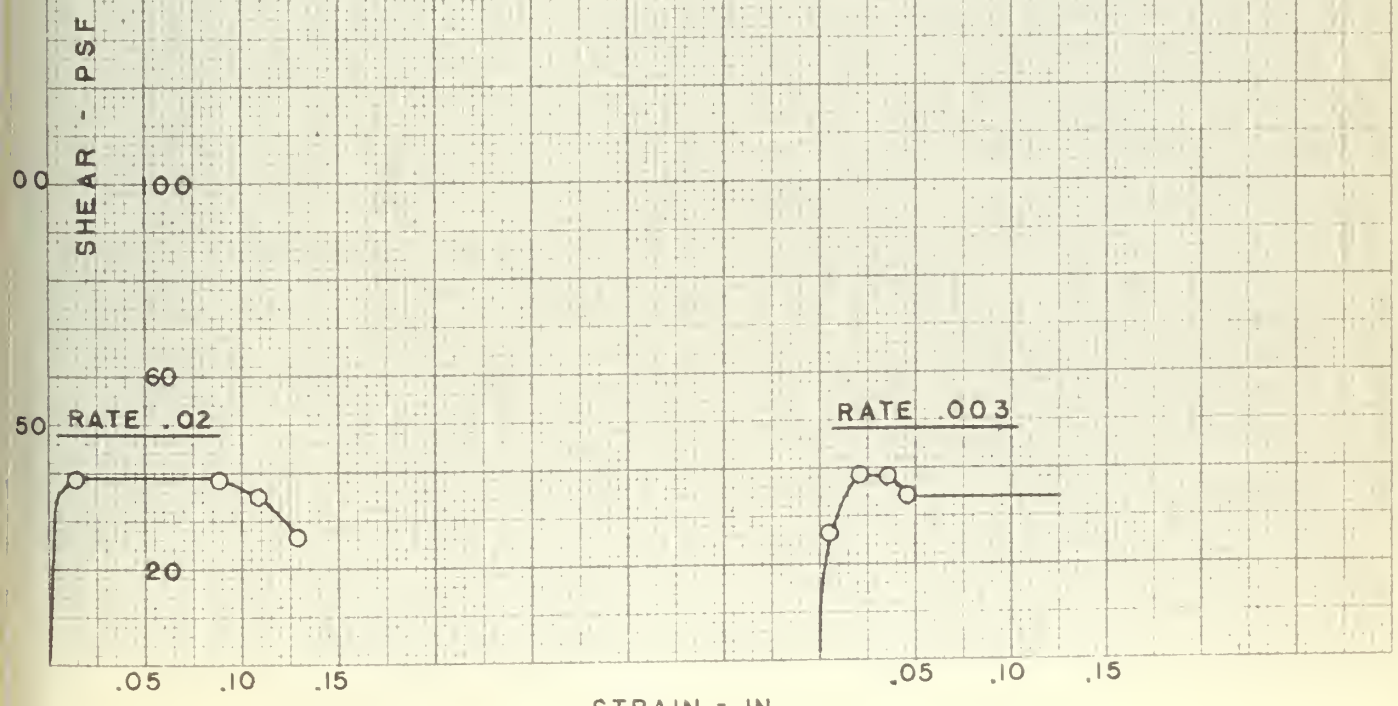

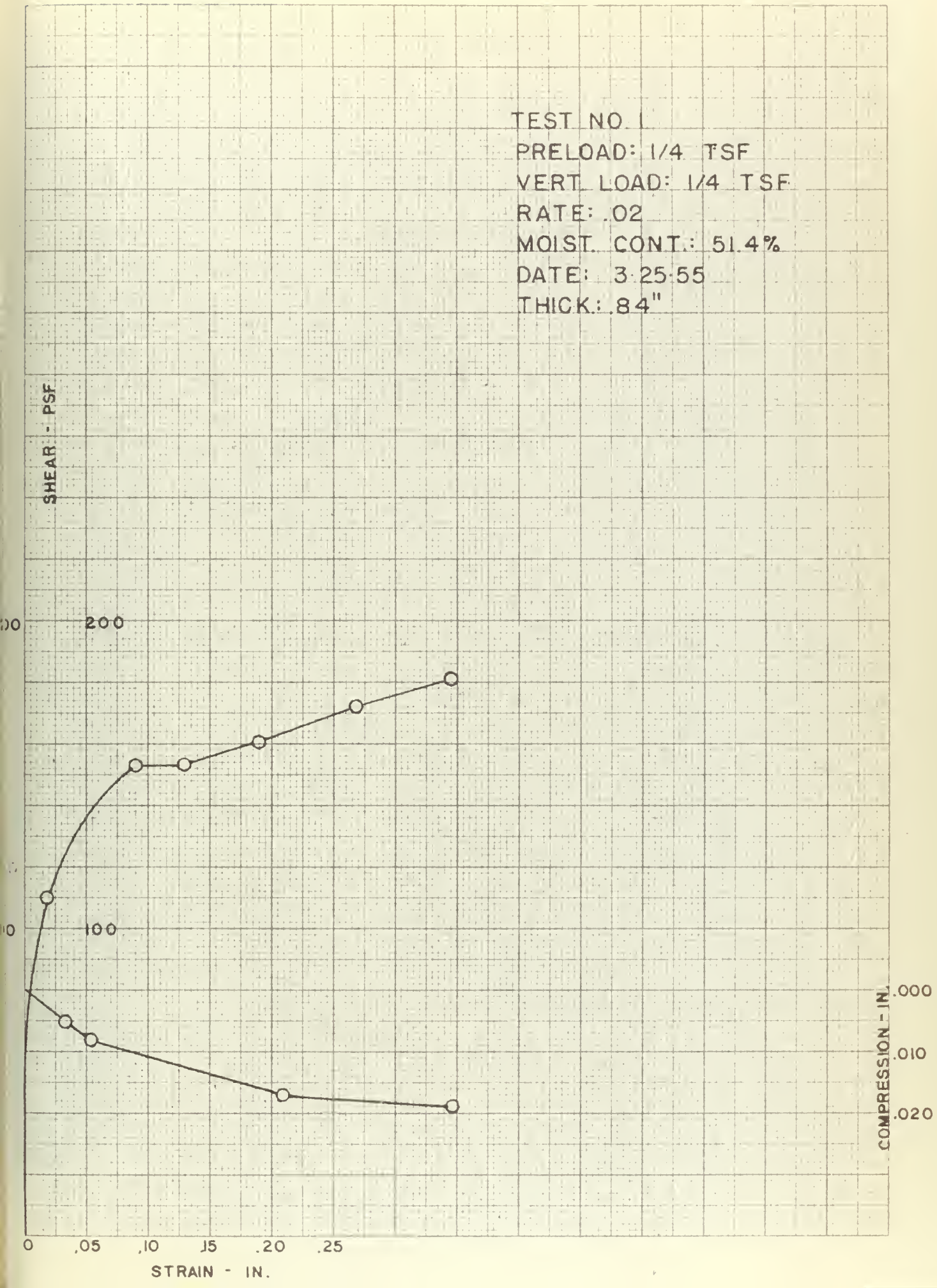
TEST NO. 1
PRELOAD: 1/4 TSF
VERT. LOAD: 1/4 TSF
RATE: .02
MOIST. CONT.: 51.4%
DATE: 3-25-55
THICK.: .84"
SHEAR - PSF
200
100
0
.05
.10
.15
.20
.25
STRAIN - IN.
COMPRESSION - IN.
.000
.010
.020

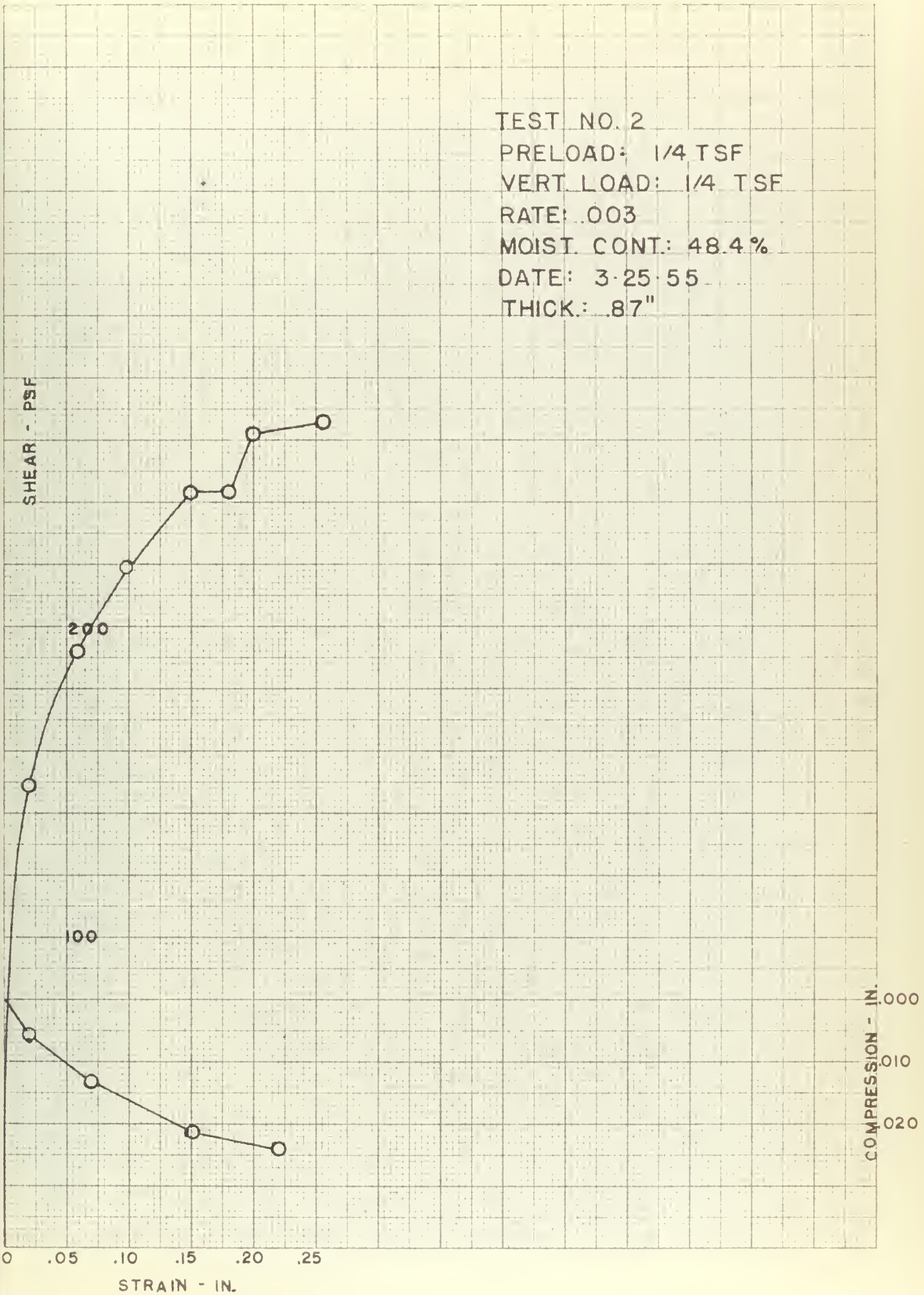
TEST NO. 2
PRELOAD: 1/4 TSF
VERT. LOAD: 1/4 TSF
RATE: .003
MOIST. CONT.: 48.4%
DATE: 3-25-55
THICK.: .87"
SHEAR - PSF
200
100
0
.05
.10
.15
.20
.25
STRAIN - IN.
COMPRESSION - IN.
.000
.010
.020

TEST NO. 3
PRELOAD: 1/2 TSF
VERT. LOAD: 1/2 TSF
MOIST. CONT.: 48.1 %
RATE: .02
DATE: 3/27/55
THICK.: .93"

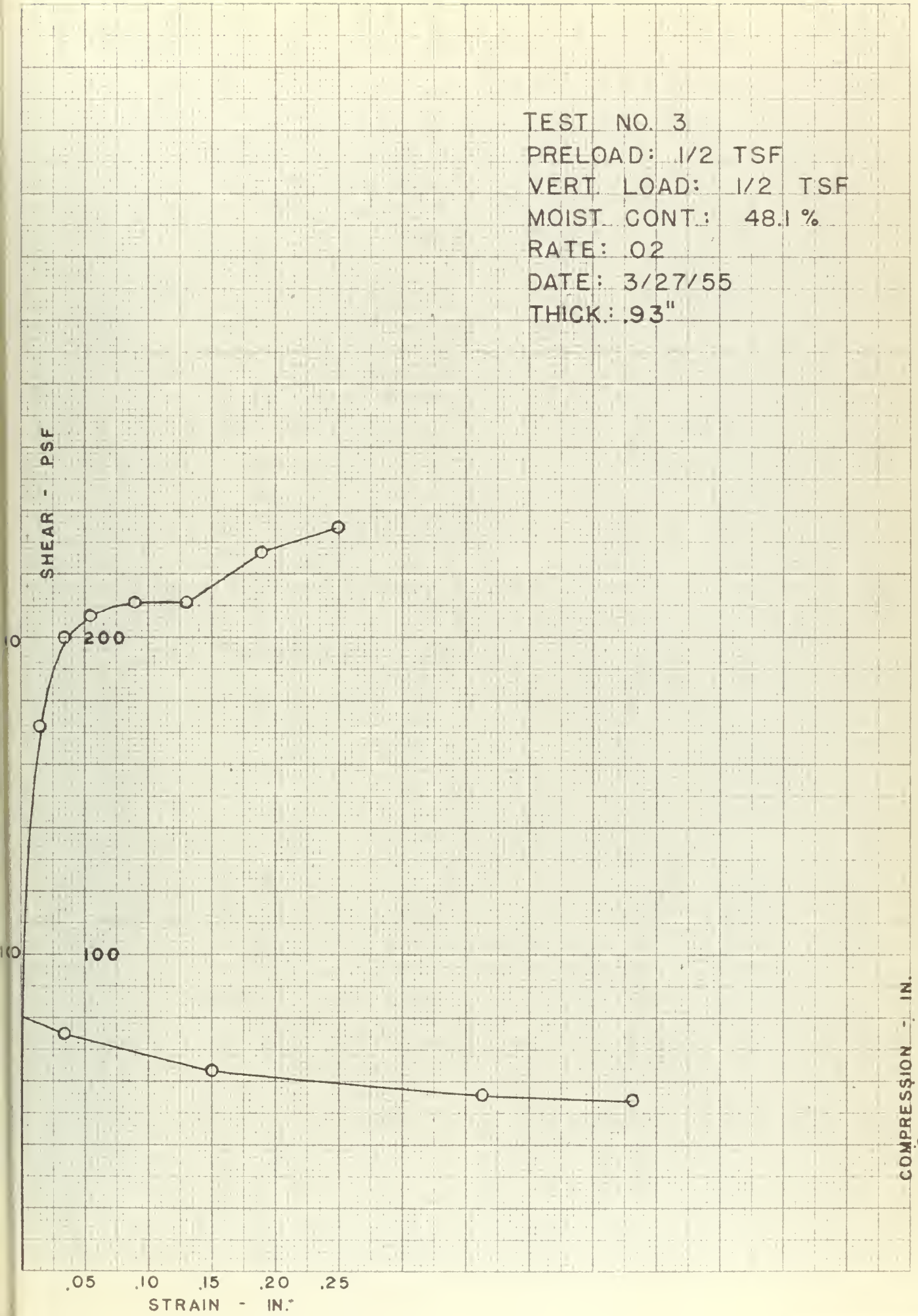

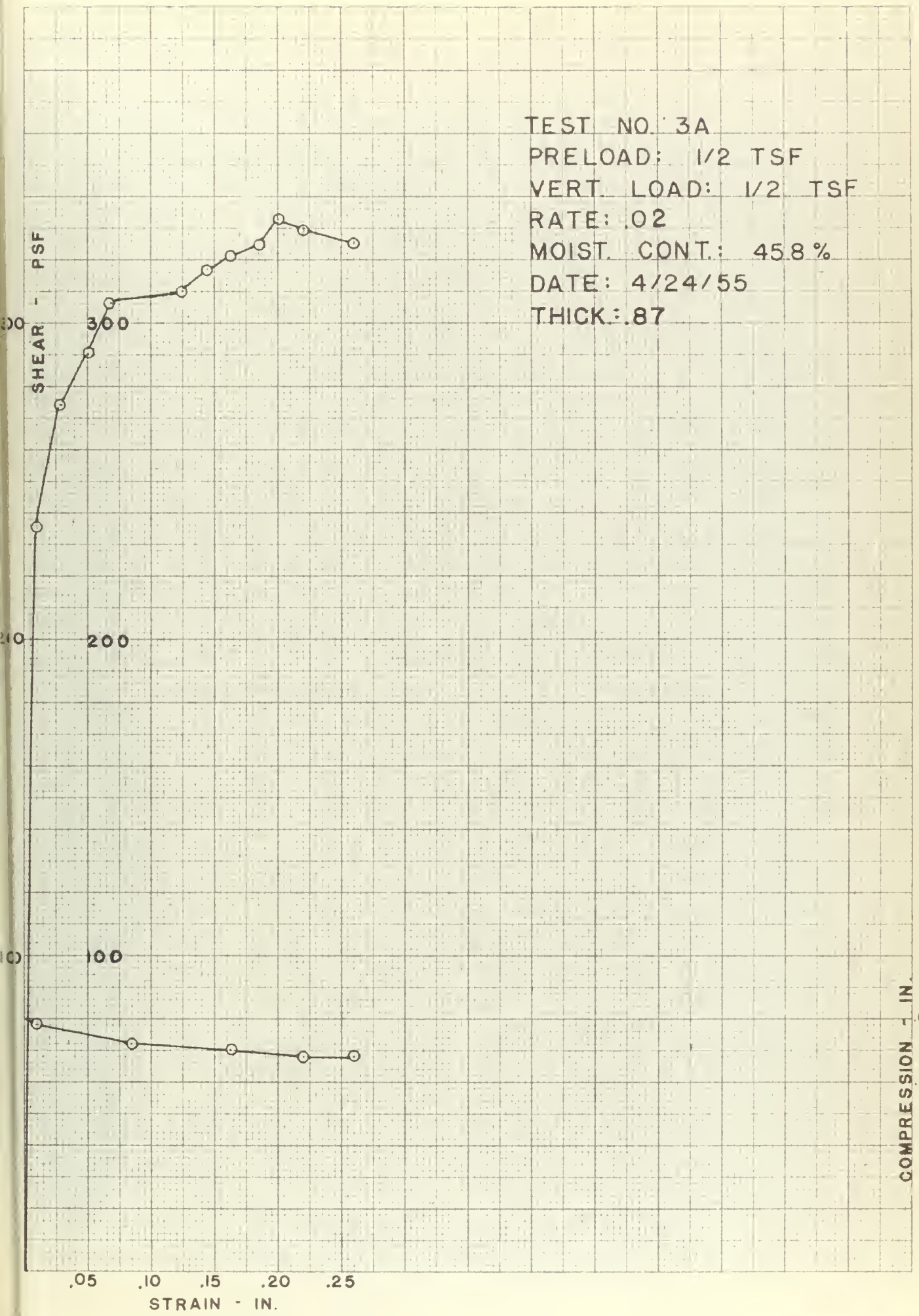
TEST NO. 3A
PRELOAD: 1/2 TSF
VERT. LOAD: 1/2 TSF
RATE: .02
MOIST. CONT.: 45.8 %
DATE: 4/24/55
THICK.: .87
SHEAR - PSF
300
200
100
.05
.10
.15
.20
.25
STRAIN - IN.
COMPRESSION - IN.
.000
.010

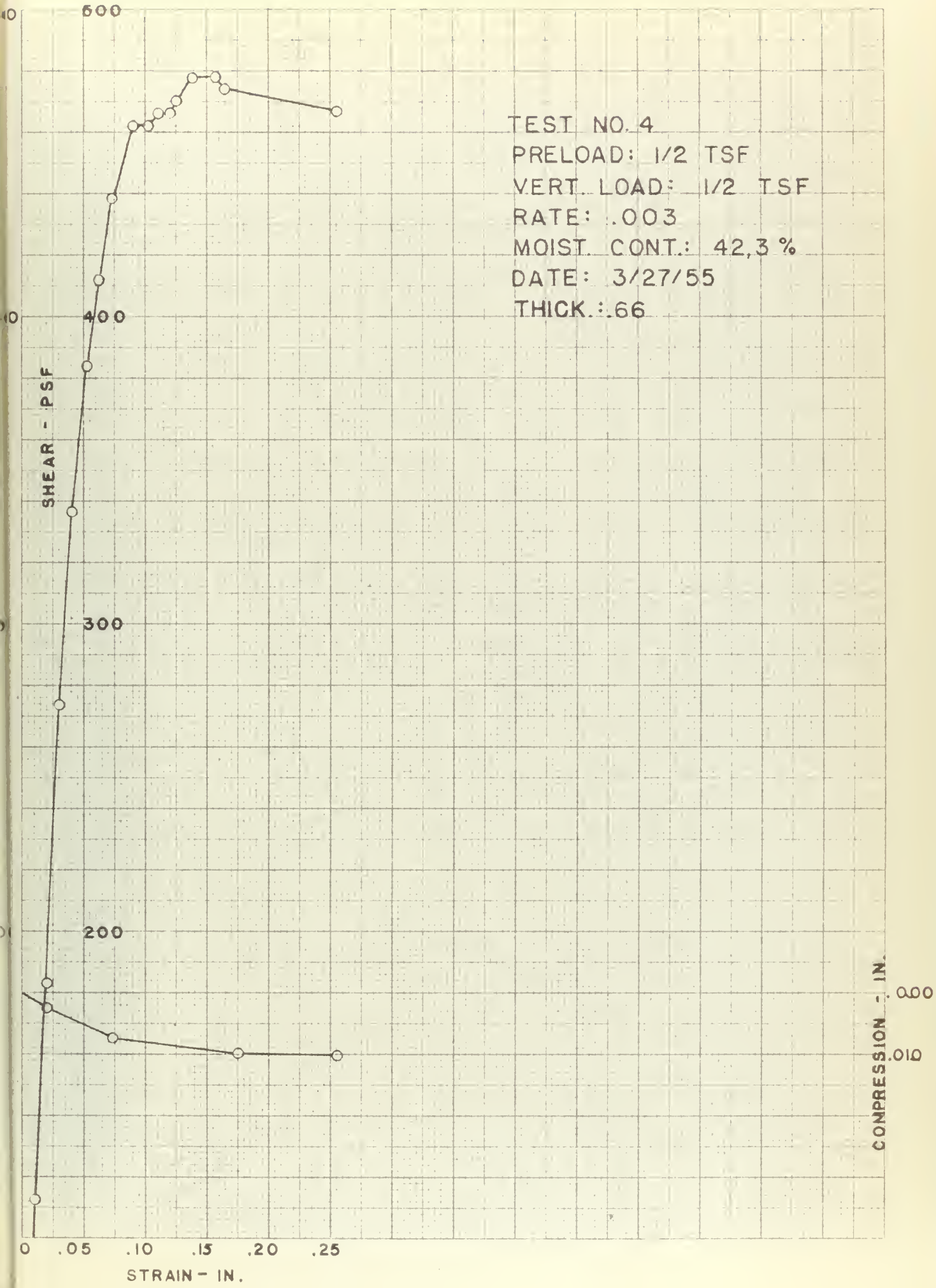
TEST NO. 4
PRELOAD: 1/2 TSF
VERT. LOAD: 1/2 TSF
RATE: .003
MOIST. CONT.: 42,3 %
DATE: 3/27/55
THICK.: .66
SHEAR - PSF
600
400
300
200
0
.05
.10
.15
.20
.25
STRAIN - IN.
COMPRESSION - IN.
.000
.010

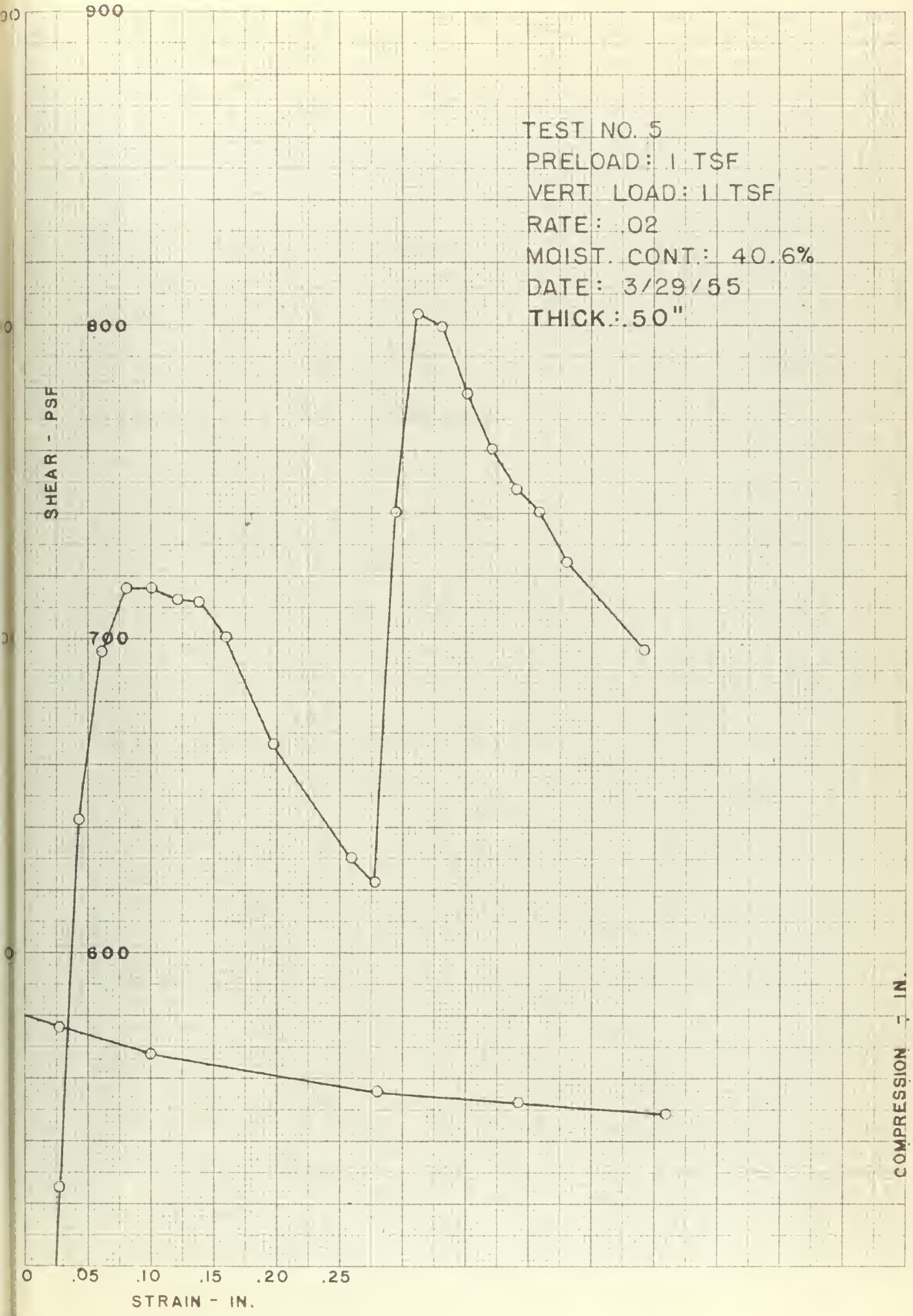
900
800
700
600
SHEAR - PSF
TEST NO. 5
PRELOAD: 1 TSF
VERT. LOAD: 1 TSF
RATE: .02
MOIST. CONT.: 40.6%
DATE: 3/29/55
THICK.: .50"
0
.05
.10
.15
.20
.25
STRAIN - IN.
.000
.010
.020
COMPRESSION - IN.

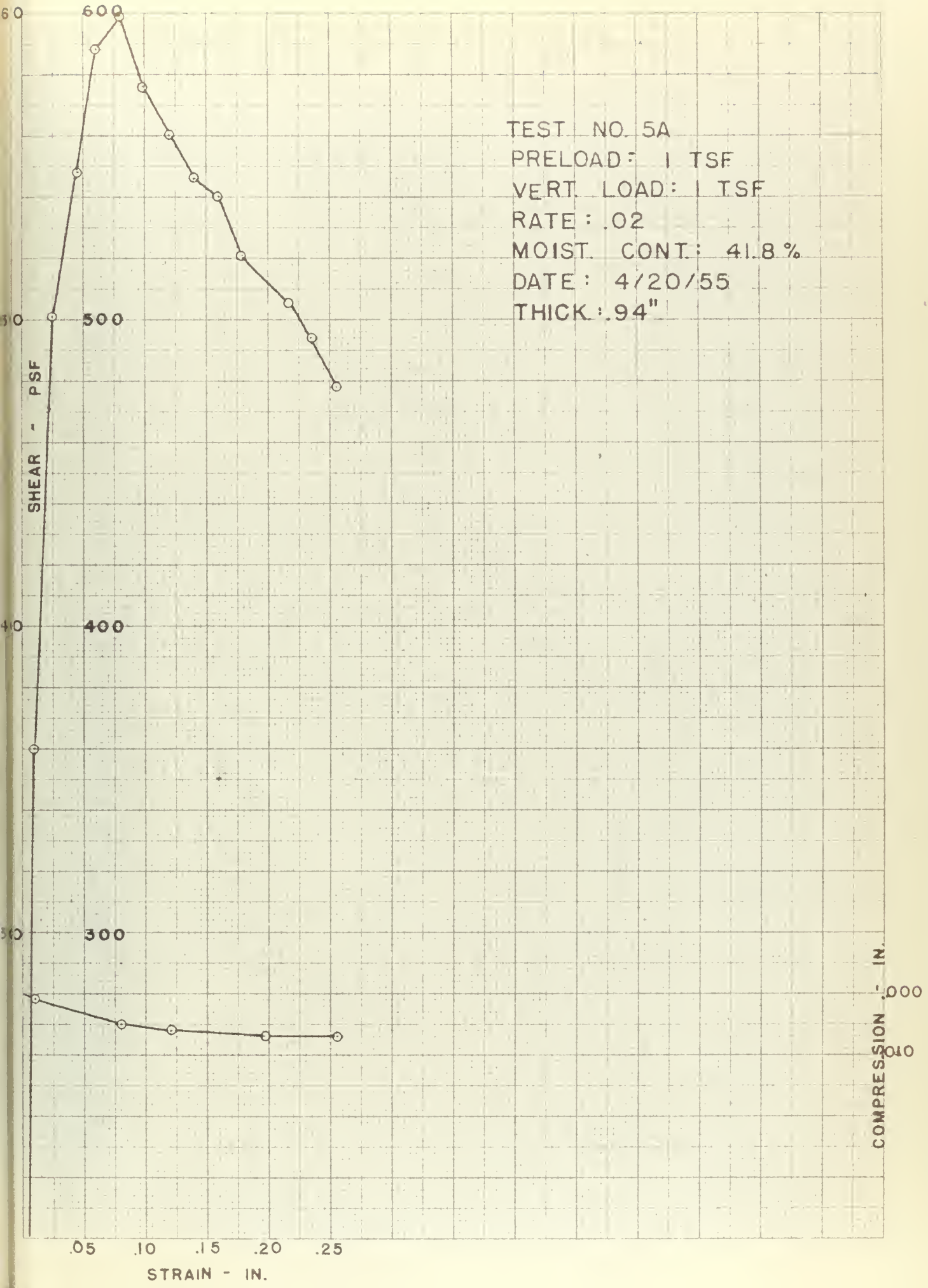
TEST NO. 5A
PRELOAD: 1 TSF
VERT. LOAD: 1 TSF
RATE: .02
MOIST. CONT.: 41.8%
DATE: 4/20/55
THICK.: .94"
SHEAR - PSF
600
500
400
300
.05
.10
.15
.20
.25
STRAIN - IN.
COMPRESSION - IN.
.000
.010

TEST NO. 6
PRELOAD: 1 TSF
VERT. LOAD: 1 TSF
RATE: .003
MOIST. CONT.: 39.0%
DATE: 3/29/55
THICK.: .94"

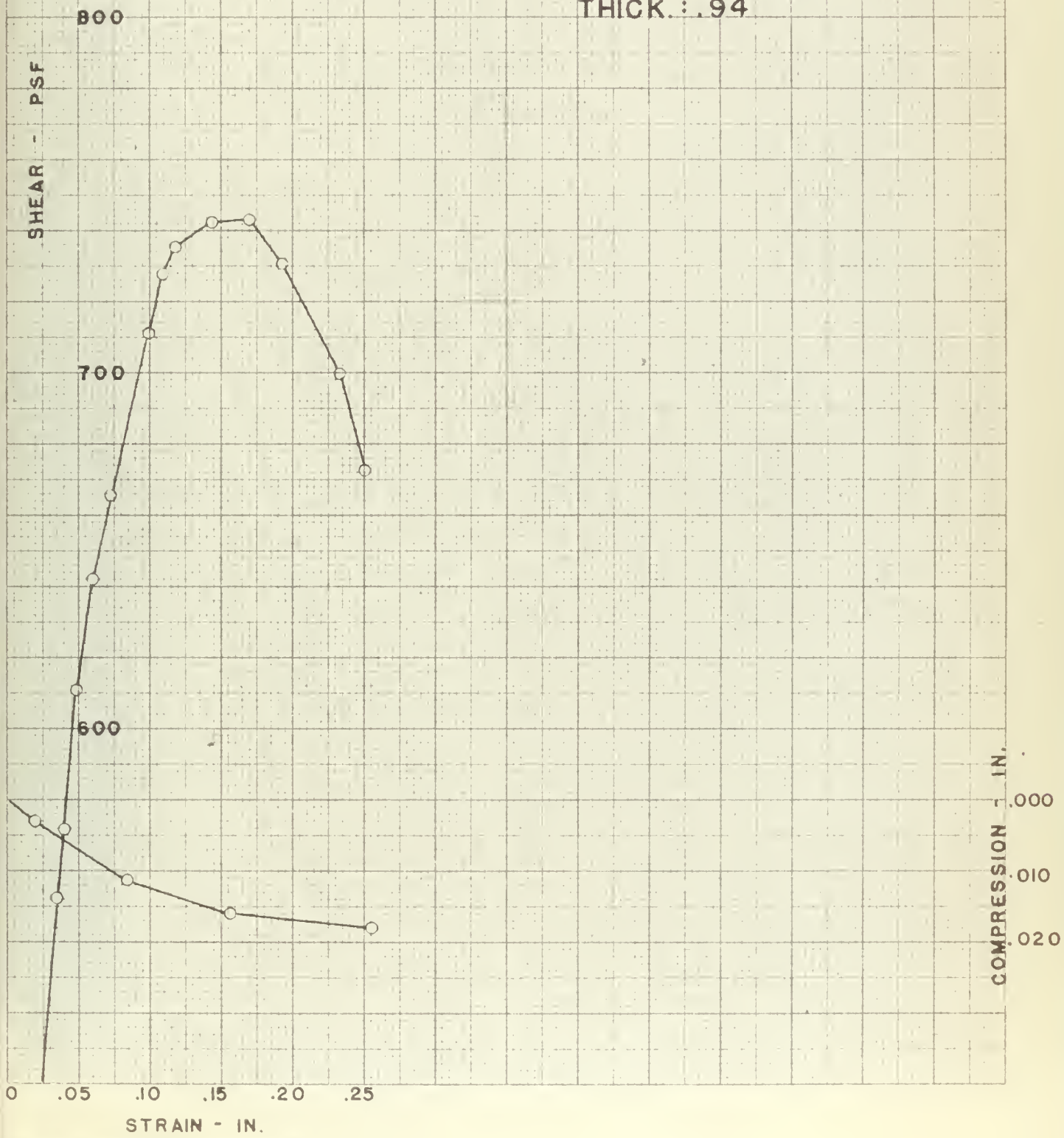

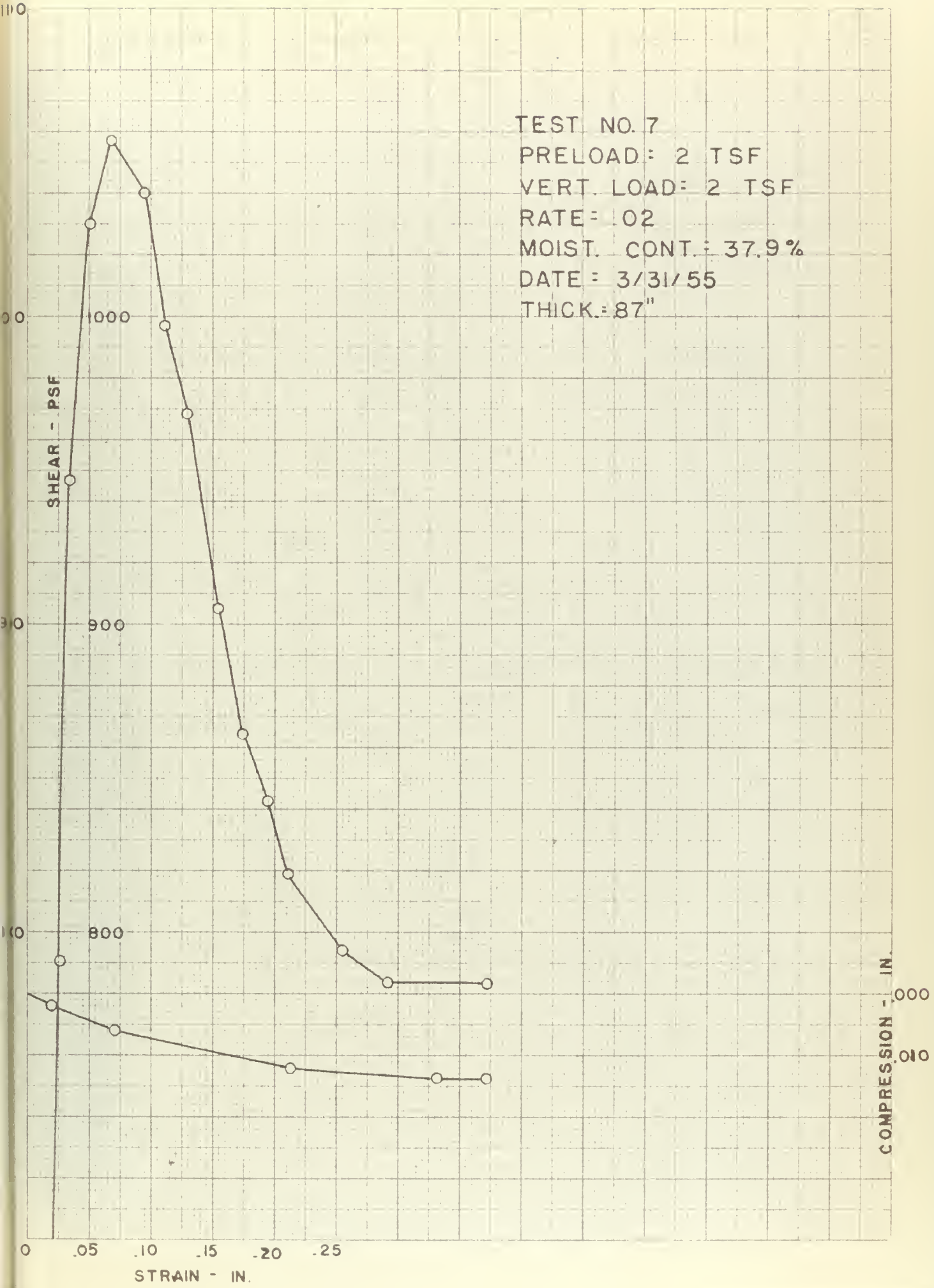
TEST NO. 7
PRELOAD: 2 TSF
VERT. LOAD: 2 TSF
RATE: .02
MOIST. CONT.: 37.9%
DATE: 3/31/55
THICK.: 87"
SHEAR - PSF
1000
900
800
0
.05
.10
.15
.20
.25
STRAIN - IN.
COMPRESSION - IN.
.000
.010

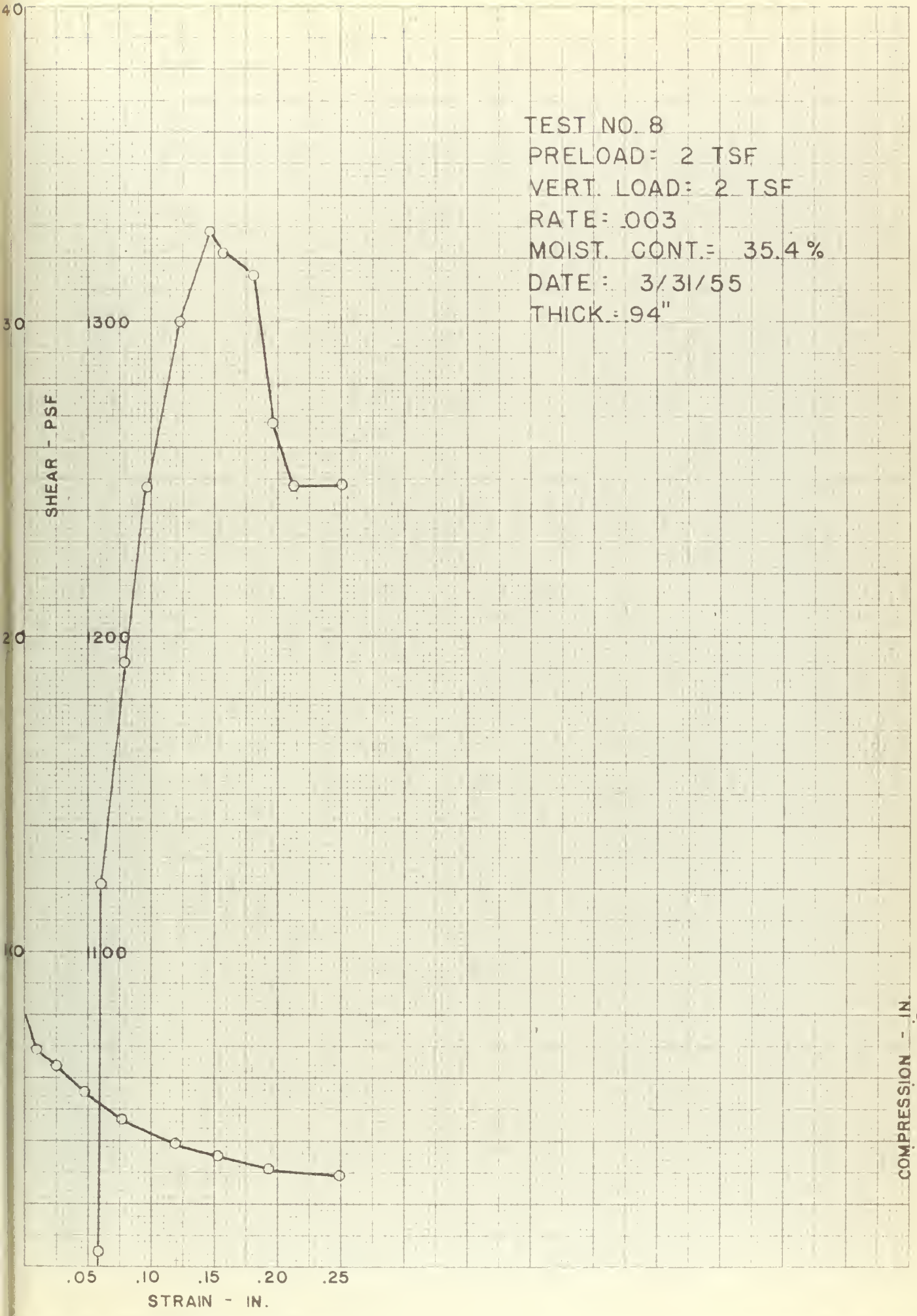
TEST NO. 8
PRELOAD = 2 TSF
VERT. LOAD = 2 TSF
RATE = .003
MOIST. CONT. = 35.4 %
DATE : 3/31/55
THICK. = .94"
40
30
20
10
1300
1200
1100
SHEAR - PSF
.05
.10
.15
.20
.25
STRAIN - IN.
.000
.010
.020
COMPRESSION - IN.

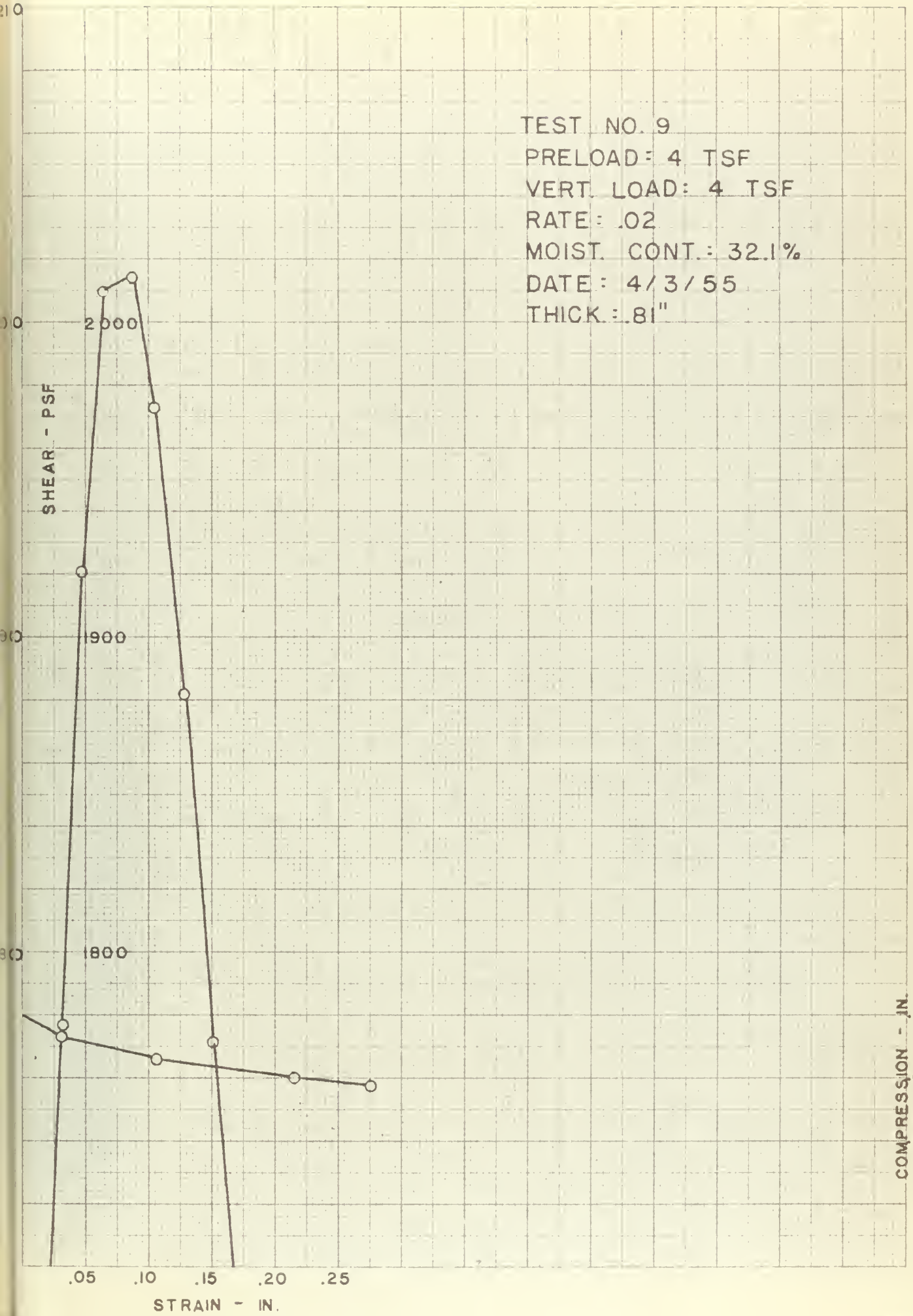
TEST NO. 9
PRELOAD: 4 TSF
VERT. LOAD: 4 TSF
RATE: .02
MOIST. CONT.: 32.1%
DATE: 4/3/55
THICK.: .81"
SHEAR - PSF
2000
1900
1800
.05
.10
.15
.20
.25
STRAIN - IN.
COMPRESSION - IN.
.000
.010
.020

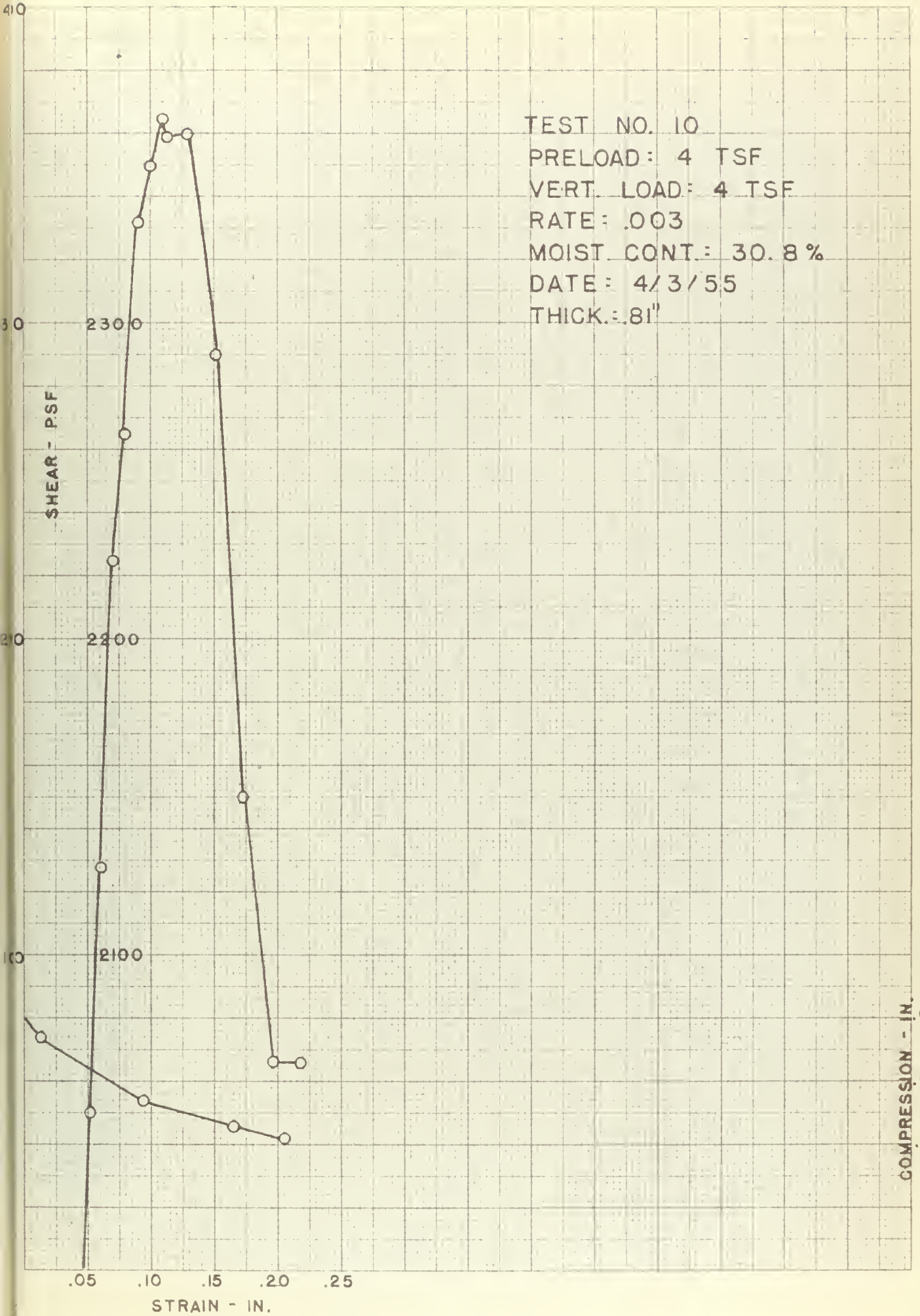
TEST NO. 10
PRELOAD: 4 TSF
VERT. LOAD: 4 TSF
RATE: .003
MOIST. CONT.: 30.8%
DATE: 4/3/55
THICK.: .81"
410
30
210
10
2300
2200
2100
SHEAR - PSF
.05
.10
.15
.20
.25
STRAIN - IN.
.000
.010
.020
COMPRESSION - IN.

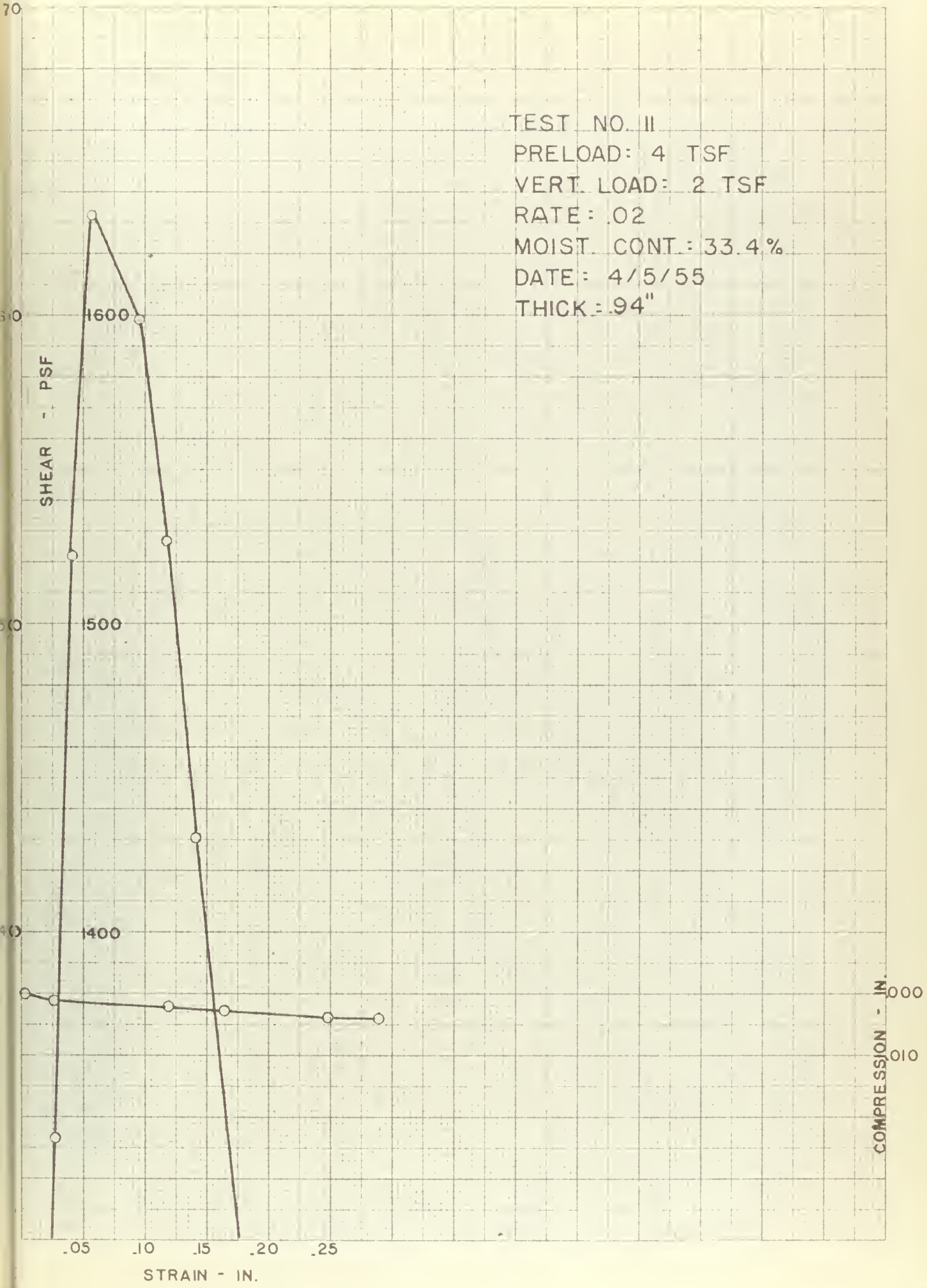
TEST NO. 11
PRELOAD: 4 TSF
VERT. LOAD: 2 TSF
RATE: .02
MOIST. CONT.: 33.4%
DATE: 4/5/55
THICK: .94"
SHEAR - PSF
1600
1500
1400
.05
.10
.15
.20
.25
STRAIN - IN.
COMPRESSION - IN.
000
010

TEST NO. 12
PRELOAD : 4 TSF
VERT. LOAD: 2 TSF
RATE: .003
MOIST. CONT.: 32.6 %
DATE: 4/5/55
THICK: 94"

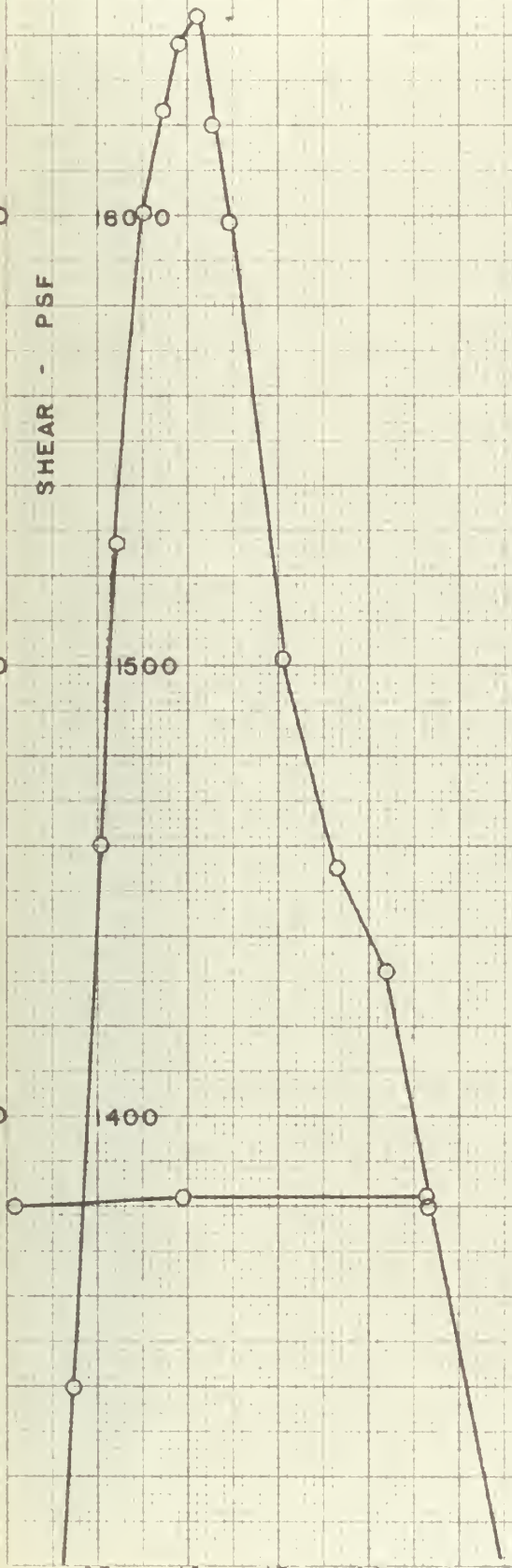

EXPANSION - IN.
.010
.000

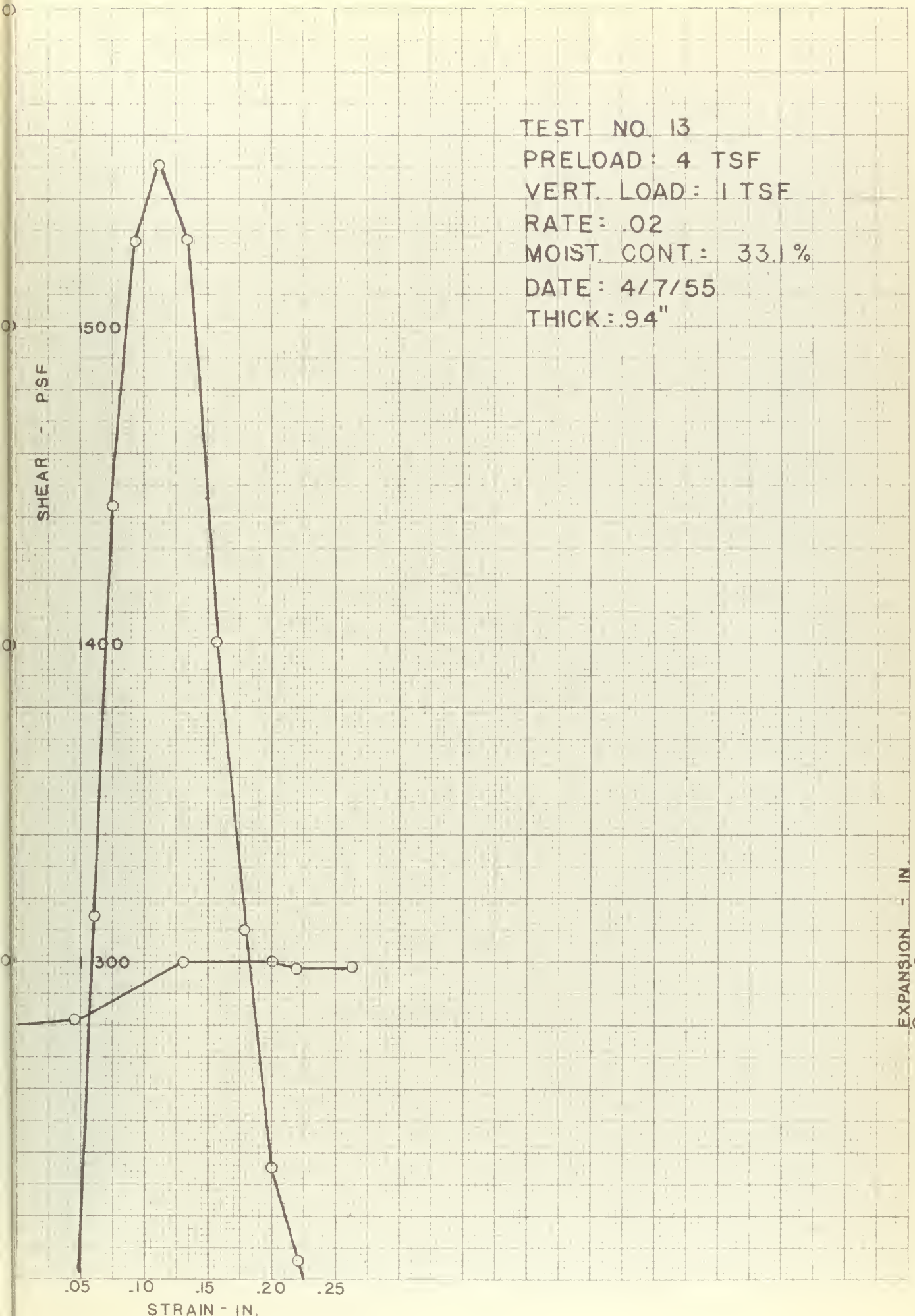
TEST NO. 13
PRELOAD: 4 TSF
VERT. LOAD: 1 TSF
RATE: .02
MOIST. CONT.: 33.1 %
DATE: 4/7/55
THICK.: .94"
SHEAR - PSF
1500
1400
1300
.05
.10
.15
.20
.25
STRAIN - IN.
EXPANSION - IN.
.010
.000

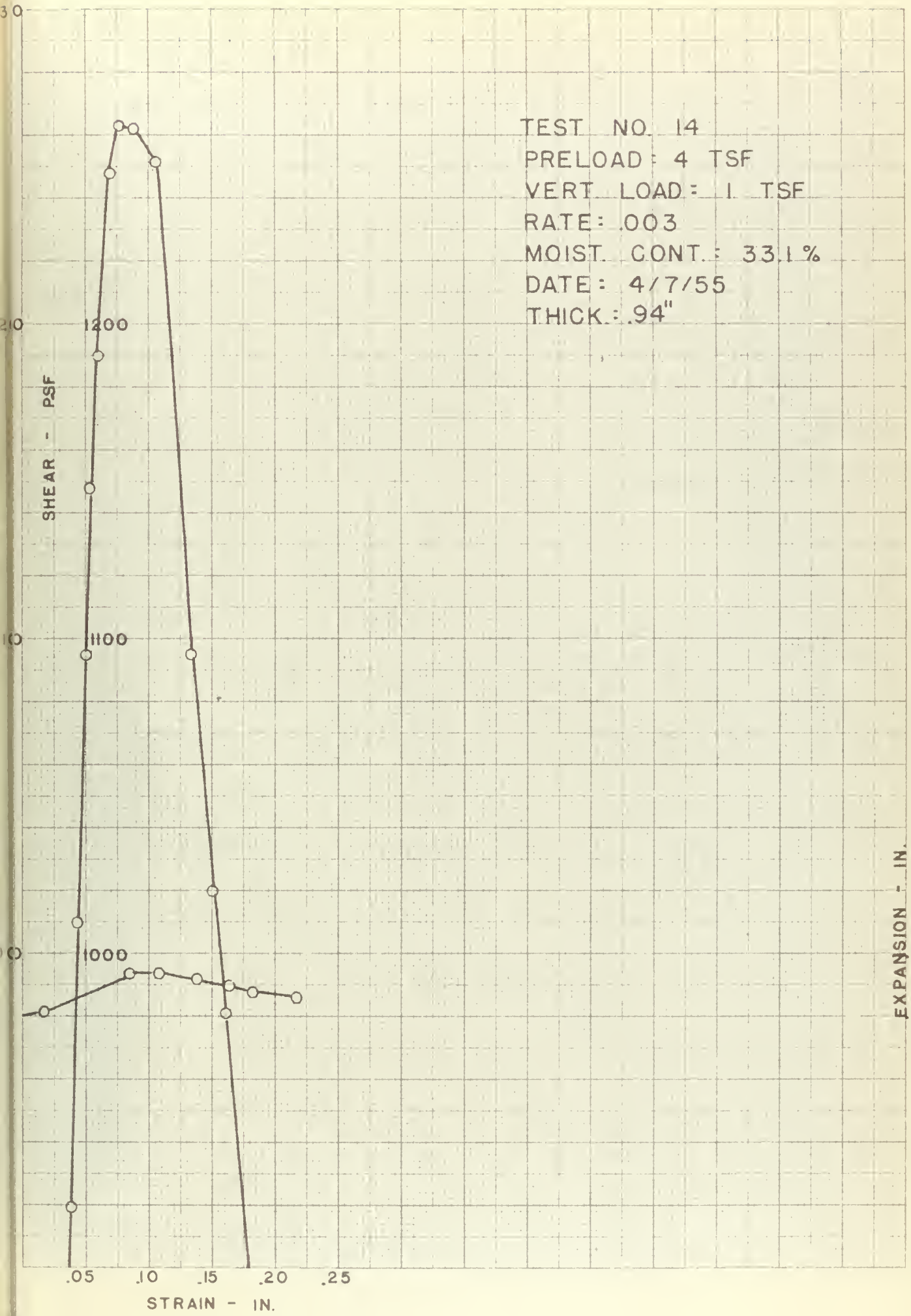
TEST NO. 14
PRELOAD: 4 TSF
VERT. LOAD: 1 TSF
RATE: .003
MOIST. CONT.: 33.1 %
DATE: 4/7/55
THICK.: .94"
SHEAR - PSF
1200
1100
1000
.05
.10
.15
.20
.25
STRAIN - IN.
EXPANSION - IN.
.010
.000

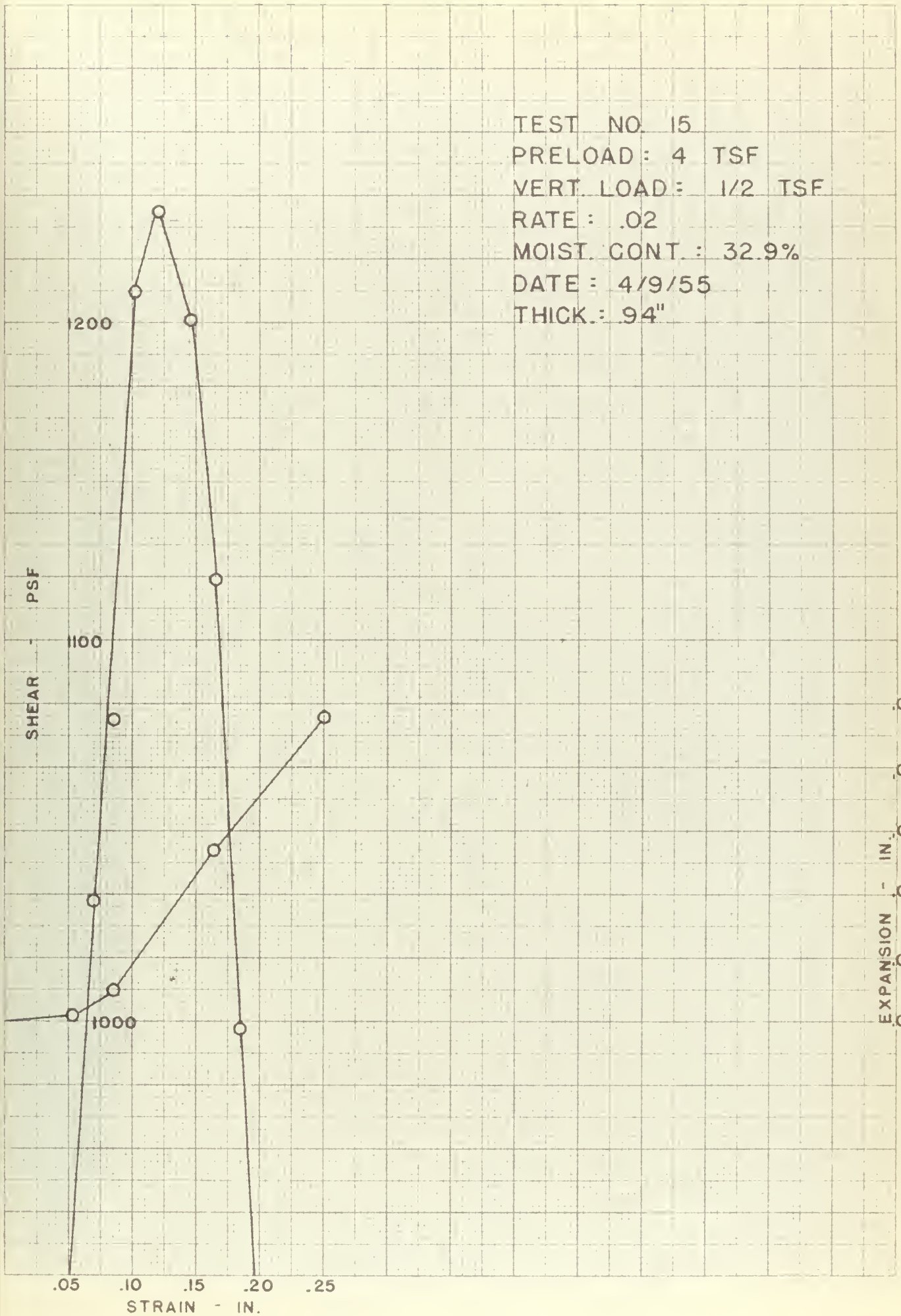
TEST NO. 15
PRELOAD: 4 TSF
VERT. LOAD: 1/2 TSF
RATE: .02
MOIST. CONT.: 32.9%
DATE: 4/9/55
THICK.: .94"
SHEAR - PSF
1200
1100
1000
.05
.10
.15
.20
.25
STRAIN - IN.
EXPANSION - IN.
.050
.040
.030
.020
.010
.000

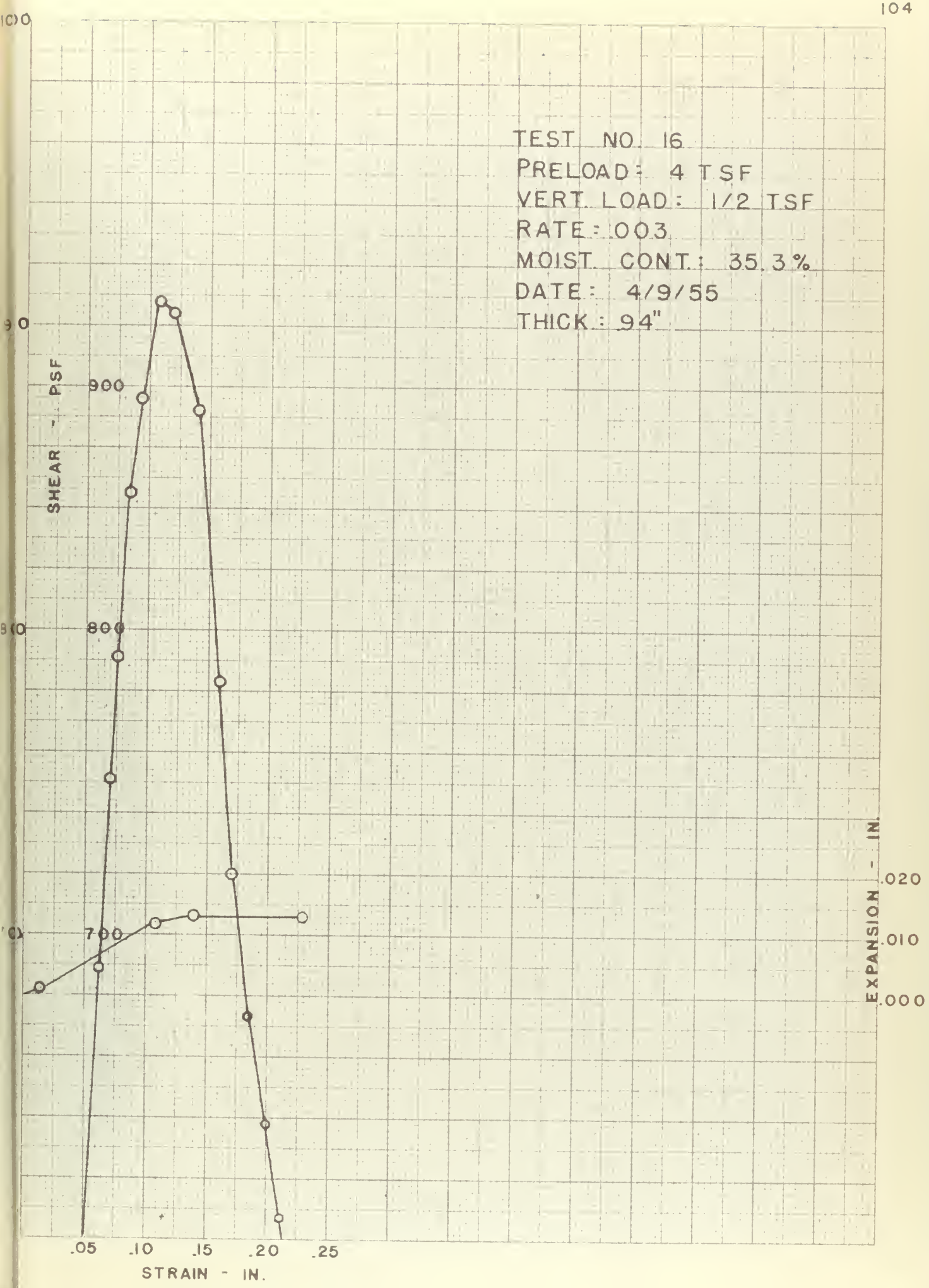
TEST NO. 16
PRELOAD: 4 TSF
VERT. LOAD: 1/2 TSF
RATE: .003
MOIST. CONT.: 35.3%
DATE: 4/9/55
THICK: .94"
SHEAR - PSF
900
800
700
EXPANSION - IN.
.020
.010
.000
.05
.10
.15
.20
.25
STRAIN - IN.

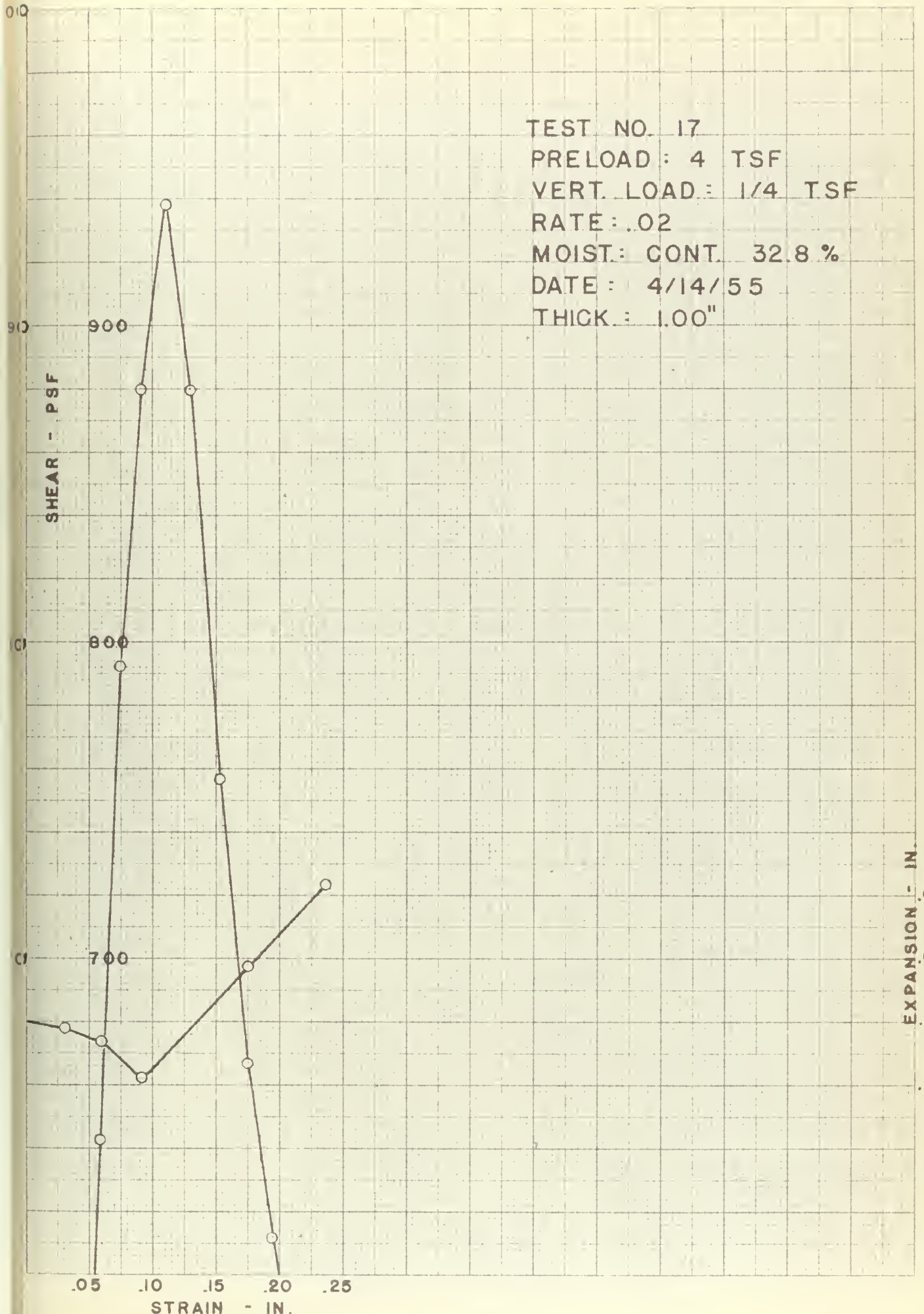
TEST NO. 17
PRELOAD : 4 TSF
VERT. LOAD : 1/4 TSF
RATE : .02
MOIST. : CONT. 32.8 %
DATE : 4/14/55
THICK. : 1.00"
SHEAR - PSF
900
800
700
.05
.10
.15
.20
.25
STRAIN - IN.
EXPANSION - IN.
.020
.010
.000
.010

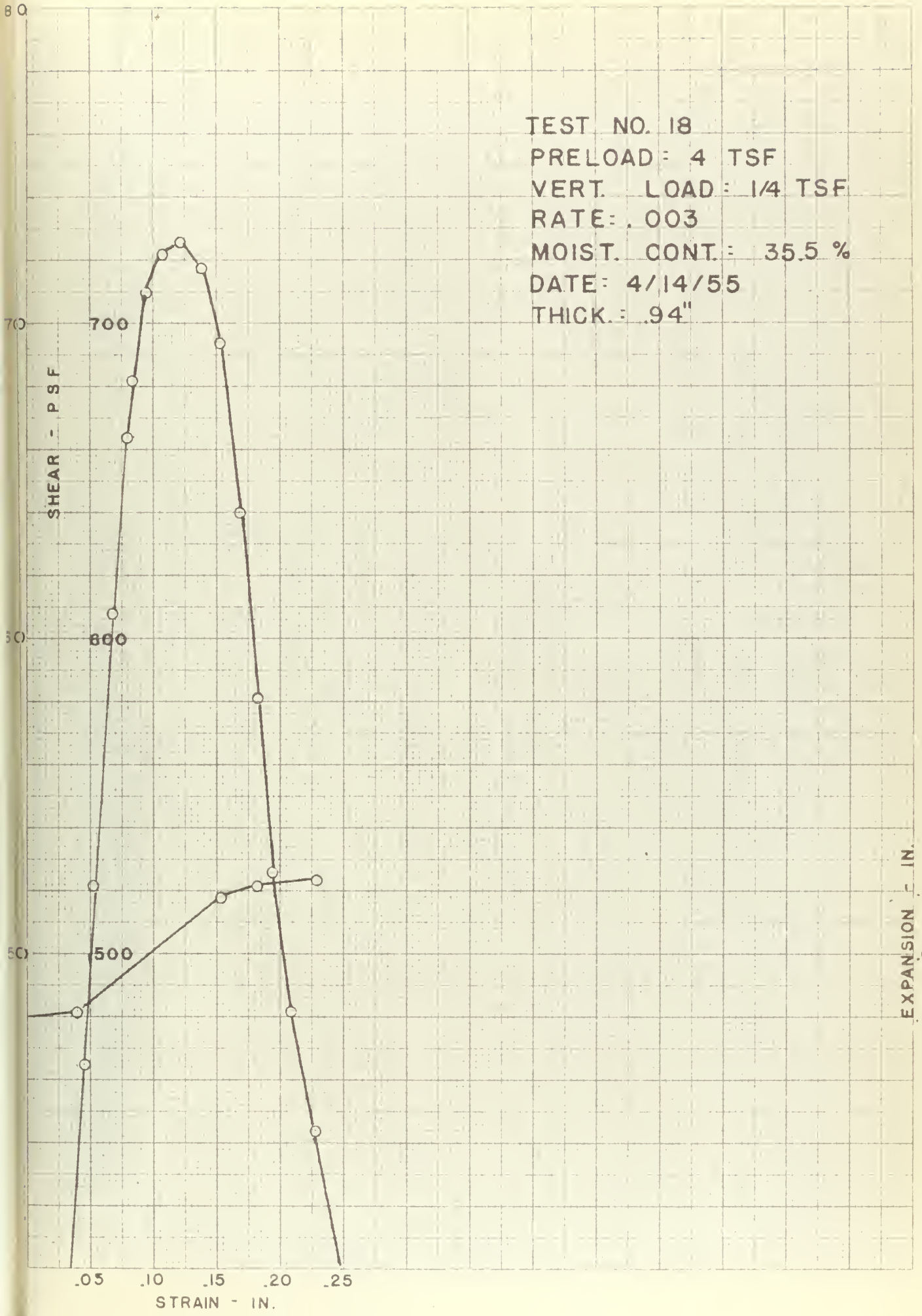
TEST NO. 18
PRELOAD: 4 TSF
VERT. LOAD: 1/4 TSF
RATE: .003
MOIST. CONT.: 35.5 %
DATE: 4/14/55
THICK.: .94"
SHEAR - PSF
700
600
500
EXPANSION - IN.
.020
.010
.000
.05
.10
.15
.20
.25
STRAIN - IN.

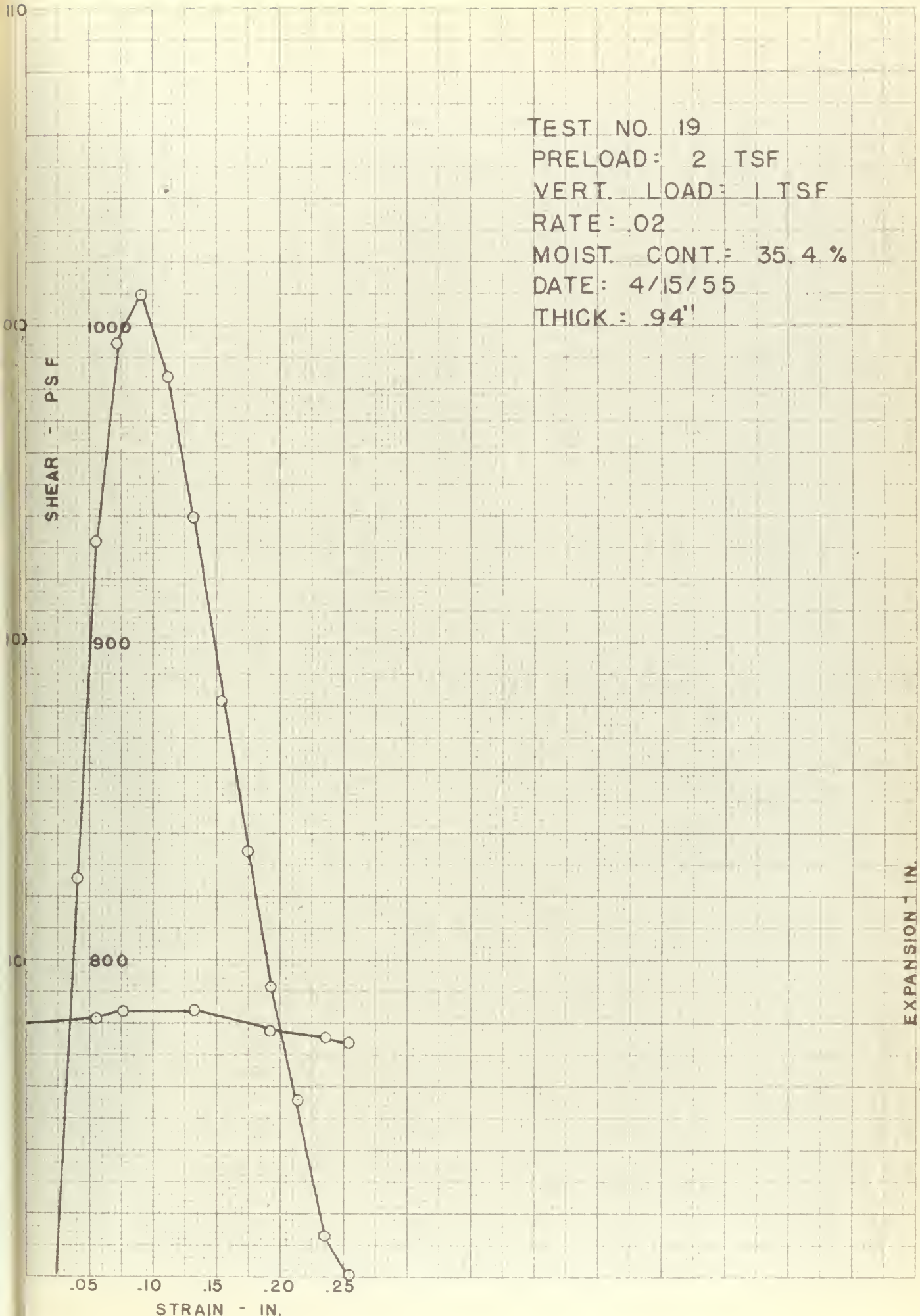
TEST NO. 19
PRELOAD: 2 TSF
VERT. LOAD: 1 TSF
RATE: .02
MOIST. CONT.: 35.4 %
DATE: 4/15/55
THICK.: .94"
SHEAR - PSF
1000
900
800
.05
.10
.15
.20
.25
STRAIN - IN.
EXPANSION - IN.
.010
.000
.010

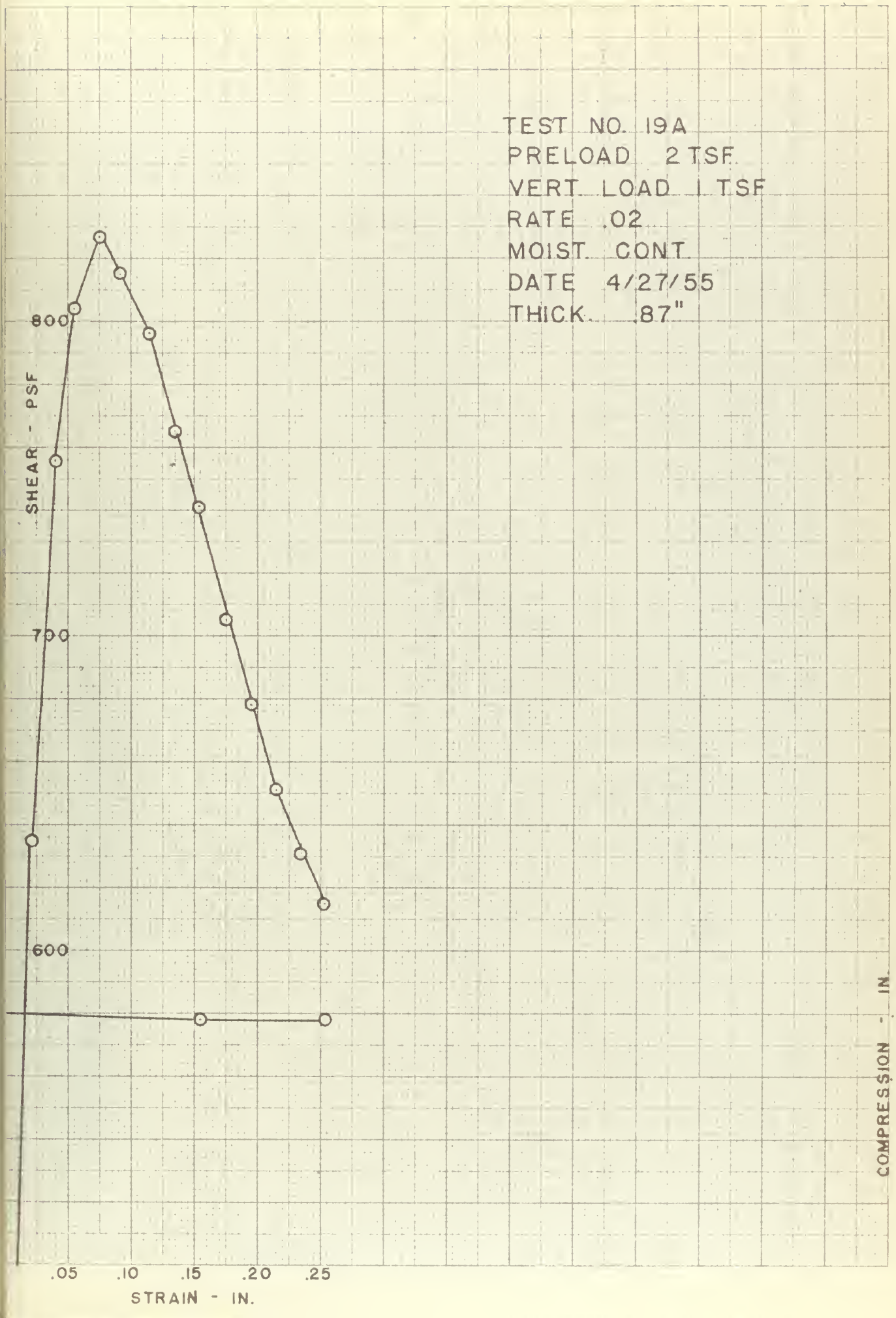
TEST NO. 19A
PRELOAD 2 TSF
VERT. LOAD 1 TSF
RATE .02
MOIST. CONT.
DATE 4/27/55
THICK. .87"
800
700
600
SHEAR - PSF
.05
.10
.15
.20
.25
STRAIN - IN.
.000
.010
COMPRESSION - IN.

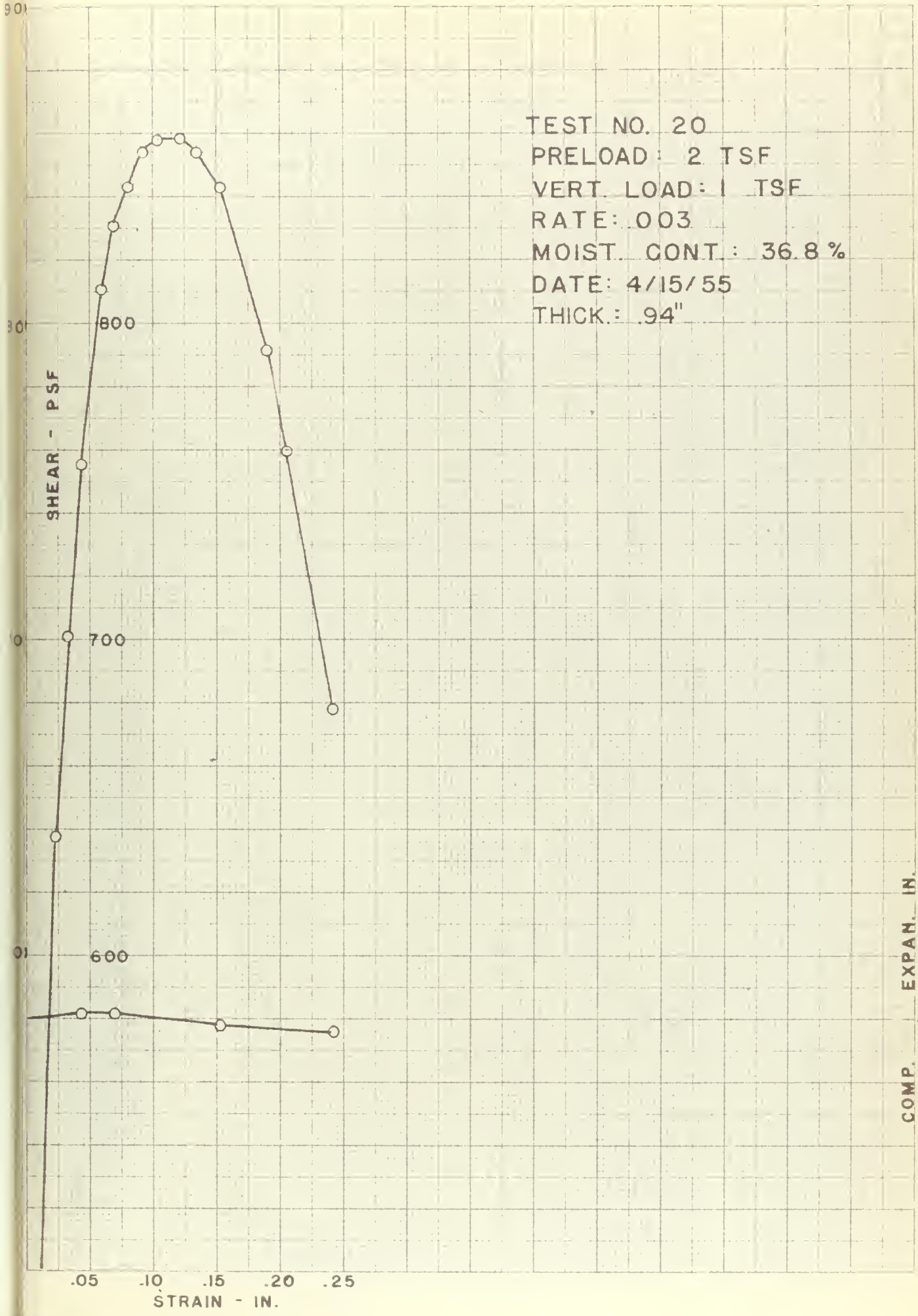
TEST NO. 20
PRELOAD: 2 TSF
VERT. LOAD: 1 TSF
RATE: .003
MOIST. CONT.: 36.8 %
DATE: 4/15/55
THICK.: .94"
800
700
600
SHEAR - PSF
.05
.10
.15
.20
.25
STRAIN - IN.
COMP.
EXPAN. IN.
.010
.000
.010

TEST NO. 21
PRELOAD: 2 TSF
VERT. LOAD: 1/2 TSF
RATE: .02
MOIST. CONT.: 35.0%
DATE: 4/16/55
THICK.: 1.00"

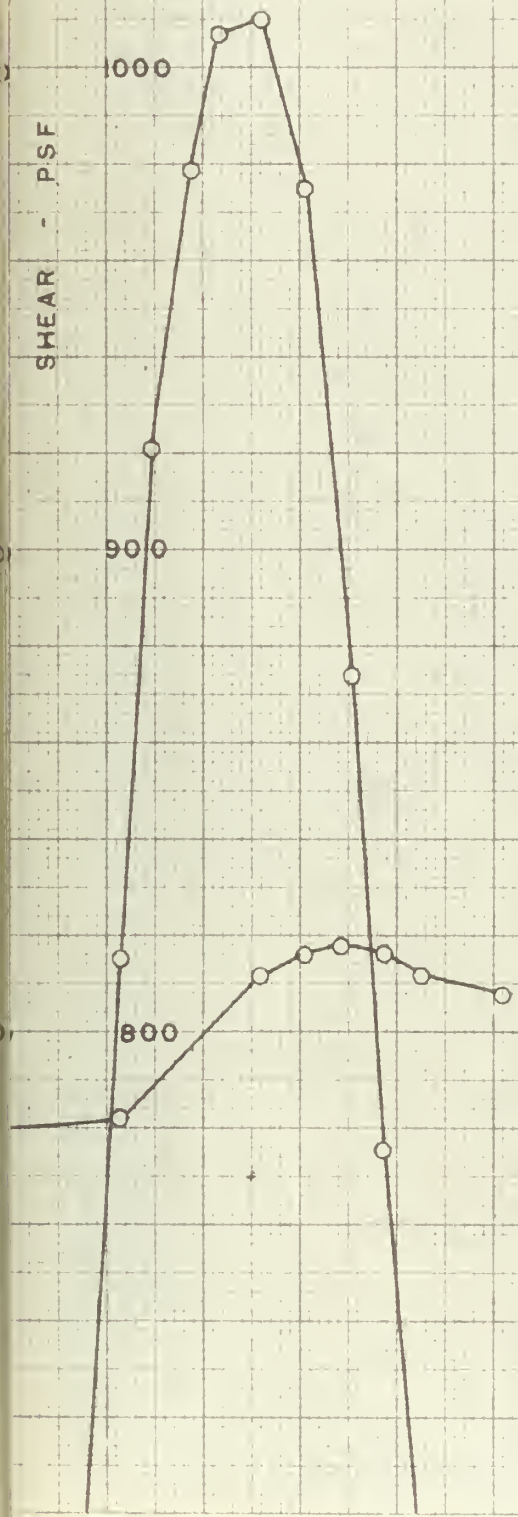

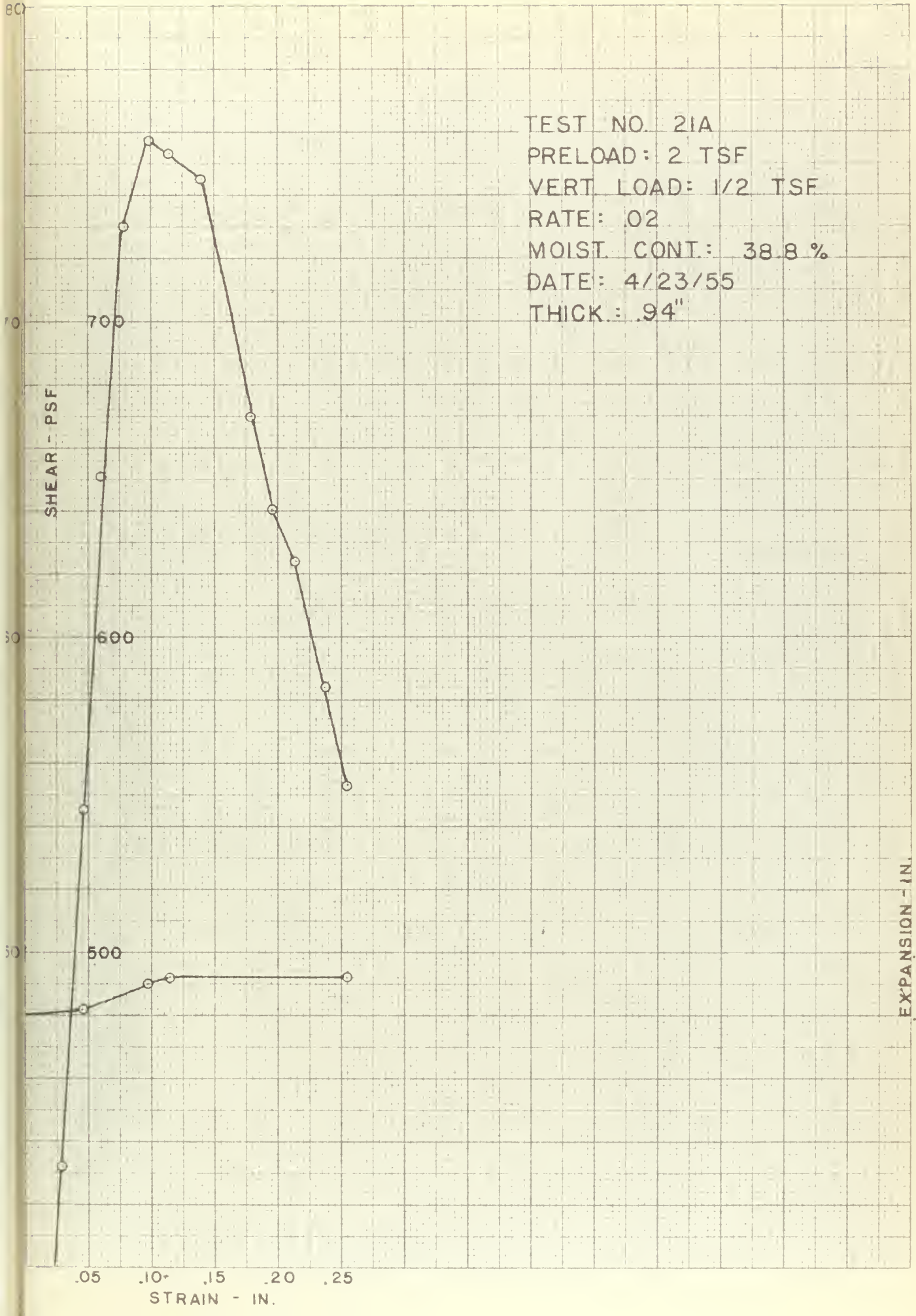
TEST NO. 21A
PRELOAD: 2 TSF
VERT LOAD: 1/2 TSF
RATE: .02
MOIST. CONT.: 38.8 %
DATE: 4/23/55
THICK.: .94"
SHEAR - PSF
700
600
500
.05
.10
.15
.20
.25
STRAIN - IN.
EXPANSION - IN.
.010
.000

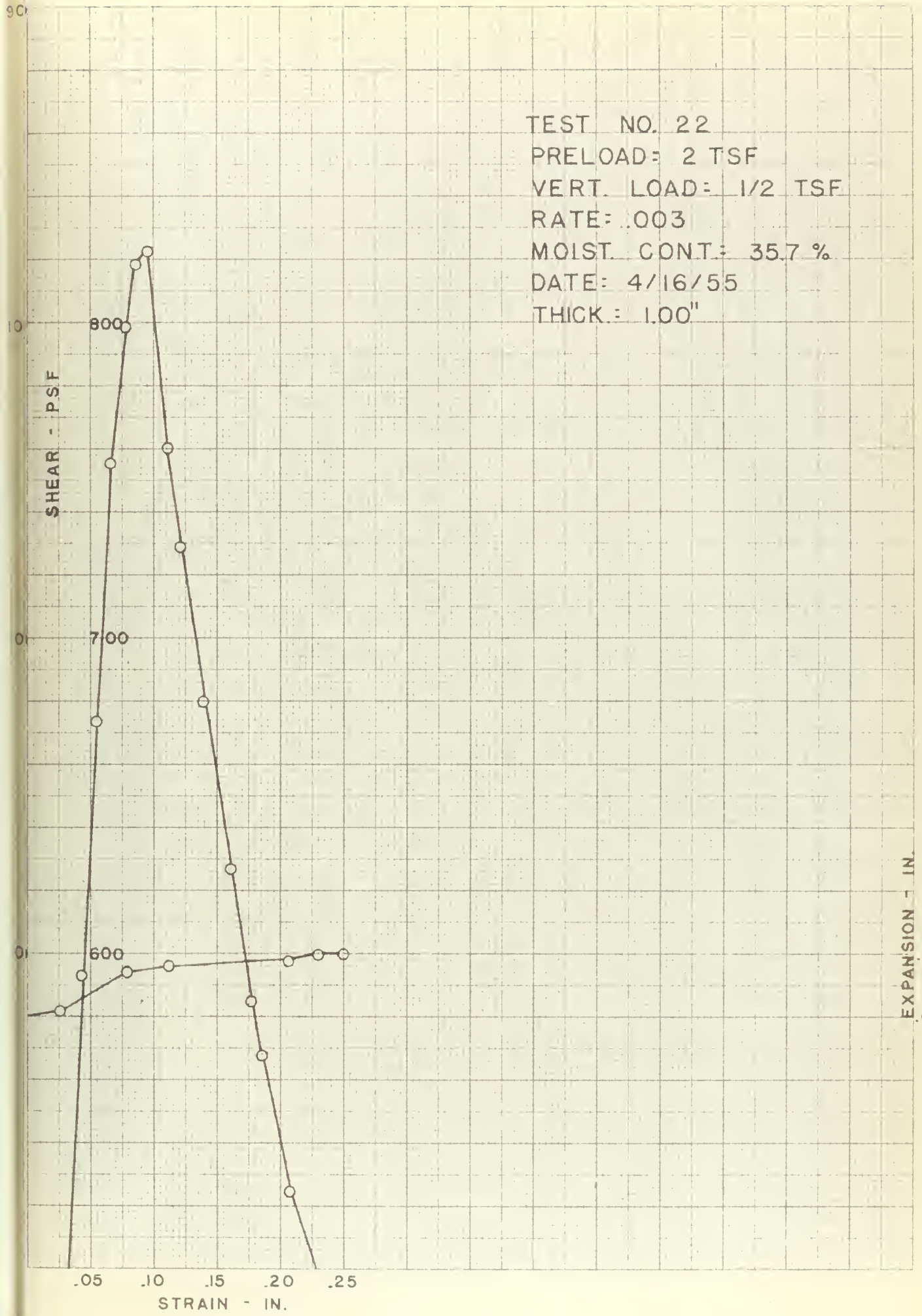
TEST NO. 22
PRELOAD= 2 TSF
VERT. LOAD= 1/2 TSF
RATE= .003
MOIST. CONT.= 35.7 %
DATE= 4/16/55
THICK.= 1.00"
SHEAR - PSF
800
700
600
.05
.10
.15
.20
.25
STRAIN - IN.
EXPANSION - IN.
.010
.000

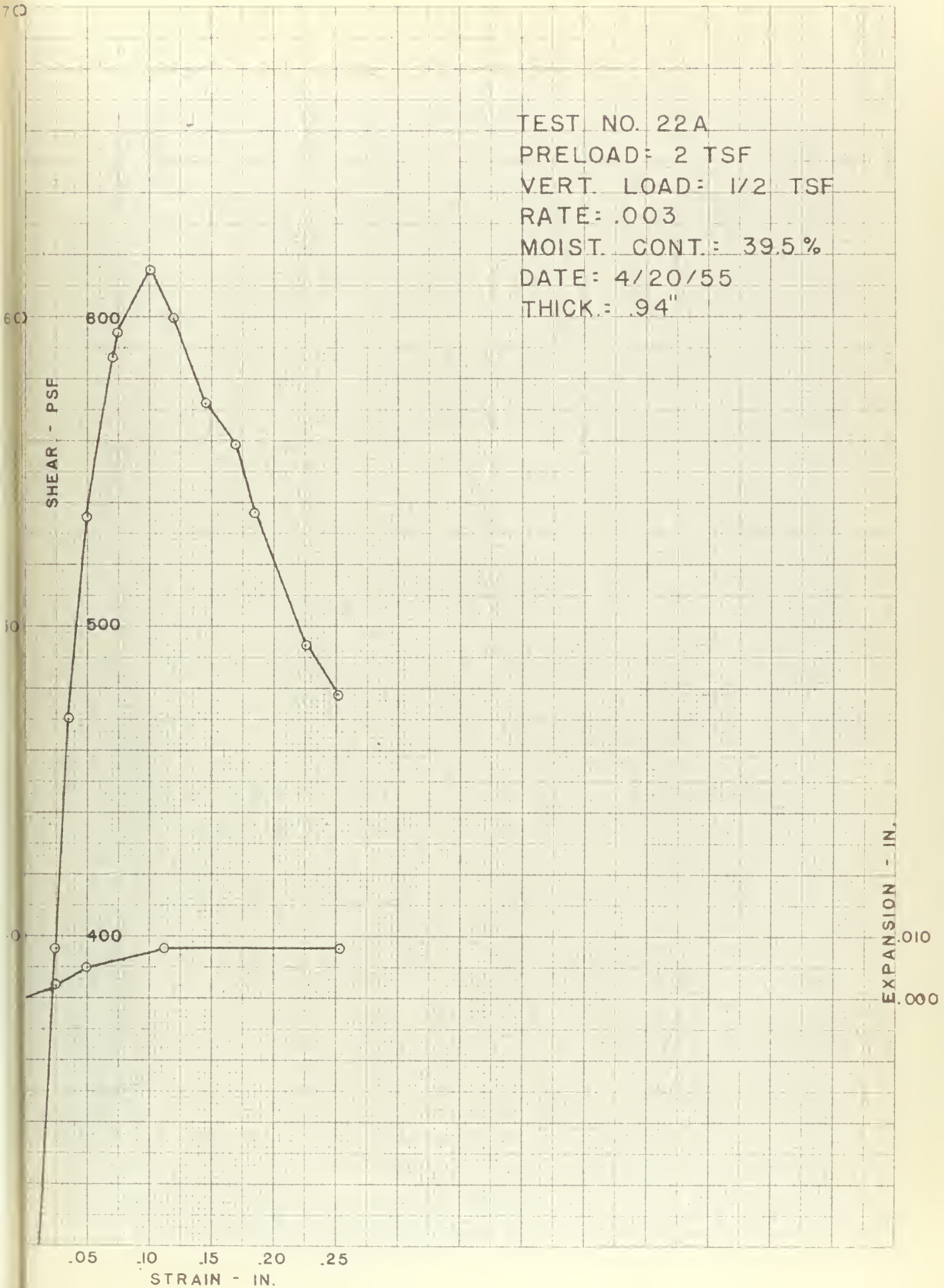
TEST NO. 22A
PRELOAD: 2 TSF
VERT. LOAD: 1/2 TSF
RATE: .003
MOIST. CONT.: 39.5%
DATE: 4/20/55
THICK.: .94"
SHEAR - PSF
600
500
400
.05
.10
.15
.20
.25
STRAIN - IN.
EXPANSION - IN.
.010
.000

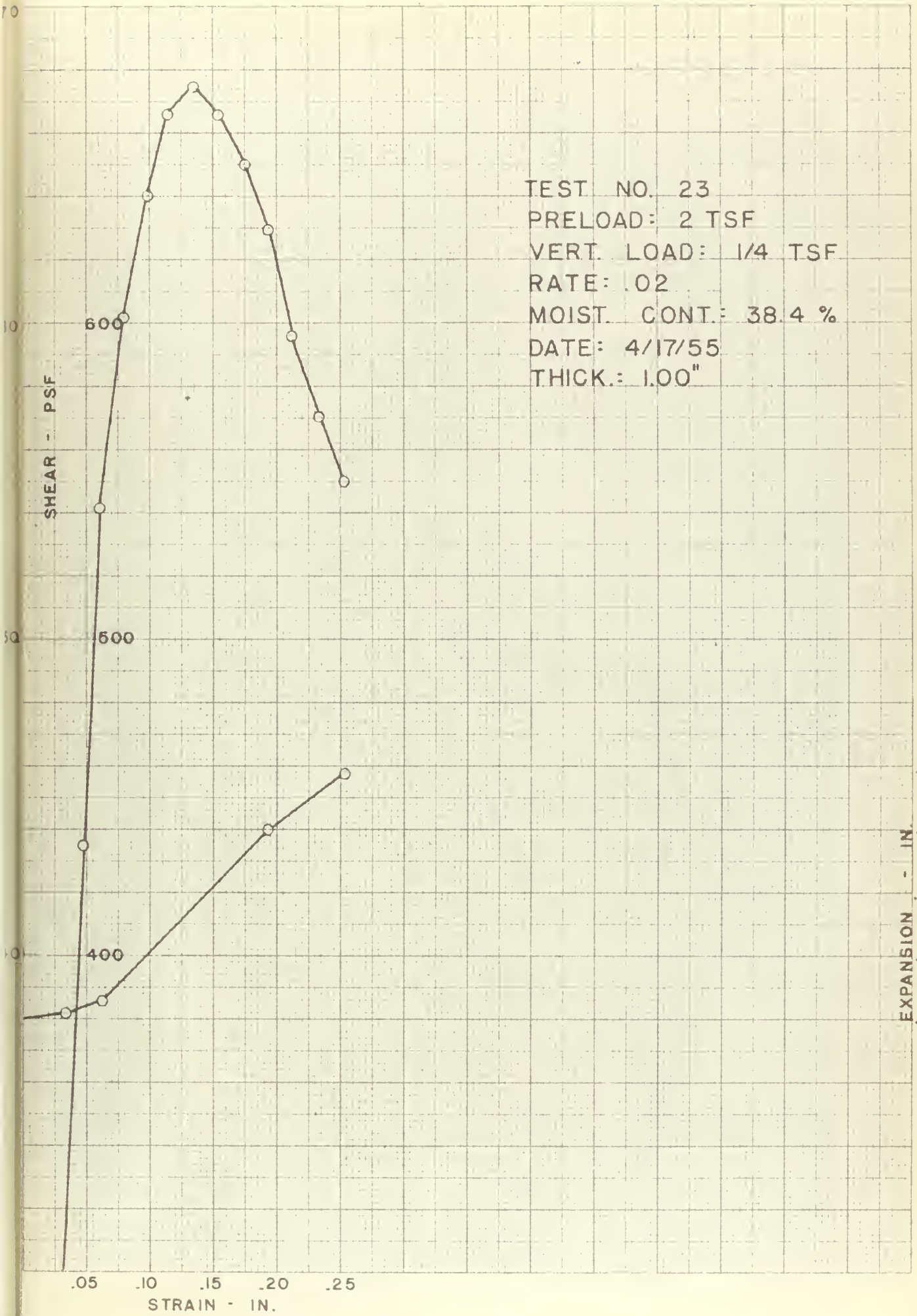
TEST NO. 23
PRELOAD: 2 TSF
VERT. LOAD: 1/4 TSF
RATE: .02
MOIST. CONT.: 38.4 %
DATE: 4/17/55
THICK.: 1.00"
SHEAR - PSF
600
500
400
.05
.10
.15
.20
.25
STRAIN - IN.
.040
.030
.020
.010
.000
EXPANSION - IN.

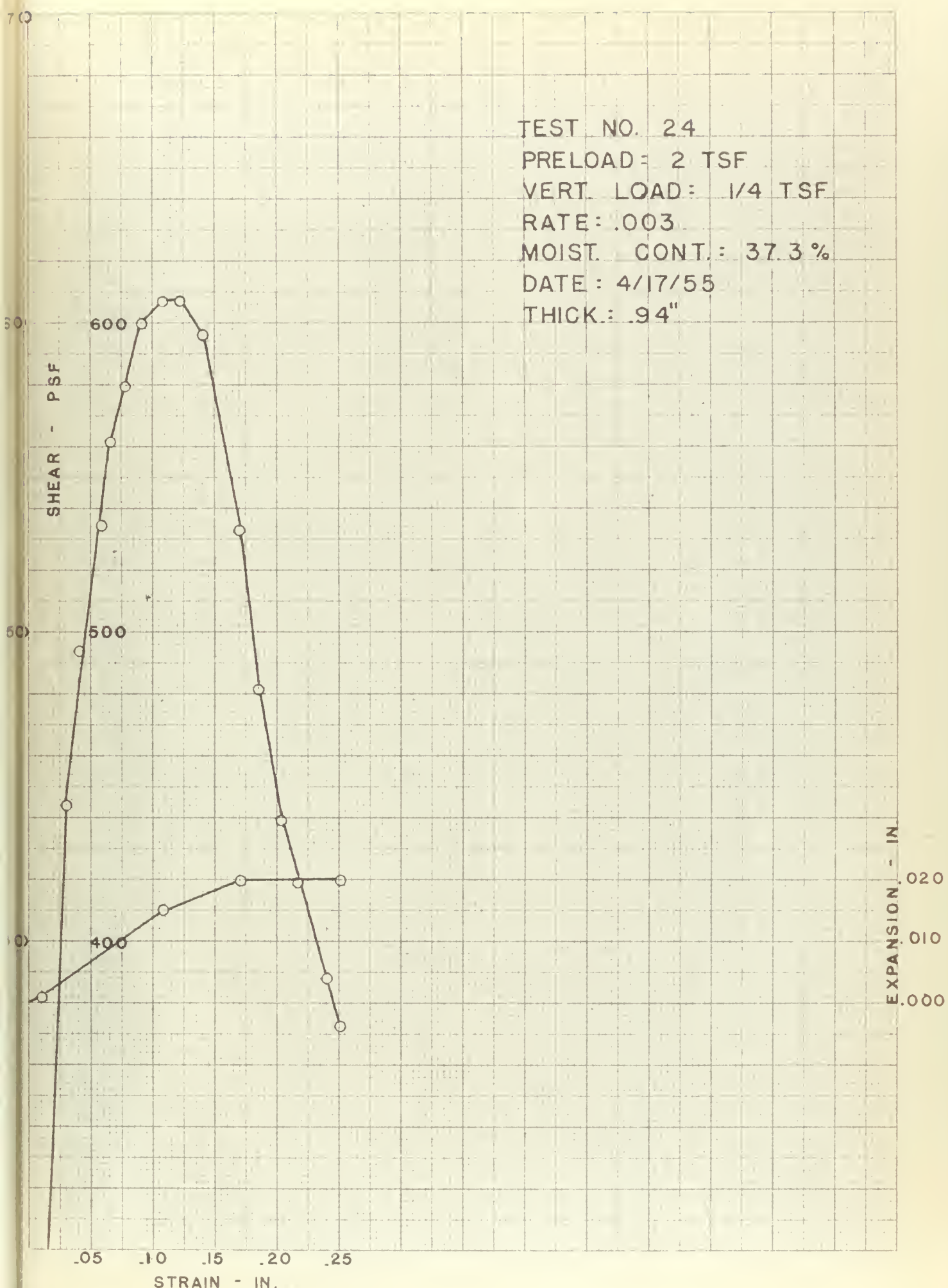
TEST NO. 24
PRELOAD: 2 TSF
VERT. LOAD: 1/4 TSF
RATE: .003
MOIST. CONT.: 37.3 %
DATE: 4/17/55
THICK.: .94"
SHEAR - PSF
600
500
400
.05
.10
.15
.20
.25
STRAIN - IN.
EXPANSION - IN.
.020
.010
.000

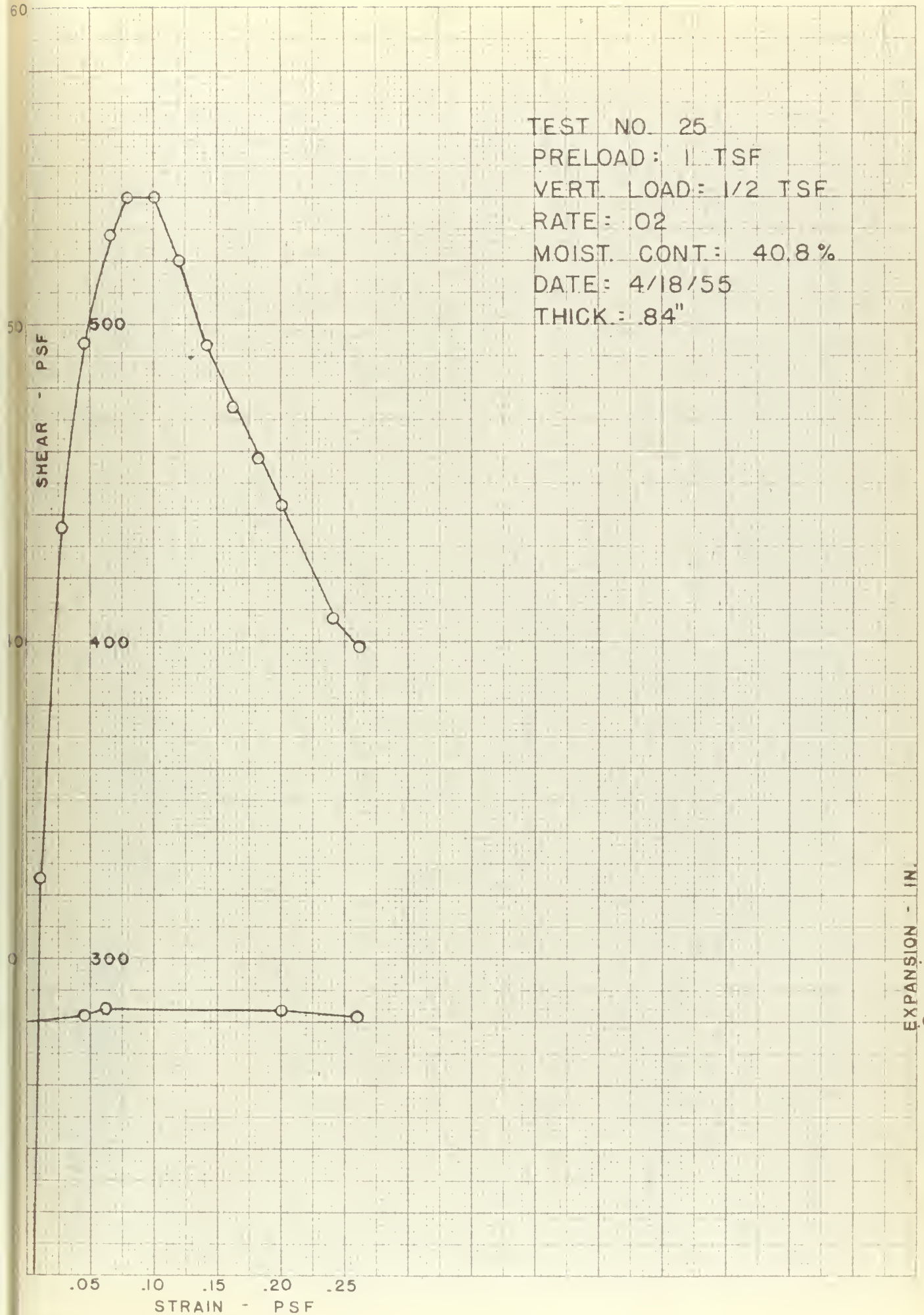
TEST NO. 25
PRELOAD: 1 TSF
VERT. LOAD: 1/2 TSF
RATE: .02
MOIST. CONT.: 40.8%
DATE: 4/18/55
THICK.: .84"
SHEAR - PSF
60
50
40
0
500
400
300
.05
.10
.15
.20
.25
STRAIN - PSF
EXPANSION - IN.
.010
.000

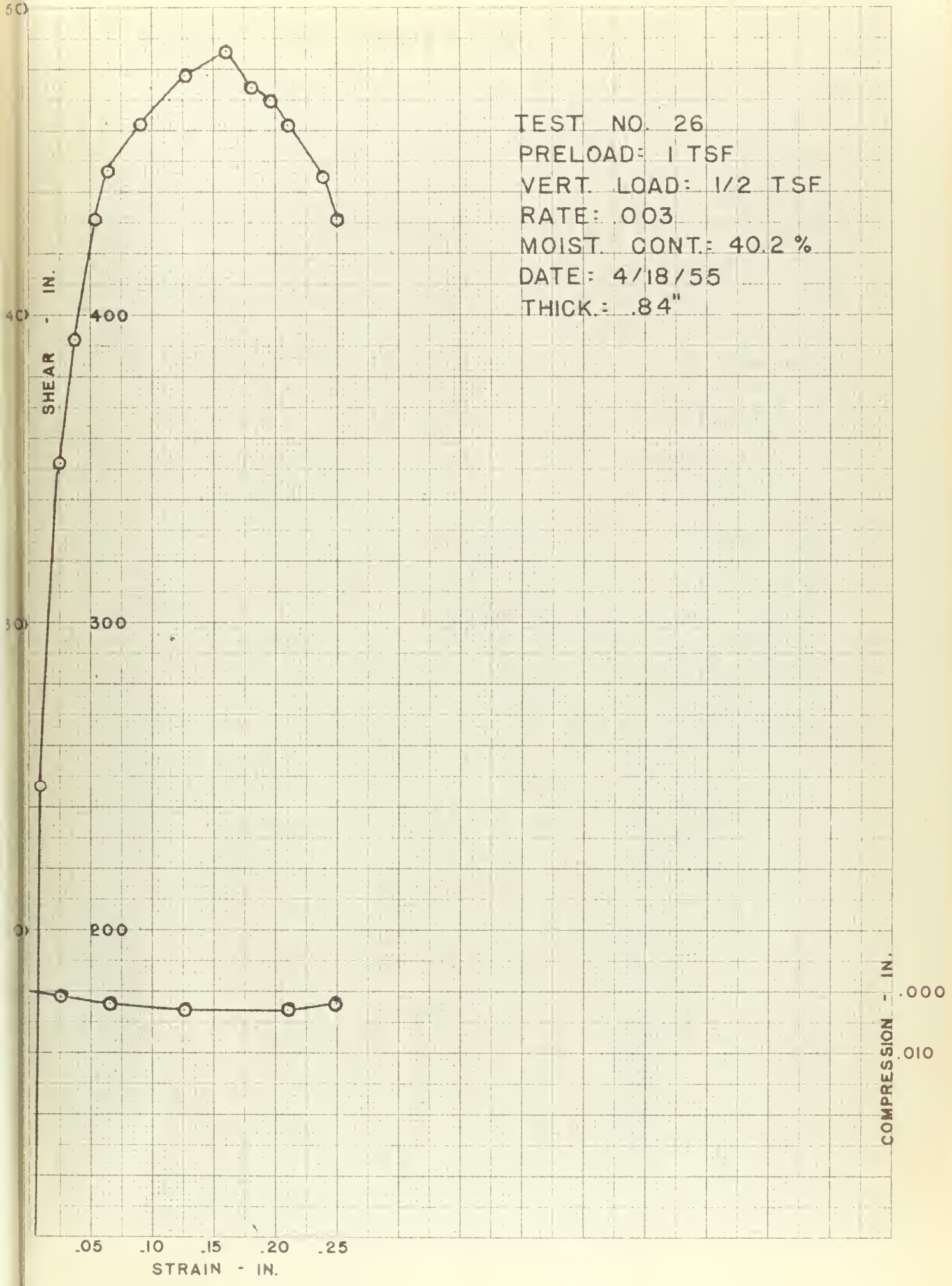
TEST NO. 26
PRELOAD: 1 TSF
VERT. LOAD: 1/2 TSF
RATE: .003
MOIST. CONT.: 40.2 %
DATE: 4/18/55
THICK.: .84"
SHEAR - IN.
400
300
200
.05
.10
.15
.20
.25
STRAIN - IN.
COMPRESSION - IN.
.000
.010

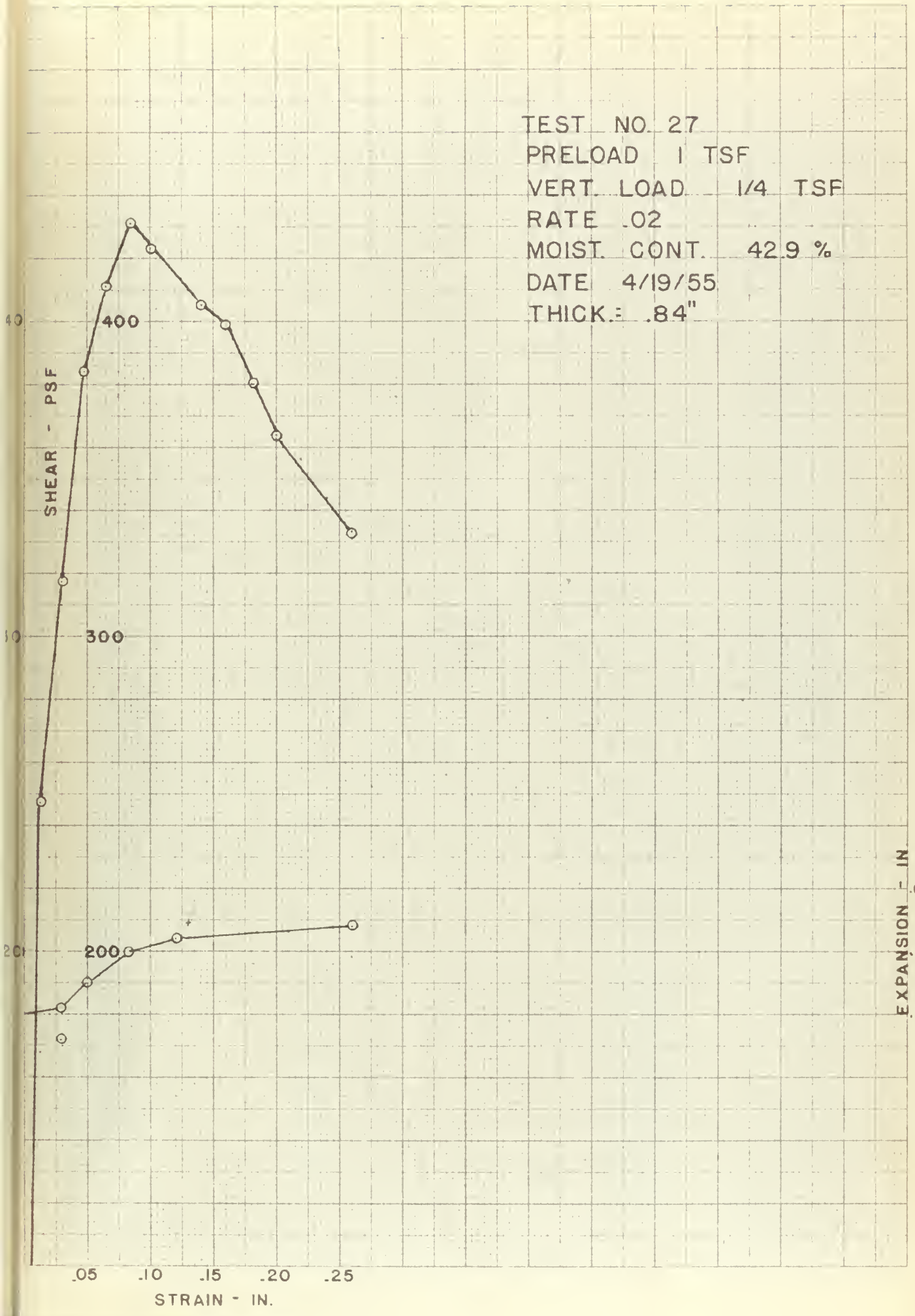
TEST NO. 27
PRELOAD 1 TSF
VERT. LOAD 1/4 TSF
RATE .02
MOIST. CONT. 42.9 %
DATE 4/19/55
THICK.= .84"
SHEAR - PSF
400
300
200
.05
.10
.15
.20
.25
STRAIN - IN.
EXPANSION - IN.
.020
.010
.000

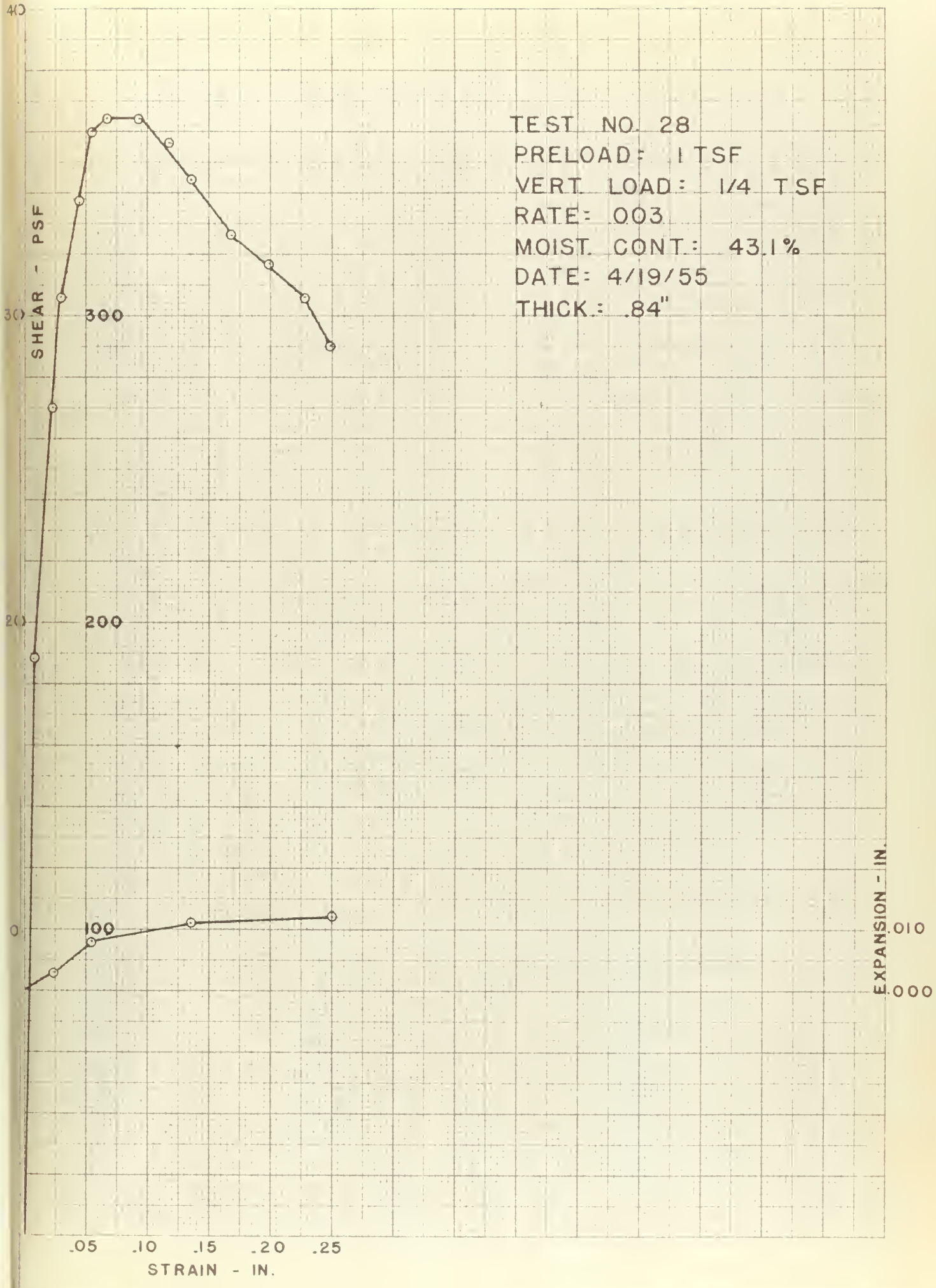
TEST NO. 28
PRELOAD: 1 TSF
VERT. LOAD: 1/4 TSF
RATE: .003
MOIST. CONT.: 43.1%
DATE: 4/19/55
THICK.: .84"
SHEAR - PSF
400
300
200
100
0
.05
.10
.15
.20
.25
STRAIN - IN.
EXPANSION - IN.
.010
.000